Designing a new cross-linkable cohesin complex for studying cohesin`s interaction with DNA

Pelin Uluocak

Wolfson College

Oxford

Dissertation submitted for the degree of Doctor of Philosophy

Department of Biochemistry, University of Oxford

January 2012

Canim Aileme / to my dear Family

Meral, Kâmil & Mehmet Uluocak

Contributions

Experiments presented in **Figure 2-8** and **Figure 2-10** were performed by Dr Maurici Brunet Roig in the laboratory of Prof Kim Nasmyth at the University of Oxford.

Experiments explained in **Chapter 3.2.2.1** and **Chapter 3.2.2.2** were performed by Dr Thomas Gligoris in the laboratory of Prof Kim Nasmyth at the University of Oxford. He initially did the bpa screening of Smc3 and provided the foundation for the experiments performed in Chapter 3.2.2.3 and Chapter 3.2.2.4. They all are presented in this thesis due to their relevance to our findings.

Table of contents

Index of Figures

Summary

Sister chromatid cohesion is essential for accurate chromosome segregation. Cohesion is generated by cohesin, a conserved multi-subunit protein complex composed of four core subunits: Smc1, Smc3, Scc1, and Scc3. Cohesin holds sister chromatids together in mitotic cells starting from S-phase, when DNA replicates, until their separation at the onset of anaphase where its Scc1 subunit is cleaved. In budding yeast, most Scc1 is destroyed by cleavage at anaphase and is only re-synthesised in late G1, whereupon it associates with the unreplicated chromatin. Although sister chromatid cohesion is known to be mediated by a topological interaction of cohesin complexes around sister DNAs, the nature of cohesin`s interaction with chromatin before DNA replication remains to be elucidated. My project aims to develop a new system in order to find out whether 'non-cohesive' cohesin interacts with chromatin topologically. This is important for two main reasons. Firstly, understanding the physical nature of cohesin's interaction with chromatin before DNA replication is essential for determining how cohesion is established during DNA replication. Another reason is that most cohesin in multicellular organisms is associated with the unreplicated chromatin of post mitotic cells where it regulates transcription. How cohesin mediates gene expression is unknown. Understanding how cohesin binds unreplicated chromatin may therefore bring insights into the mechanisms by which cohesin complex performs its non-canonical functions.

In order to address this, we needed a situation where cohesin is already loaded onto chromosomes, but either DNA replication or cohesion establishment is prevented. Therefore, we used a temperature sensitive allele of Eco1 (required for establishment of cohesion). Quantitative measurement of cohesin levels on chromosomes in either wild type allele or temperature sensitive allele of Eco1 showed that the amount of cohesin associated with centromeric and inner pericentromeric regions in both strains are almost indistinguishable from each other throughout the whole cell cycle. Despite normal levels of cohesin, we confirmed by minichromosomal assay that no sister chromatid cohesion is established in the absence of functional Eco1 protein.

If "non-cohesive" cohesin interacts with the chromatin in a topological manner when there is no sister chromatid cohesion, then its association with chromatin should be resistant to denaturing conditions in the presence of a modified version of the cohesin complex that can be covalently circularized. To test this prediction, a cross-linkable cohesin molecule was needed, which should be resistant to SDS denaturation and should not have major cohesion defects due to the modifications making it to be cross-linkable. The previously created cross-linkable cohesin molecule had cohesion defects due to the presence of Smc3-Scc1 fusion protein. In addition, this fusion alone could bypass the requirement for Eco1, and therefore we could not test how "non-cohesive" cohesin interacts with chromatin, using this version of cross-linkable cohesin complex.

We tried two different methods to conditionally close Smc3/Scc1 interface in a way resistant to protein-denaturants and create a new cross-linkable cohesin complex. In our first attempt, the C-terminus of Smc3 and the N-terminus of Scc1 were fused to FRB and FKBP12 respectively, proteins that can form a complex upon addition of rapamycin. Crystal structure of the ternary complex of FKP12/rapamycin/FRB enabled us to design cysteine pairs for the crosslinking of FRB and FKBP12 only in the presence of rapamycin. A more efficient *in vivo* crosslinking was achieved between the Smc3 and Scc1 in our second attempt. Amino acids within the coiled coil region of Smc3 were replaced by the unnatural photo-cross-linkable amino acid ρ-benzoyl-phenylalanine that can be induced to form covalent bonds with neighbouring proteins (T.Gligoris, unpublished data). Photo and chemically cross-linkable interfaces of cohesin were then integrated with each other to generate a new version of cross-linkable cohesin molecule.

Chapter 1 – Introduction

1.1. The life history of cells and chromosomes

1.1.1. Cell-division cycle

Despite the variety and diversity of life on Earth, all organisms, from unicellular to multicellular ones, are built from similar molecular components, indicating that every living cell today has arisen from a common ancestral cell that came into being over a billion years ago. Continuity of life has been dependent on a vital process, called cell division, which ensures the transmission of the complete genetic information from generation to generation.

Cell division operates in a cycle (Figure 1-1A). This cycle is comprised of a series of phases, which leads to the duplication and equal distribution of cell`s content into the daughter cells. Based on the morphology and movements of the chromosomes, the cell cycle can be subdivided into interphase and M (mitotic) phase, which is composed of nuclear division (mitosis) and cell division (cytokinesis). M phase is also divided into four substages: prophase, metaphase, anaphase and telophase (Figure 1-1B). The first stage of mitosis is prophase, where chromosomes start to compact in a rod shaped structure and become visible under light microscope. In metaphase, chromosomes are then positioned in the center of the cell waiting for the signal to separate, and when the right time comes, sister chromatids are pulled towards opposite poles of the cell in anaphase. Mitosis is then completed in telophase, when the chromosomes and other nuclear components are packaged into identical daughter nuclei. Cell cycle is finished by the separation of two cells via the formation a new cell membrane.

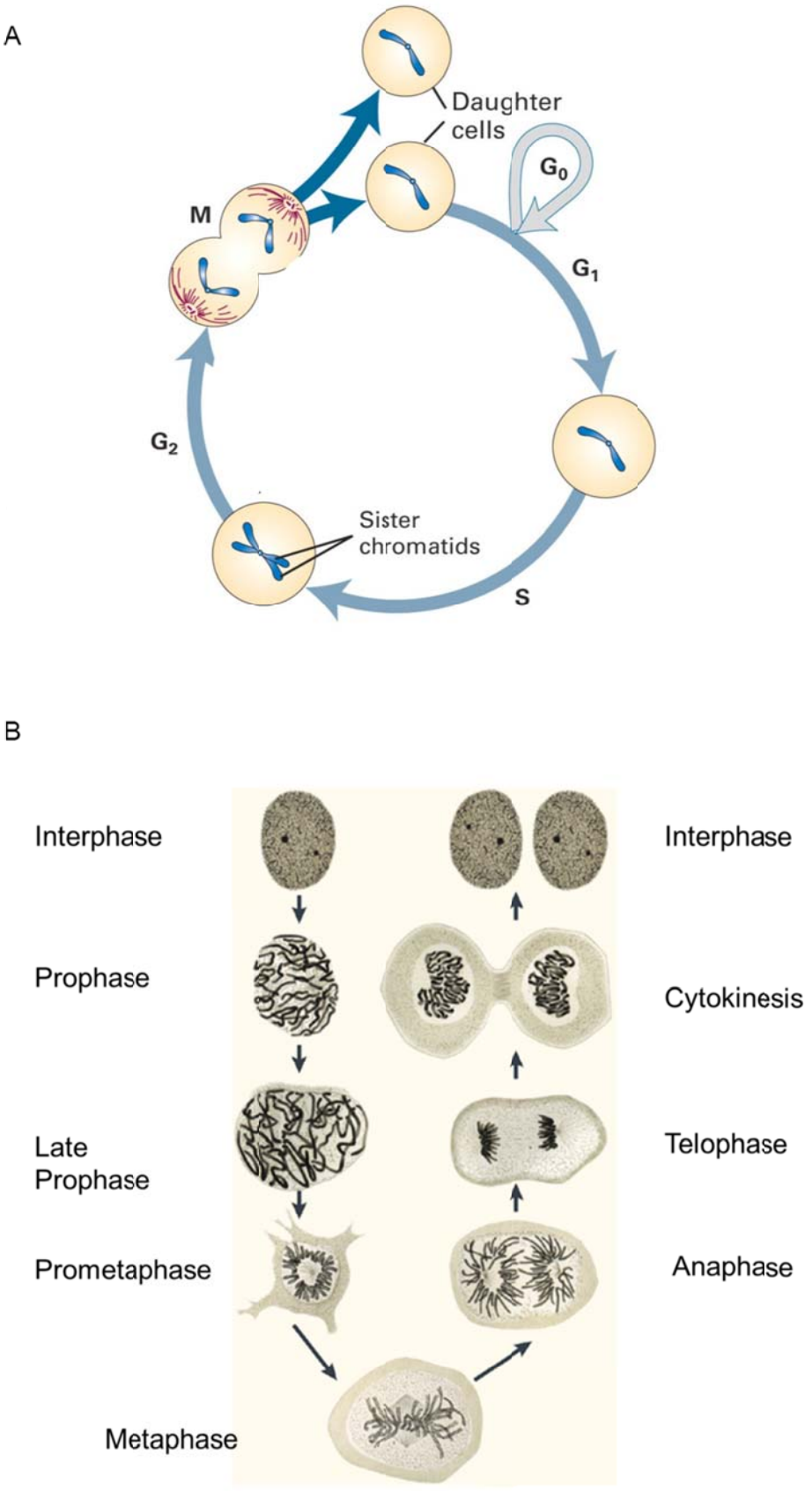
A
Daughter cells
G_0
M
G_1
G_2
Sister chromatids
S
B
Interphase
Prophase
Late Prophase
Prometaphase
Metaphase
Interphase
Cytokinesis
Telophase
Anaphase

Figure 1-1

Figure 1-1: The eukaryotic cell cycle

(A) In proliferating cells, G1 is the period between "birth" of a cell following mitosis and the initiation of DNA synthesis. Chromosomes are replicated in S-phase followed by M-phase comprising of both nuclear and cell division. Most non-proliferating cells in vertebrates leave the cell cycle in G1-phase, entering the G0 state, where cells differentiate into different cell types. Cytokinesis gives rise to two daughter cells; (adapted from Lodish *et al*., Molecular Cell Biology, 2003).

(B) Walter Flemming`s drawing of mitotic chromosome structure. Mitosis begins with prophase, where skein-like form of nuclear threads change into the star-like configuration at prometaphase. Threads then move to the equatorial plate (metaphase), and subsequently evolve into the double star configuration (anaphase). Once the threads arrive at the position of the daughter-cell nucleus, the double skein (telophase) can be observed (Images reproduced from Paweletz *et al*., 2001).

Interphase is the period between two consecutive M-phases (the end of one and the beginning of the next), and known as “preparatory phase”, since most proteins, RNAs and other cellular macromolecules necessary for S-(synthesis) and M-phases are being produced and accumulated during this stage. It is comprised of S-phase, and two gap (G) phases, G1 and G2.

In eukaryotic cells, DNA replication takes place in S phase. The G1- and G2- phases of the cell cycle occur between DNA synthesis and mitosis. In the first gap, G1-phase, the cell is preparing for the DNA synthesis. The G2-phase is the second gap during which the cell gets ready for mitosis.

Cells give a critical decision for their fate in G1-phase, as they either decide to continue cell division or exit the cell cycle depending on the growth conditions. When cells are in an unfavourable environment or receive inhibitory signals for their growth, they can temporarily arrest cell proliferation or permanently quit the cell cycle to enter a “quiescent” state or a G0 (G zero) phase. G0-phase is also referred to as a "post-mitotic" state, as G0-phase cells are in a non-dividing state. Many cells in an adult multicellular organism, such as nerve and heart muscle cells have to exit the cell cycle in order to reach a post-mitotic stage where they are terminally differentiated to perform a unique function. During the differentiation process, changes are happening in cell’s size, metabolic activity, and responsiveness to signals, which are mainly due to the modifications in gene expression. Therefore, cells are now programmed to carry out their specialized function.

When cells fail to receive a life-maintaining signal, they actually start to produce proteins necessary for self-destruction, a process called apoptosis (programmed cell death). Death by apoptosis prevents unnecessary reproduction of cells and avoids release of potentially toxic cell constituents. Programmed cell death is a critical process in homeostasis, development

and functioning of our bodies, by providing a balance between cell proliferation and removal of unneeded, old cells.

1.1.2. Cell cycle regulation

Execution of these cell cycle events is under the strict control of check point mechanisms. During the cell cycle, a series of biochemical switches initiate progression through the three major regulatory checkpoints. An important function of these checkpoints is to verify whether the DNA has been damaged, which is being recognised by sensor mechanisms at the end of each phase of the cell cycle, before allowing progression into the next phase. The first checkpoint is called Start or G1/S checkpoint, giving the decision of whether the cell should divide, delay division, or enter a resting stage. In the absence of environmentally favourable conditions for cell proliferation, the progression through Start is blocked by repression of the G1/S- and S-phase CDKs (cyclin dependent kinase). The G2/M checkpoint is the second checkpoint, ensuring that the cell is ready to enter mitosis. The molecular nature of this checkpoint involves examining whether DNA replication was completed accurately, therefore preventing the transmission of any damaged DNA into the daughter cells. The third major checkpoint is the metaphase-to-anaphase transition, whose role is to verify that all the chromosomes are properly aligned on the mitotic plate being under bipolar tension.

The cell cycle control system behaves like a biochemical timer in order to initiate cell cycle events in the correct order and to provide enough time for each event to be correctly completed before proceeding to the next one (Hartwell and Weinert, 1989). Cyclin-dependent kinases (CDKs) are the main players of the cell cycle control system. CDKs are activated through binding to their partner proteins called cyclins, whose phosphorylation they control. Changes in the amounts of cyclins lead to the oscillations in CDK activity during cell cycle.

Different types of cyclins are synthesised at different cell cycle stages, causing the formation of specific cyclin-CDK complexes initiating different cell cycle phases (Figure 1-2; Morgan *et al*, 1997).

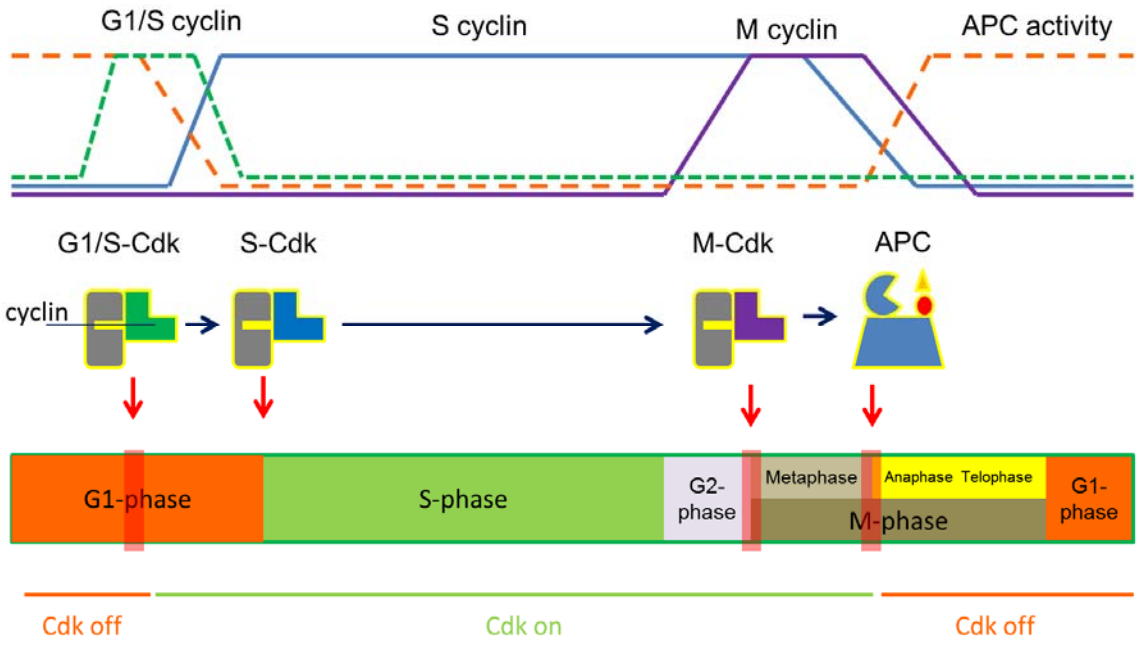

Figure 1-2: A general overview of cell cycle control

A cell enters a new division cycle by the formation of active G1/S-Cdk complexes in late G1-phase. The S-Cdk complexes, activated by G1/S-Cdks, trigger DNA replication at the beginning of S-phase. After the M/Cdk activation occurring at G2/M phase, mitosis is initiated. Activation of APC/C then leads to the sister chromatid separation at the metaphase-to-anaphase transition, causing the destruction of S- and M-phase cyclins. This results in completion of mitosis and cytokinesis. (Image reproduced from Morgan, 2007).

In early G1-phase, cyclin-CDK concentrations in the cell are low due to the decrease in cyclin gene expression, presence of high concentrations of CDK inhibitors (CKIs) and the increase of cyclin degradation through the activation of the anaphase-promoting complex/cyclosome (APC/C), which is an ubiquitin-protein ligase. Once the cells have entered a new cell division cycle, the G1 cyclins induce the activation of APC/C-Cdh1, a form of APC/C activated by the Cdh1 (Cdc20 homolog 1) protein (Visintin *et al.,* 1997), which leads to the degradation of S-phase inhibitors by causing their polyubiqutination by SCF (Skp1-Cul1-F-box) ubiquitin ligase (Cardozo and Pagano, 2004). Formation of active G1/S cyclin-CDK complexes promotes cell cycle progression. The rise in G1/S cyclin-CDK levels is paralleled by an increase in S cyclin-CDKs. Presence of S cyclin-CDKs activates pre-replication complexes and initiates DNA replication. The "once-and-only-once" nature of DNA replication is achieved by dividing the initiation process into two temporally distinct steps. The timing of both steps in the initiation of DNA synthesis is governed by the cell cycle control system (reviewed in Bell and Dutta, 2002). First, in late mitosis and early G1, a large complex of proteins called pre-replicative complex (preRC) binds to specific DNA sequences, generally called replication origins and prepares them for firing (reviewed in Blow and Tanaka, 2005). Assembly of the preRC at replication origins only takes place in late mitosis and early G1, when CDK activity is low and APC/C activity is high. The multi-subunit replication machinery preRC, consists of the ORC (origin recognition complex), together with Cdc6 (cell division cycle 6), Cdt1 (chromatin licensing and DNA replication factor 1) and the Mcm2-7 (mini-chromosome maintenance) complex proteins (reviewed in Diffley, 1995; Stillman, 2005). Second, in early S phase, the pre-replicative complex is transformed into a pre-initiation complex that unwinds the replication origins and loads the DNA synthesis machinery (reviewed in Waga and Stillman, 1998). Once an origin has been activated, the preRC disassembles, and its reassembly is prevented at origins until the

following G1-phase since CDKs have been reactivated by binding to their partner cyclins and the APC/C has been inactivated until late mitosis. Therefore, following DNA replication, the chromosomes no longer have the ability to initiate DNA synthesis, ensuring that DNA duplication occurs only once per cell cycle (reviewed in Rao and Johnson, 1970).

After the completion of S-phase, M cyclin-CDK concentrations increase as the cell begins to enter mitosis and the concentrations peak at metaphase. They phosphorylate multiple proteins that promote chromosome condensation, assembly of the mitotic spindle apparatus, and alignment of condensed chromosomes at the metaphase plate. Activation of APC/C-Cdc20, a form of APC/C activated by the Cdc20 protein, then causes sister-chromatid separation at the metaphase-to-anaphase transition and destruction of S and M cyclins, leading to the completion of mitosis and cytokinesis (Nasmyth *et al*, 2001).

1.1.3. DNA compaction into chromosomes

Eukaryotic chromosomes contain an enormous amount of DNA, which requires an elaborate system to package the chromosomal DNA into the nucleus. Considering the fact that a human cell contains about 2 meters of DNA in a nucleus, which is only about 6 μm in diameter, DNA compaction is a serious and complicated task which cells must accomplish during the course of cell cycle. So, how is that entire DNA packaged so tightly into a tiny nucleus?

The answer to this question lies in the fact that the thin thread of DNA in each chromosome is compressed in chromatin by a variety of proteins. This process does not only fold the long DNA molecules into durable and compact forms, but also gives them a flexible structure, so that the proteins that regulate gene expression, DNA replication and DNA repair can still access the DNA.

While the overall chromatin structure is significantly different between the stages of the cell cycle, the packaging ratio of chromatin also varies dramatically in different regions of the genome. When examined under the microscope after DNA staining, an interphase cell nucleus typically looks like a mosaic image as a result of dense and thin regions of chromatin. Lighter regions are known as "euchromatin" and darkly stained compartments refer to "heterochromatin" (Heitz *et al*., 1928). While euchromatin is rich in transcriptionally active genes and easily accessible by transcriptional activators and RNA Polymerase II (RNAPII), heterochromatin is less accessible to the transcription machinery, tightly packaged, and mainly found around the centromeres and telomeres (reviewed in Grewal and Moazed, 2003). Although heterochromatin exerts a silencing effect on gene expression, transcription of non-coding RNAs from heterochromatic repeats has also been observed in several systems including fission yeast (Volpe *et al*., 2002; Verdel *et al*., 2004). During the M-phase, the chromatin packs more tightly to facilitate chromosome segregation and to cope with large mechanical forces pulling them into each of the two daughter cells (reviewed in Teif and Bohinc, 2011).

The basic unit of DNA packaging is the nucleosome, which consists of approximately 147 base pairs of double stranded DNA wrapped around an octamer of core histone proteins (two copies of each histone H2A, H2B, H3 and H4) (Luger *et al*., 1997; reviewed in Felsenfeld & Groudine, 2003). Histones are a family of small, positively charged proteins, and are among the most highly conserved eukaryotic proteins known. Since DNA is negatively charged due to the phosphate groups in its phosphate-sugar backbone, lysine- and arginine- rich histone proteins can be tightly bound to the DNA.

The packaging of DNA into nucleosomes starts by shortening the fiber length about six to seven fold, also known as "11 nm" fibre, which can be seen under EM in low ionic strength conditions (Figure 1-3). This first level of chromatin structure is often described as "beads-

on-a-string" (Oudet et al. 1975), where "beads" correspond to nucleosomes. Adjacent nucleosomes are connected by a linker DNA, which varies from 10 -to 80 base pairs in length depending on species and tissue type, and is bound by the linker histone H1. Despite this compaction, chromatin is still too long to fit into the nucleus, and therefore, the basic "11 nm" fibre is further coiled into an even shorter and thicker order, termed the "30 nm" fibre, which was also observed by EM of HeLa cell metaphase chromosomes (Marsden and Laemmli, 1979).

Although the structure of these fibers is not clear, adjacent nucleosomes have been thought to interact with each other in a zigzag arrangement, which is facilitated by histone "tails" (Bernard *et al*., 1998). Each histone has a flexible, 10-30 amino acids long, positively charged N terminal tail, which extends from the surface of histone octamer. Properties of histone tails are changed through the covalent modifications such as acetylation, phosphorylation, methylation and ubiquitination, and this creates binding sites for non-histone proteins controlling chromatin structure and function (reviewed in Jenuwein and Allis, 2001).

The different types of modifications, which have been called the "histone code," are put in place by a variety of different enzymes. For instance, several lysines in histones H3 and H4 are modified by acetylation. Acetyl groups are incorporated by histone acetyltransferases (HAT) and removed by histone deacetylases (HDA). Acetylation carries in a negative charge, causing the neutralisation of the positive charge in the histone tail. This therefore, reduces the interactions between the tail and the negatively charged DNA, results in a loosening of the coil, transforms the condensed chromatin into a more relaxed form, and eventually leads to an increase in the levels of gene transcription (Kurdistani and Grunstein, 2003).

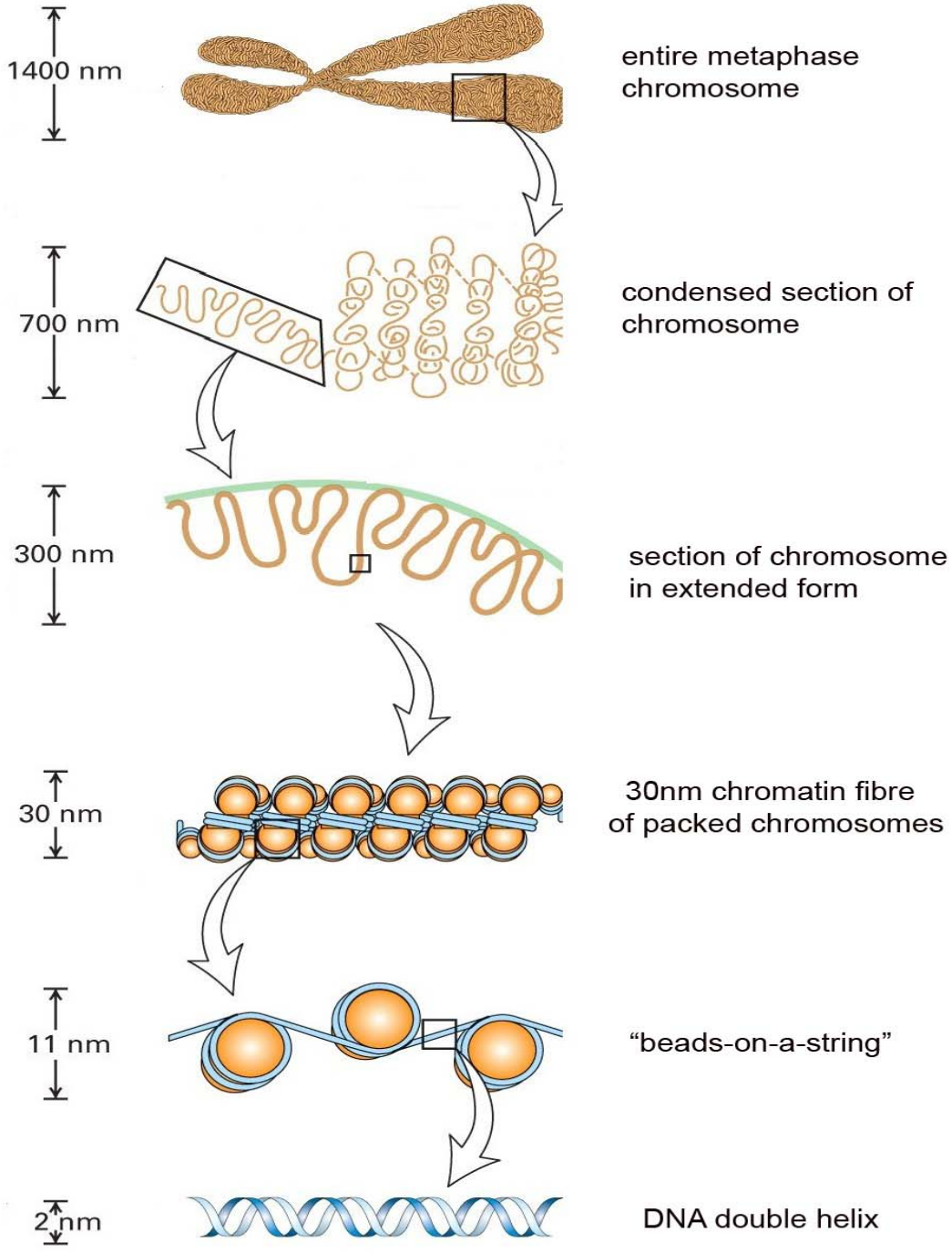

Figure 1-3: Different levels of chromatin compaction

The basic 2nm thick DNA molecule is compacted in several ways to give rise to about 10 000-fold compacted structures of the mitotic chromosomes. Nucleosomes can be arrayed in the loosely packed “beads-on-a-string” form of chromatin. The 30nm fibre can be packed at different densities by expansion or contraction of the fiber along its length (adapted from Lodish et al., Molecular Cell Biology, 2003).

In addition to histone-modifying enzymes, members of a large and diverse class of enzymes, called chromatin remodeling complexes, use ATP hydrolysis also to mobilize and restructure nucleosomes in order to provide access to the underlying DNA to enable transcription, chromatin assembly, and DNA repair. For example, prior to transcription in budding yeast, one of the major types of chromatin remodeling machines, called the SWI/SNF and SAGA histone acetylase complex, is recruited to the HO gene promoter by the SWI5 activator, which slides the nucleosomes along the DNA so that RNA polymerase II can reach the promoter regions of the DNA (Struhl, 1999).

1.1.4. Chromosomes are reorganized in mitosis

Entry into mitosis initiates dramatic structural changes in the chromosomes. When DNA replication is completed in S phase, sister DNAs are in a fragile and intertwined form. At this stage any segregation attempts would have catastrophic consequences for the cell, since it might cause DNA breakage as sister DNAs are pulled apart. To avoid this, the sister chromatids are compacted into rod-like, durable structures by chromosome condensation. Such a structural change strengthens the architecture of sister chromatids and prevents them from becoming entangled with each other, thereby allowing their proper segregation to opposite poles of the cell.

Chromosome condensation starts in early prophase resulting in the formation of thick, rod-shaped chromosomes. Although not much is known about the structural basis of the mitotic chromosome changes, a class of protein complexes called condensins seem to be required for this process. Condensins share functional and structural similarities to another protein complex, named cohesin (see section 1.2.). Condensin contains two members of a large family of chromosomal ATPases, known as structural maintenance of chromosome (SMC) proteins, SMC2 and SMC4, form V-shaped heterodimers whose nucleotide binding domains

(NBDs) are connected by the non-SMC subunit Cap-H, causing the formation of a ring-shaped structure. It has been proposed that condensin compacts DNA by encircling different parts of the same DNA molecule within a single chromatid using the energy provided by the ATP hydrolysis (reviewed in Nasmyth and Haering, 2005). It could also be argued that condensin generates intra-chromatid cohesion by linking together adjacent segments of a given DNA molecule (reviewed in Nasmyth and Haering, 2009).

In addition to its role in chromosome condensation, condensin also participates in sister-chromatid resolution, a process in which sister chromatids are rearranged into distinct units so that they can be easily separated in anaphase. Condensation and resolution progress in parallel during metaphase, so that chromosomes are "metamorphosed" into compact and distinct sister chromatids, which are only joined together at their centromeres awaiting mitosis. Following cell division, chromosomes start to decondense again, gaining their G1-phase characteristics back.

1.2. The cohesin complex and its role in holding sister chromatids together

The main purpose of mitosis is to distribute equally the duplicated sister chromatids into the two daughter nuclei, being dependent on the accurate sister chromatid separation at anaphase. In early stages of mitosis, by resisting the pulling forces of microtubules coming from the opposite poles of the cell, sister chromatid cohesion was thought to create tension, suggested to be required for the accurate alignment of chromosomes on the metaphase plate (Nicklas, 1998). A sudden loss of cohesion was proposed then to initiate sister chromatid separation during anaphase (Miyazaki and Orr-Weaver, 1994).

However, for a long time, it was unclear how sister chromatid cohesion is mediated. In other words, the question of what holds sister chromatids together until the onset of anaphase remained unknown until 15 years ago. It has been proposed that sister chromatids might be held together by DNA catenation, which is the extensive intertwining of replicated DNA molecules that arise when two replication forks meet during DNA synthesis (reviewed in Murray and Szostak, 1985). Although most of this catenation is resolved during metaphase by the enzyme topoisomerase II, resolution of catenates only makes a minor contribution to destroy the connection between cohesed sisters at this point, indicating the existence of another protein or protein complexes that function to hold sister chromatid together (Koshland and Hartwell, 1987; Farcas *et al*., 2011).

1.2.1. Discovery of the cohesin complex

After having found out that the ubiquitin-protein ligase, APC/C (Anaphase Promoting Complex/Cyclosome), promotes the destruction of proteins that control the metaphase to anaphase transition and is therefore essential for sister chromatid separation, it was presumed that sister chromatid cohesion might be regulated by proteins which are targets of APC/C (King *et al*., 1995; Irniger *et al*., 1995). Identification of APC/C as an essential step in the degradation of proteins that control the metaphase to anaphase transition and therefore its requirement for sister chromatid separation, led to the presumption that sister chromatid cohesion might be regulated by proteins that are targets of the very same APC/C. Independent genetic studies performed by two research groups in *S. cerevisiae* have led to the discovery of specific proteins involved in sister chromatid cohesion (Guacci *et al*., 1997; Michaelis *et al*., 1997). Both studies reasoned that inactivation of the proteinaceous “links” between sister chromatids would separate them in the absence of APC/C activity. Koshland laboratory identified a gene called *Mcd1* (*Mitotic cell determinant*) in a screen based on a

microtubule- depolymerizing agent that arrest cells in metaphase. The screen aimed at identifying mutants which are defective in holding sisters chromatids together and therefore separate precociously during the mitotic arrest (Guacci *et al*., 1997). Studies from Nasmyth laboratory identified four genes *Scc1* (*Sister chromatid cohesion 1*, identical to *Mcd1*), *Scc2* (*Sister chromatid cohesion 2*), *SMC1* and *SMC3 (Structural Maintenance of Chromosomes 1* and *3)* in a screen for mutants that could separate the sister chromatids in the absence of APC/C activity (Michaelis *et al*., 1997). A follow-up screen for mutants able to separate sister chromatids in the absence of anaphase inhibitor Pds1 (Funabiki *et al*., 1996; Cohen-Fix *et al*., 1996) added *Scc3* and several other genes, including *Eco1 (Establishment of cohesion)* (Skibbens *et al*., 1999; Toth *et al*., 1999). Since all these proteins are involved in the generation of the cohesive force required to withstand the pulling forces of the mitotic spindle, this group of proteins were named "cohesin". Immunopurification experiments performed in *Xenopus laevis* egg extracts have shown that Smc1, Smc3, Rad21 (the ortholog of Scc1) and SA1 and SA2 (two different orthologs of Scc3) form a stable protein complex, and therefore named as "core cohesin complex" (Losada *et al*., 1998; Toth *et al.,* 1999; Losada *et al*., 2000; Sumara *et al*., 2000). Cohesin homologs have been found in all eukaryotic species studied today, indicating that the function of this complex in the process of sister-chromatid cohesion has been highly conserved throughout the evolution.

In *S. cerevisiae,* all components of the core cohesin complex are associated with DNA from S-phase until the onset of anaphase, where cohesin`s dissociation from DNA leads to the segregation of sister chromatids towards opposite spindle poles (Toth *et al*., 1999). Remarkably, it was found that cohesin`s dissociation from DNA coincides with and depends on the proteolytic cleavage of Scc1 subunit by a site-specific thiol protease Esp1 (Extra Spindle Pole Bodies), also called separase (Uhlmann *et al*., 1999; Uhlmann *et al*., 2000). Experiments, in which the original separase-cleavage sites of Scc1 were replaced by cleavage

sites recognised by the exogenous site-specific Tobacco Etch mosaic Virus (TEV) protease, demonstrated that artificial cleavage of Scc1 is sufficient to initiate anaphase (Uhlmann *et al*., 2000; Oliveira *et al*., 2010; Tachibana-Konwalski *et al.,* 2010).

1.2.2. The structure of the cohesin complex

Having discovered the key players required for proper chromosome segregation, the immediate questions to be addressed regarded the structure of the cohesin complex and the manner in which it performs its function of holding sister chromatids together.

The cohesin complex is comprised of four subunits: Smc1, Smc3, Scc1 and Scc3 (Figure 1-4). Two of the cohesin subunits, Smc1 and Smc3, are members of a structurally related family of proteins, called Structural Maintenance of Chromosome (SMC) proteins. Their names reflect their fundamental roles in multiple aspects of chromosome metabolism. In eukaryotes, six different SMC proteins form the cores of three discrete complexes. Smc1 and Smc3 together with two non-Smc proteins form the cohesin complex; the Smc2 and Smc4 proteins are involved in the assembly of the condensin complex, necessary for mitotic chromosome structure. Finally, the Smc5 and Smc6 proteins are the main subunits of a yet unnamed complex that has crucial roles in DNA repair and recombination (reviewed in Nasmyth and Haering, 2005).

Both Smc1 and Smc3 subunits contain an N- and a C-terminal globular nucleotide binding domain. SMCs fold back on themselves at the level of a central "hinge" domain, forming 50nm long, rod-shaped molecules, having intra-molecular antiparallel coiled-coils that connect the hinge to the NBDs. This brings N- and C-terminal globular domains in close proximity to each other, building an ABC (ATP binding cassette)-like ATPase "head" domain (Melby *et al*., 1998; Haering *et al*., 2002; reviewed in Hirano, 2006). The folded Smc1 and

Smc3 proteins interact with each other at their hinge domains creating a large V-shaped molecule, which has been observed by electron microscopic analysis of purified cohesin complexes (Figure 1-4, Anderson *et al*., 2002).

While each Smc NBD is constructed from two halves, one from N-terminal and the other from C-terminal, the hinge domain is encoded by amino acids from the center of the polypeptide. The interaction at the hinge interface of Smc1 and Smc3 is mainly hydrophobic and tight, with low nanomolar dissociation constant (K_D). The crystal structure of a homodimeric bacterial hinge domain from *Thermotoga maritima,* and the crystal structure of a Smc1/Smc3 hinge heterodimer complex from *Mus musculus* revealed that the hinge dimer is a doughnut shaped protein containing two interacting interfaces, with a channel in the middle that is lined by several positively charged amino acid residues (Kurze *et al*., 2011; reviewed in Nasmyth and Haering, 2009). Each interaction surface is sufficient for dimerization and required to build stable sister chromatid cohesion (Mishra *et al*., 2010).

The crystal structure of the *Thermotoga maritima* SMC head showed that while the N-terminal portion of the SMC protein contributes the Walker A motif, the C terminal part comprises of a Walker B and ABC signature motifs, generating an ABC-like ATPase domain (Lowe *et al*., 2001). The ATPase head domains of an SMC dimer sandwich ATP in order to interact with each other (Hopfner *et al*., 2000). Mutagenesis of highly conserved Walker B glutamate residues prevents the hydrolysis of ATP at either site. Cohesin complexes containing such mutations cannot associate with chromatin correctly or build sister chromatid cohesion (Arumugam *et al*., 2003; Weitzer *et al*., 2003).

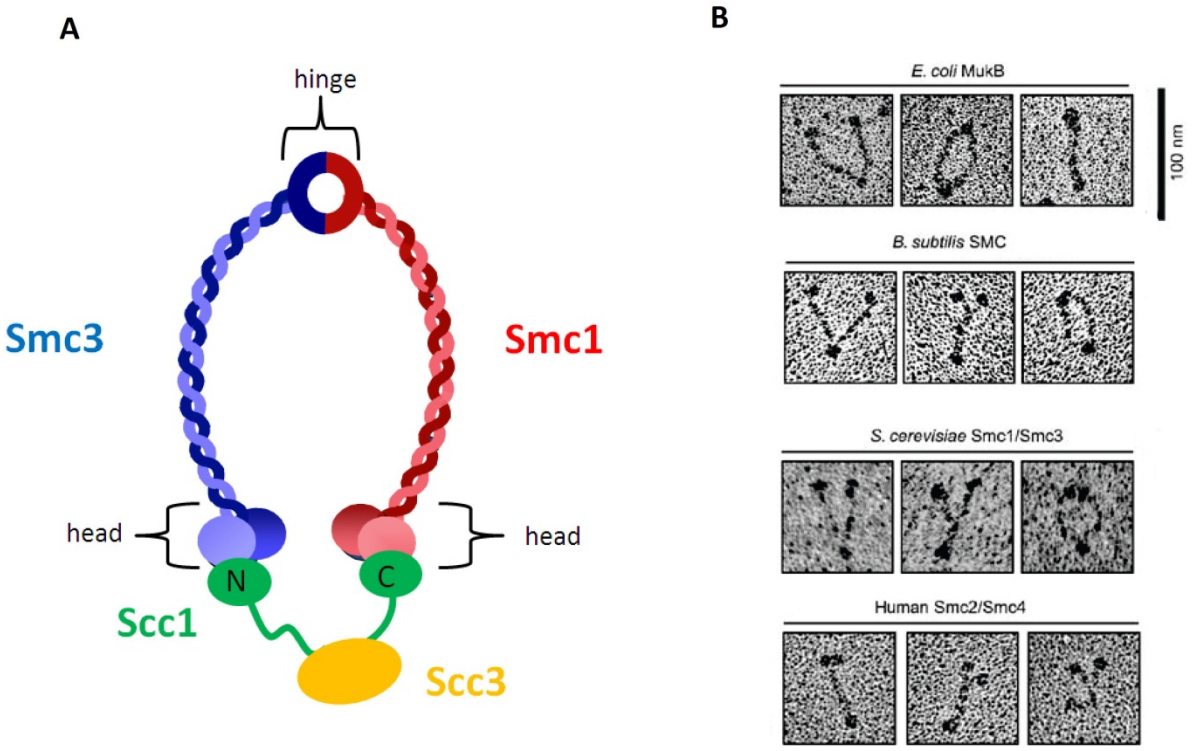

Figure 1-4: Cohesin is a large ring-shaped protein complex

(A) The four core cohesin subunits Smc1, Smc3, Scc1 and Scc3 are shown (adapted from Nasmyth and Haering, 2005).

(B) Electron micrographs show soluble cohesin complexes from different species (reproduced from Melby *et al.*, 1998; Haering *et al*., 2002; Anderson *et al*., 2002).

While ATP-binding and hydrolysis has been suggested to trigger a conformational change promoting association or dissociation of the two ATPase heads according to a very similarly structured DNA repair protein Rad50, a stable Smc1/3 head-head interaction *in vivo* requires the binding of an additional protein Scc1 (Haering *et al*., 2002; Gruber et al, 2003; reviewed in Hopfner and Tainer, 2003; Arumugam *et al*., 2006). Binding of the N-and C-terminal domains of Scc1 to the Smc3 and Smc1 ATPase heads, respectively, results in the formation of a large tripartite ring structure with a diameter of at least 40 nm that can be observed under electron microscopy (Haering *et al*., 2002; Anderson *et al*., 2002). Interaction between the ATPase head domain of Smc1 and the C-terminal region of Scc1 was also verified by X-ray crystallography (Haering *et al*., 2004). Both domains of Scc1 are found in members of the so-called kleisin family of proteins. This family includes subgroups, comprised of SMC-interacting proteins, where orthologs of Scc1 actually belongs to the α-kleisins.

Little is known about the fourth subunit of core cohesin complex, Scc3. It was shown that Scc3 interacts with the tripartite ring by binding to a region adjacent to the carboxy-terminal Smc1-binding domain of Scc1 (Haering *et al*., 2002). Although Scc3 is not a part of the ring structure, it was purified together with Scc1/Smc1/Smc3 complex in a stoichiometric manner (Losada *et al*., 2000; Sumara *et al*., 2000).

1.2.3. Cohesin loading onto chromatin

Association of cohesin with chromatin at all sites within the genome depends on the activity of the so-called cohesin loading factor Scc2/Scc4, identified in all eukaryotes examined so far (Ciosk *et al.,* 2000; reviewed in Nasmyth and Haering, 2009). Scc2 is a large and highly conserved HEAT-repeat protein and a member of Scc2/Nipped-B family (Neuwald and Hirano, 2000). The less-conserved Scc4 is composed of TPR (tetratricopeptide) repeats,

which are similar to HEAT-repeats and are thought to be involved in protein-protein interactions (Watrin *et al*., 2006).

In *S.cerevisiae*, cohesin`s loading onto chromatin takes place in late G1/just before S phase, when α-kleisin Scc1`s synthesis is initiated (Michaelis *et al*., 1997; Ciosk *et al*., 2000), while in metazoa cohesin loading starts already in telophase of the previous cell cycle (Warren *et al*., 2000; Gerlich *et al*., 2006). There is accumulating evidence that cohesin`s association with chromosomes requires additional factors, other than Scc2/4 complex. It has been shown that in egg extracts from *Xenopus laevis*, the presence of the pre-replication complexes (pre-RC) is required for the recruitment of Scc2/Scc4 and therefore cohesin to the DNA (Takahashi *et al*., 2004; Gillespie and Hirano, 2004). Cdc7/Drf1 kinase (DDK) has been identified as the key player that mediates the interaction between Scc2/Scc4 and pre-RCs in *Xenopus* (Takahashi *et al*., 2008). However, in *S. cerevisiae*, pre-RCs do not seem to be required for recruiting cohesin to the DNA since cohesin still associates with the DNA in the absence of DNA replication when the Cdc6 component of preRC is depleted (Uhlmann and Nasmyth, 1998).

Loading of cohesin onto chromatin is not only limited to postmitotic or G1 cells. In yeast, cohesin has been shown to associate with chromosomes when the Scc1 subunit is expressed after S phase (Uhlmann and Nasmyth, 1998; Ocampo-Hafalla *et al.*, 2007). The question of how cohesin is loaded onto the DNA by Scc2/Scc4 complex is still waiting to be addressed. Based on the ring model for cohesion, the Scc2/Scc4 complex may function by promoting the entrapment of chromatin fibers by cohesin. Scc2/Scc4 has been anticipated to act by regulating the ATPase activity of SMC heads, where ATP hydrolysis is required for cohesin`s stable association with DNA (Weitzer *et al*., 2003). Although the manner in which the ATP hydrolysis assists cohesin loading onto the DNA is still unknown, the energy release from ATP hydrolysis is thought to be capable of opening the cohesin ring such that the DNA can

pass through. Studies from Gruber *et al*., 2006 have suggested that cohesin`s loading onto DNA involves opening of the hinge domain, which acts as the entry gate for the DNA into the cohesin ring. This finding was based on experiments in yeast, where cohesin`s hinge domains are conditionally locked by fusing them to FRB and FKBP12 proteins, which form a complex upon addition of the drug rapamycin. Rapamycin addition prior to replication locks the modified hinges and reduces cohesin's association with the DNA, thereby preventing the establishment of cohesion. However, locking the hinge after replication did not affect the establishment or maintenance of cohesion (Gruber et al., 2006).

1.2.4. Establishment and maintenance of cohesin

Although loading of cohesin onto the chromosomes can take place during the entire cell cycle, cohesion establishment in an unperturbed cell cycle is limited to S-phase (Uhlmann and Nasmyth, 1998; Haering *et al*., 2004). An evolutionarily conserved protein called Eco1 (establishment of cohesin protein 1) mediates this process (Uhlmann and Nasmyth, 1998; Toth *et al*., 1999; Skibbens *et al*., 1999; Lengronne *et al*., 2006). Orthologs of Eco1 are encoded by most but not all eukaryotic organisms (reviwed in Nasmyth and Haering, 2005). Humans contain two related orthologs, Esco1 and Esco2; mutations in *Esco2* have been shown to be causative for the Roberts/SCphocomelia (RBS/SC) syndrome (Vega *et al*., 2005; Schule *et al*., 2005). Cells from RBS/SC patients show clear defects in chromosome segregation (reviewed in Dorsett, 2007).

It had been known from *in vitro* studies that Eco1 possess an acetyl-transferase activity (Ivanov *et al*., 2002). The two conserved lysine residues, K112 and K113, on the upper surface of Smc3's NBD were identified as the targets of Eco1-mediated acetylation (Ben-Shahar *et al*., 2008; Unal *et al*., 2008; Zhang *et al*., 2008; Rowland *et al*., 2009). Mutating both residues into arginines, that mimic un-acetylated lysines, results in cell death due to

cohesin defects. Acetylation of Smc3 was found to be essential for establishment of sister chromatid cohesion and tightly regulated during the cell cycle, where it increases as cells undergo DNA replication in S phase and then starts to decrease as they enter anaphase (Ben-Shahar *et al*., 2008; Beckouet *et al*., 2010). Although it has been suggested that replication-coupled acetylation is due to the recruitment of Eco1 to the replication forks by binding to PCNA (proliferating cell nuclear antigen) polymerase clamps (Moldovan *et al*., 2006), there is no convincing evidence that this occurs *in vivo* at the moment. Strikingly however, the positively charged residues within the hinge interface were shown to be required for efficient acetylation of Smc3`s NBD and therefore cohesion establishment, indicating that transient hinge opening may be involved in the acetylation process facilitating the entrapment of sister chromatids during DNA replication. (Kurze *et al*., 2011).

Not much is known on how acetylation of Smc3 contributes to cohesion establishment. This modification could either allow the entrapment of sister DNAs within cohesin rings, or stabilize such structures after they have been produced. In yeast, cleavage of Scc1 at the onset of anaphase triggers the deacetylation of Smc3, which is dependent on a histone deacetylase called Hos1(Beckouet *et al*., 2010; Borges *et al*., 2010; Xiong *et al*., 2010). The fact that Smc3 acetylation persists between DNA replication and anaphase, and overexpression of Hos1 in M-phase induces Smc3 deacetylation accompanied by a loss of sister chromatid cohesion raise the possibility that acetylation of Smc3`s NBD might have the role of locking cohesin rings shut in order to keep sister DNAs permanently entrapped within the cohesin ring (Beckouet *et al*., 2010).

Apart from Smc3, three additional proteins, Scc3, Pds5 and Rad61 (the yeast ortholog of human Wapl (wings apart-like), seemed to be involed in regulating sister chromatid cohesion, as suppressor mutations wihtin the genes encoding Scc3, Pds5 and Rad61 were found to suppress the lethality of *Eco1* mutants in yeast (Ben-Shahar *et al*., 2008; Rowland *et al*.,

2009). Suprisingly, all three proteins were found to form a complex *in vitro,* which is recruited to the core cohesin complex via an interaction with the Scc1 subunit (Rowland *et al*., 2009). In human cells, a stable complex has also been observed to form between Wapl, Scc1, SA1 and Pds5A (a specific form of Pds5 protein that has been predicted to have a role in arm cohesion) (Gandhi *et al*., 2006; Kueng *et al*., 2006).

Pds5 (precocious dissociation of sisters) is a HEAT-repeat containing protein conserved from fungi to vertebrates, and required for establishment and maintenance of cohesion (Hartman *et al*., 2000; Panizza *et al*., 2000). It is recruited by cohesin to chromosomes, where it binds to the same sites as cohesin (Hartman *et al*., 2000; Lengronne *et al*., 2004). Although Pds5`s role in the maintenance of cohesion is well established, the function of Rad61/Wapl is still under debate. Very different phenotypes were observed by inactivating Rad61 in yeast and Wapl in human cells. Depletion of Wapl by RNA interference (RNAi) in HeLa cells blocks cohesin`s dissociation from chromosomes during the early stages of mitosis, indicating that Wapl promotes a separase-independent way of removing cohesin from the DNA (Gandhi *et al*., 2006; Kueng *et al*., 2006). In contrast to what has been shown in HeLa cells, in *S.cerevisiae*, Rad61 does not reduce cohesin`s association with chromosomes (Rowland *et al*., 2009; Sutani et al., 2009). In fact, in the yeast strains where *Rad61* has been deleted the amount of cohesin associated with chromatin was found to be decreased. Nevertheless, it is still possible that these orthologs function in a similar way since they both form stable stoichiometric complexes with Pds5 (Gandhi *et al*., 2006; Kueng *et al*., 2006; Rowland *et al*., 2009). Their state of modification and the cell cycle stage that they are in may affect whether they promote or reduce association of cohesin with chromosomes.

In animal cells, DNA replication and acetylation during S-phase promotes the recruitment of one further protein called Sororin, which seems to be required for maintaining cohesion during G2- and M-phases (Rankin *et al*., 2005; Schmitz *et al*., 2007; Lafont *et al*., 2010;

Nishiyama *et al*., 2010). It has been proposed that Sororin displaces Wapl from its binding partner Pds5, but not from cohesin, by causing a reorganization in the topology of these cohesin-associated proteins. These changes are thought to inhibit Wapl's ability to dissociate cohesin from DNA, and that the resulting stable interaction of cohesin with DNA enables cohesin to mediate cohesion (Nishiyama *et al*., 2010). Sororin orthologs have yet to be identified in yeast, but it is likely that cohesion establishment in yeast requires equivalent conformational changes in the properties of cohesin. The current proposed model regarding cohesion establishment and maintenance in yeast is that while the complex of Scc3, Pds5 and Rad61/Wapl promotes maintenance of cohesion by preventing the ring opening, acetylation of Smc3`s NBD by Eco1 temporarily inhibits the "anti-establishment" or "maintenance" function of Rad61/Wapl, Pds5 and Scc3 in S phase and thereby promotes cohesion establishment (Rowland *et al.,* 2009).

Despite all the recent findings in cohesion establishment, how chromatin-bound cohesin is converted to cohesion during DNA replication is unknown. Eco1 is known to interact with the DNA processivity factor PCNA *in vitro*, and Ctf4 and Ctf18, which are components of the clamp loader Replication Factor C (RF-C), suggesting a link between DNA replication and cohesion establishment (Hanna *et al*., 2001; Mayer *et al*., 2001; Lengronne *et al*., 2006; Moldovan *et al*., 2006). The cohesin rings associated with chromatin may be converted at/by replication forks into rings that entrap sister DNA. According to one model, this could happen by passing the replication machinery through the cohesin ring. Or in an alternative model, it has been proposed that transient ring opening without dissociating from chromatin, which might be triggered by Eco-1 mediated acetylation of Smc3, could allow the replication fork passage and thereby entrapment of both sister DNAs.

Establishment of cohesion is normally limited to S-phase in undamaged cells (Uhlmann and Nasmyth, 1998). Recent studies in budding yeast have shown that cohesion can also be

generated by an Eco1- and Scc2/Scc4- dependent but replication-independent mechanism in response to double strand breaks (DSBs) in G2/M phase (Strom *et al*., 2007; Unal *et al*., 2007). The findings that genome-wide cohesion can also be generated by overexpression of Eco1 in G2/M cells in the absence of DSBs, and that Eco1-mediated acetylation of Scc1 is responsible in establishing cohesion upon DSB induction (Heidinger-Pauli *et al*., 2008; Heidinger-Pauli *et al*., 2009), suggest that Eco1 does not have only important roles in S-phase but also during DSB-induced cohesion generation.

1.2.5. Cohesin`s dissociation from chromosomes

In budding yeast cohesion between sister chromatids is lost at the onset of anaphase, when the α-kleisin subunit Scc1 is cleaved by separase resulting in sister chromatid separation (Uhlmann *et al*., 1999; Uhlmann *et al*., 2000). In vertebrates, however, the majority of cohesin was observed to dissociate from chromosome arms already in prophase, independent from Scc1`s cleavage (Losada *et al*., 1998; Sumara *et al*., 2000; Waizenegger *et al*., 2000). This process, called "the prophase dissociation pathway", requires activity of the Wapl protein (Kueng *et al*., 2006; Gandhi *et al*., 2006) and phosphorylation of the Scc3/SA subunit of the cohesin complex by Polo-like kinase 1 (Plk1)/Aurora B (Losada *et al*., 2002; Sumara *et al*., 2002; Hauf *et al*., 2005). The remaining cohesin still holds sister centromeres together until metaphase and its cleavage triggers the loss of sister chromatid cohesion (Hauf *et al*., 2001). Centromeric cohesin is protected from dissociation by a protein called shugoshin (Sgo). Sgo1 is mostly localized at kinetochores in a Bub1 and Aurora B dependent mechanism (McGuinness *et al*., 2005; Salic *et al*., 2004) , and stably associates with PP2A (protein phosphatase 2 A) which counteracts phosphorylation of Scc1 and SA2/Scc3, thereby maintaining cohesion at centromeres (Kitajima *et al*., 2005; Kitajima *et al*., 2006; Riedel *et al*., 2006). The exact mechanism of how cohesin is removed from chromosome arms by the

prophase pathway is still not understood. One thing which is clear is that the remaining small fraction of cohesin on chromosomes after prophase is sufficient to oppose the spindle forces. Since the large soluble pool of cohesin generated by the prophase pathway has not undergone separase cleavage at the metaphase-to-anaphase transition and it reassociates with chromosomes as soon as cells exit mitosis (Waizenegger *et al*., 2000), it has been suggested that this pool of cohesin could have important functions other than holding sister chromatids together by regulating transcription and chromatin structure during interphase (reviewed in Peters, Tedeschi and Schmitz, 2008).

Since the destruction of cohesin by the proteolytic cleavage of Scc1 is not reversible in anaphase, any mistakes made in the attachments of sister kinectochores cannot be corrected afterwards. Therefore, the timing of anaphase is controlled by the spindle assembly checkpoint (SAC), which monitors the attachment of sister chromatids to the spindle and allows anaphase to occur only after bi-orientation was achieved. During prometaphase, incorrectly attached kinetochores generate an inhibitory signal that blocks APC/C-Cdc20 activity, and thereby securin destruction and sister chromatid separation. In the presence of such spindle defects, the spindle checkpoint component Mad2 (mitotic arrest deficient 2) associates tightly with Cdc20 and inhibits its funtion as an APC/C activator, which keeps the SAC active. Once all chromosomes have properly bi-oriented at the metaphase plate, Mad2 dissociates from Cdc20 which turns on the APC/C activity and inactivates SAC system (De Antoni *et al*., 2005; Mapelli *et al*., 2006; reviewed in Musacchio and Salmon, 2007) .

During mitosis, phosphorylation of separase protein Esp1/Cut1(extra spindle poles protein 1;cell ultimately torn protein 1) by Cdk1 induces stable binding of cyclin B/Cdk1, which inactivates the protease (Stemmann *et al*., 2001; Gorr *et al*., 2005). Securin/Pds1 (premature dissociation of sisters) is a regulatory chaperone that binds to separase keeping it also inactive for most of the cell cycle. Separase is only fully activated when all chromosomes have

completed bi-orientation, which triggers the activation of APC/C-Cdc20. Cyclin B and securin/Pds1 are then recruited by Cdc20 to the APC/C-Cdc20, leading to their ubiquitylation and subsequent proteolysis. Upon liberation from securin and cyclin, separase gets activated and cleaves the Scc1 subunit of cohesin, which leads to dissociation of the cohesin complex from chromatin, resulting in sister chromatid separation (Uhlmann *et al*., 1999).

In budding yeast, there is one exception known in which cleavage of Scc1 does not trigger separation of the genomic loci. Due to high rates of transcription, tandem rDNA repeats on chromosome XII are held together via a poorly understood cohesin- independent mechanism, which might require intercatenation (Sullivan *et al*., 2004). A different mechanism, possibly DNA decatenation, must trigger dissolution of sister rDNAs.

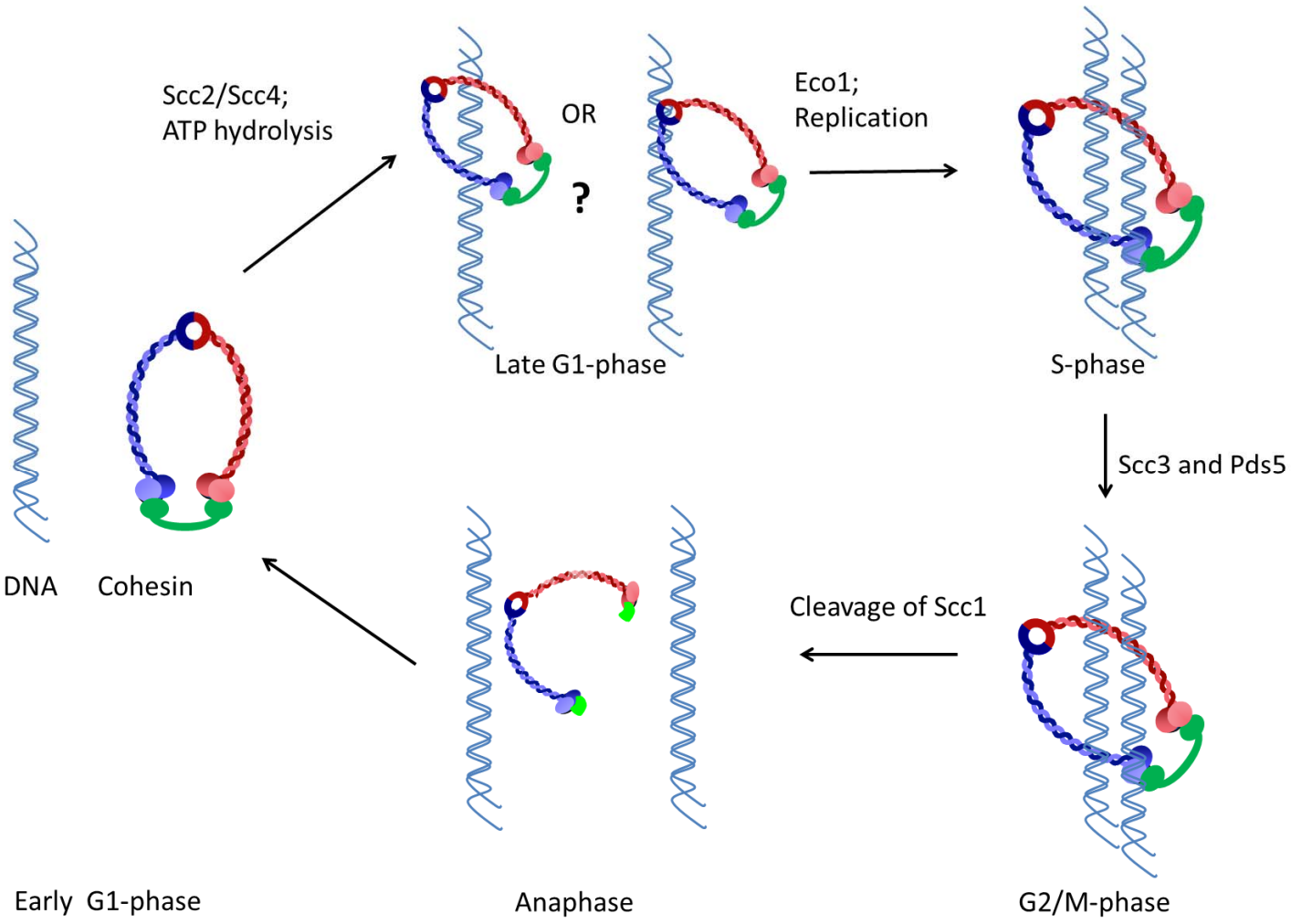

Figure 1-5: An overview of the cohesin cycle in yeast

Association of cohesin with chromatin takes place in late G1, assisted by Scc2/Scc4 complex and ATP hydrolysis. At this stage whether cohesin entraps unreplicated chromatin into its ring is unknown. During replication, cohesion is established by Eco1, and Scc3 and Pds5 support the maintenance of cohesion during G2/M-phase. All chromosome associated cohesin is cleaved by separase at the onset of anaphase.

1.3. Distribution of cohesin

Genome-wide cohesin mapping studies performed in budding yeast through chromatin immunoprecipitation followed by hybridization to DNA microarrays (ChIP-CHIP) has provided evidence that cohesin binds to DNA approximately every 11 kbp, and is being almost exclusively located between convergently transcribed genes (Glynn *et al*., 2004; Lengronne *et al*., 2004). These arm sites are so-called cohesin-associated regions (CARs), mainly comprised of A-T rich DNA sequences without having any common nucleotide sequence motif (Laloraya *et al*., 2000). Cohesin has also been shown to accumulate predominantly around centromeres (spanning 20-50kbp around centromere), which is dependent on the presence of kinetochore proteins and 125bp centromeric DNA sequence (Megee *et al*., 1999; Tanaka *et al*., 1999; Weber *et al*., 2004). Cohesin`s association with the centromere-flanking region of a minichromosome was reduced upon centromere excision in cells arrested in metaphase (Megee *et al*., 1999). Furthermore, even when the centromere was moved to an ectopic location, e.g. arm locus, it has been observed that kinetochores are still able to mediate increased cohesin association over a broad chromatin region, indicating that cohesin might slide laterally along the DNA (Weber *et al*., 2004; Hu *et al.,* 2010). Based on this "sliding cohesin ring model", it has also been proposed that once cohesin is loaded onto the DNA, it is moved by transcribing RNA polymerases to sites of convergent transcription. Indeed, changes in transcription in CAR or near the centromere sequence have the ability to remove cohesin from these and neighbouring sites (Tanaka *et al*., 1999; Glynn *et al*., 2004; Lengronne *et al*., 2004). Moreover, the distribution of the cohesin loading factor Scc2/Scc4 was found to be different from cohesin`s localisation pattern (Lengronne *et al*., 2004; Hu *et al.,* 2010). According to ChIP-CHIP data analysis, while cohesin is initially associated with Scc2 binding sites, it then progressively repositions to the regions between convergently

transcribed genes (Lengronne *et al*., 2004; Hu *et al.,* 2010). Consistent with a sliding ring model, repositioning of cohesin does not seem to require the continuous activity of the Scc2/Scc4 complex (Bausch *et al*., 2007). However, the idea that cohesin complexes are pushed along the DNA fiber by the elongating RNA polymerase and therefore accumulate in the regions of convergent transcription has been challenged by the finding that no cohesin enrichment is being detected at the 3' ends of several induced genes, which would be indicative of sliding. This suggests that the cohesin ring may also be disassembled (Bausch *et al*., 2007).

Cohesin rings with mutant NBDs that can bind but not hydrolyse ATP (Arumugam *et al*., 2003) have recently been shown to accumulate at core centromeres at very high levels. Binding of ATP hydrolysis-defective cohesin rings to core centromeres is very unstable and dependent on the activity of Scc2/Scc4 complex. This suggests that mutant cohesin complexes can initiate the loading reaction, which is hydrolysis independent but then fail to entrap sister chromatids, which is a process dependent on the energy provided by ATP hydrolysis (Hu *et al*., 2010). This finding is therefore consistent with the notion that cohesin is first loaded onto the core centromeres and then relocates into neighbouring sequences.

Distribution of cohesin in *S.pombe* is similar to the one in *S.cerevisiae*, cohesin being concentrated at the centromeres and at the regions between convergently transcribed genes (Lengronne *et al*., 2004). Cohesin is recruited to the centromeres in a manner dependent on the Mis4/Ss13 (Scc2/Scc4 homologs in fission yeast) loading complex activity, and its binding to chromatid is mediated through an interaction between Psc3 (Scc3 homolog in fission yeast) and the heterochromatic protein Swi6/HP1 (Bernard *et al*., 2001; Bernard *et al*., 2008; Nonaka *et al*., 2002). Swi6 is required for association of cohesin with centromeres but not with chromosome arms, indicating that Swi6 acts to distinguish cohesion at centromere from cohesin along chromosome arms (Bernard *et al*., 2001). Bi-directional transcription of

repetitive sequences and retroposons resulting in production of double-stranded RNAs is required for Swi6 recruitment to heterochromatin. These RNAs are processed by the RNAi-machinery promoting the methylation of H3K9 (trimethylated lysine 9 on histone H3), thereby providing a binding site for Swi6/HP1 (reviewed in Verdel and Moazed, 2005).

Results from Gullerova *et al*. in fission yeast have provided new insights into a function of cohesin accumulation between convergent genes. The study indicates that the mechanism of double-stranded RNA-induced recruitment of cohesin at centromeres is also responsible for the enrichment of cohesin at sites of convergent transcription (Gullerova and Proudfoot, 2008). Read-through transcription of convergent gene pairs during G1 was proposed to cause the formation of double-stranded RNAs. This leads to activation of the RNAi pathway, which in turn causes the transient formation of heterochromatin. The classical marks of heterochromatin, trimethylation of H3K9 and binding of Swi6 protein, can then be detected in convergently transcribed gene pairs during G1-phase. Consistent with earlier observations (Bernard et al., 2001; Nonaka et al., 2002), deletion of Swi6 led to a decrease in cohesin binding of these regions during G2-phase, and similarly to a deletion of Scc1, a dramatic increase in read-through transcripts. Moreover, removal of the component of RNAi pathway caused read-through transcription during G2-phase. These results suggest that accumulation of cohesin between convergently transcribed genes during G1 due to the heterochromatin formation prevents read-through transcription during G2, indicating that apart from the centromere, cohesin can also be recruited to other genomic regions through double-stranded RNA-induced heterochromatin formation.

In contrast to fission yeast, budding yeast does not have the RNAi pathway and heterochromatin marks (H3K9 trimethylation and Swi6/HP1). However, it is likely that an alternative mechanism exists in *S.cerevisiase* since cohesin also accumulates at sites of convergent transcription in this eukaryote. A different type of heterochromatin proteins, Sir

(silent information regulator) proteins, might be good candidates to mediate cohesin targeting at sites of convergently transcribed genes since they also mediate silencing and are involved in targeting cohesin to the silent mating type locus *HMR (Hidden MAT Right)* in budding yeast (Chang *et al*., 2005). Cohesion establishment at this locus was also found to depend on silencing and a presence of a tRNA gene (Dubey and Gartenberg, 2007).

Recent genome-wide ChIP maps in fly and mammalian cell lines show that the pattern of cohesin on chromosomes appears to be different from that in yeast. Cohesin was found to localize at intergenic sites and actively transcribed genes, and unlike in yeast no accumulation is observed between convergent genes (Parelho *et al*., 2008; Wendt *et al*., 2008; Misulovin *et al*., 2008). Moreover, *Drosophila* loading factor Nipped-B was observed to display a distribution pattern very similar to that of cohesin (Misulovin *et al*., 2008). Surprisingly, in mammalian cell lines a strong similarity was found between the genomic distribution of cohesin and CTCF (CCCTC binding factor), which is a highly conserved sequence-specific zing-finger DNA binding protein required for transcriptional gene insulation (Parelho *et al*., 2008; Wendt *et al*., 2008; Stedman *et al*.,2008; Rubio *et al*., 2008). Unlike in yeast or flies, cohesin also prefers to bind a GC-rich consensus sequence in mammalian cells. Although a direct physical interaction could not be demonstrated between cohesin and CTCF, knockdown of CTCF extensively reduced the association of cohesin to CTCF binding sites, but not the amount of chromatin-bound cohesin, suggesting that cohesin`s positioning at CTCF sites throughout the genome is dependent on the CTCF protein (Wendt *et al*., 2008). Depletion of CTCF did not lead to any mitotic defects, indicating that sister chromatid cohesion was not affected. Moreover, knockdown of the Scc1/Rad21 cohesin subunit had no effect on CTCF binding (Parelho *et al*., 2008).

1.4. Non-canonical functions of cohesin

1.4.1. Cohesin in DNA repair

Studies in yeast and vertebrate cells have provided the first indications that cohesin plays a role in the repair of DNA-DSBs during mitosis and meiosis (Sjoergen and Nasmyth, 2001; Klein *et al*.,, 1999). While Scc1/Rad21 mutants were defective in repairing DNA damages when they are exposed to γ-irradiation, absence of Rec8 (Recombination 8; meiosis-specific cohesin subunit) protein led to defects in recombination between homologous chromosomes in *S.pombe* (Birkenbihl and Subramani, 1992). Cohesin`s involvement in DSB repair was later noticed by the observation that upon induction of DSBs in S- and G2- phase cells the amount of cohesin associated with DNA was highly increased at the lesion sites as well as covering the regions of 50-100kbp adjacent of the damaged DNA (Unal *et al*., 2004; Strom *et al*., 2004). Cohesin was found to assist DSB repair by homologous recombination, which is active during S- and G2-phases and repairs damaged chromosomes using the sister chromatid as a template, instead of promoting repair by non-homologous end joining, which operates during G1-phase in the absence of a sister chromatid. *De novo* generation of sister chromatid cohesion in G2-phase has been shown to be required for an efficient DSB repair. It has been observed that DNA repair was impaired when Scc2/Scc4 and Eco1 proteins are inactived in G2-phase, indicating that only newly recuited cohesion-generating cohesin is able to promote DSB repair (Unal *et al*., 2004; Strom *et al*., 2004). Cleavage of pre-existing cohesin complexes by separase has also been suggested to be required for efficient DSB repair (Nagao *et al*., 2004). As opposed to S-phase induced cohesion, which requires acetylation of Smc3 by Eco1, it has been suggested that G2-phase DSB-induced cohesion is mediated through the acetylation of Scc1 by Eco1 (Heidinger-Pauli *et al*., 2009). Moreover, generation of cohesion in response DSBs has been shown to trigger a genome-wide cohesin

establishment independent of the lesion site in an Eco1 dependent manner in G2-phase (Unal *et al*., 2007). In addition to Scc2/Scc4, Eco1 and cohesin`s recruitment at the DSBs, a colloboration with Smc5/6 heterodimer is also necessary to promote recombination-mediated DNA repair (Potts *et al*., 2006).

In addition to its role in DSB repair in G2-phase, cohesin has also been suggested to be involved in the DNA-damage response/signalling pathway, due to the phosphorylation of Smc1 by ATM or ATR (ataxia telangiectasia mutated or ATM related). ATM and ATR are DNA damage signalling kinases required for the activation of S-phase checkpoint upon ionising radiation (reviewed in Watrin and Peters, 2006).

1.4.2. Cohesin and gene regulation

In addition to its roles in sister chromatid cohesion and post-replicative double-strand break repair, cohesin seems to be involved in the regulation of gene expression. Studies in yeast have shown that cohesin has a role in restricting the spread of heterochromatin formation and regulate transcriptional termination. In *S. cerevisiae,* cohesin is known to regulate establishment and extent of the silenced domain at the silent mating type locus *HMR.* Formation of boundary elements in the *HMR* mating cassette was impaired at the restrictive temperature in temperature-sensitive *smc1* and *smc3* mutants, resulting in heterochromatin spreading beyond its normal limits into neighbouring regions (Donze *et al*., 1999). Furthermore, mapping studies have later shown that cohesin binds to the *HMR* locus (Blat and Kleckner, 1999; Laloraya *et al*., 2000; Lengronne *et al*., 2004). Full repression of the *HMR* locus is mediated by the cleavage of α-kleisin subunit Scc1 during the previous mitosis (Lau *et al*., 2002). Cohesin's association with this region is dependent on Sir proteins, which mediate silencing in yeast (Chang *et al*., 2005).

As described in Chapter 1.3., studies in fission yeast have indicated that accumulation of cohesin at sites of convergently transcribed genes prevents the generation of double-stranded RNAs from these regions, and therefore inhibits heterochromatin formation (Gullerova and Proudfoot, 2008). Cohesin might promote transcript termination by creating a boundary to block the passage of RNA Polymerase II. These results illustrate that cohesin appears to have important roles in regulating the structure of chromatin through creating boundaries, which in turn prevents heterochromatin spreading.

In metazoans, the implications, that cohesin has a function in regulating gene expression, has derived from the findings that Nipped-B (the ortholog of Scc2 in fly) and Pds5 were found to control gene expression in *D.melanogaster*. Mutations in *Nipped-B* have shown to reduce gene expression of *cut* gene by preventing long-range promoter-enhancer communications at the *cut* and *Ubx* loci (Rollins *et al*., 1999). Interestingly, depletion of cohesin was later on found to result in an increase in the *cut* gene expression. This indicates that while Nipped-B promotes the interaction between promoter and enhancers, cohesin inhibits their communication by acting as a repressor (Rollins *et al*., 2004).

As opposed to yeast where the role of cohesin in gene regulation appears to be linked to the cell cycle, studies in *Drosophila* have provided the evidence that cohesin can control transcription in noncycling cells. A transposon insertion screen identified two cohesin subunits, Smc1 and Scc3/SA, as important factors for neuronal development whose absence affect axon patterning of mushroom body γ- neurons (Schuldiner *et al*., 2007). The ecdysone hormone receptor is directly involved in the regulation of genes required for neuronal development. It has been shown that while expression of *EcR-B1* (ecdysone B-receptor) gene decreases in the absence of functional Smc1, overexpression of EcR-B1 protein partially rescues the neuronal defects caused by the absence or mutations in cohesin subunits, indicating that cohesin may be involved in the control of neuronal patterning via the

regulation of EcR-B1 expression (Schuldiner *et al*., 2007). A separate study performed by Pauli *et al.* using transgenic flies expressing a TEV-cleavable version of Scc1/Rad21 has also showed that cohesin ring could be destroyed in specific tissues or developmental times by TEV protease-induced cleavage of Scc1/Rad21 (Pauli *et al*., 2008). Cleavage of cohesin has been demonstrated to cause defects in axonal pruning in non-dividing cells, indicating that cohesin has a role in the removal of axon projections. Subsequent studies using a temperature-sensitive system to induce TEV protease have showed that within four hours, inactivation of cohesin leads to changes in the expression of cohesin-binding genes in the ecdysone steroid hormone pathway. Specifically, TEV-induced cleavage of Scc1 caused a decrease in transcription of the Ecdysone-inducible *Eip74EF* locus in *Drosophila* salivary glands, providing evidence for a direct role in gene regulation (Pauli *et al*., 2010).

Identification of cohesin`s genome wide distribution in mammalian cells has also indicated that cohesin plays additional roles other than holding sister chromatids together. Several studies demontrate that the cohesin complex plays an important role in gene regulation by the insulator protein CTCF (Wendt *et al*., 2008; Parelho *et al*., 2008; Stedman *et al*., 2008). As mentioned in Section 1.3., the genomic distribution of cohesin showed a high degree of similarity with the localization of CTCF. Cohesin has previously been shown to facilitate CTCF-mediated long-range enhancer-promoter chromatin interactions, and knockdown of Scc1/Rad21 or Smc3 causes the loss of CTCF-mediated insulator activity. Moreover, the teamwork between CTCF and cohesin has been reported to be essential for the transcriptional control of the imprinted, differentially silenced *H19/IGF2* (H19 non-coding RNA; IGF2 insulin like growth factor 2) locus in mammalian cell (Wendt *et al*., 2008). At the imprinted *H19/IGF2* locus, while *H19* ICR (interlocus control region) makes sure that *H19* is only transcribed from the maternal allele, the *IGF2* gene is only expressed from the paternal allele (Bartolomei *et al*., 1991; DeChiara *et al*., 1991). Only the unmethylated maternal allele can

bind to CTCF, which prevents *IGF2* promoters from interacting with the enhancers. ICR methylation on the paternal chromosome prevents CTCF from binding, leading to the activation of the IGF2 promoters by the enhancers (Bell and Felsenfeld, 2000; Hark *et al*., 2000; Kanduri *et al*., 2000). At the *H19/IGF2* locus, cohesin is enriched at the ICR, and only binds to the unmethylated maternal allele (Wendt *et al*., 2008). Notably, removal of cohesin has been observed to cause an increase in *IGF2* transcription and, a decrease in *H19* transcription; CTCF depletion had the same effect in this experiment. Considering the fact that similar results were obtained when these experiments were performed in G1- and G2-synchronized cells, this role of cohesin appears to be independent of its role in cohesion. How cohesin contributes to regulation of gene expression at mechanistic level is unknown. The finding that cohesin is capable of encircling DNA fibers *in trans* (Haering *et al*., 2008) led to the proposal that cohesin might control gene expression by facilitating interactions between distant DNA elements in *cis*, via the formation or maintenance of chromatin loops (Figure 1-6).

Two recent studies have provided evidence that cohesin together with another protein complex, named Mediator, cooperate in mediating long range interactions between enhancers and promoters by organizing chromatin into loop structures (Kagey *et al*., 2010; Ebmeier and Taatjes, 2010). Mediator is a coactivator complex that can bridge enhancer-bound transcription factors and promoter bound RNA polymerase II (reviewed in Kornberg *et al.,* 2005). It has been revealed that in a screen aimed to detect regulators required to maintain the expression of transcription factor Oct4 in murine embryonic stem cells (ESCs), knockdown of genes encoding subunits of Mediator or Cohesin caused reduced Oct4 protein levels (Kagey *et al*., 2010). Interestingly, both Cohesin and Mediator were found to be localized at the enhancer and core promoter regions of a set of active genes in ESCs, including *Oct4* and *Nanog.* This led to the proposal that Cohesin and Mediator contribute to

DNA looping between the enhancer and promoter of these genes. Consistently, through the usage of 3C technology, the promoters of *Oct4* and *Nanog* genes were found to be in close to enhancer sites in ESCs, which is indicative of DNA looping. Importantly, this interaction was not observed in murine embryonic fibroblasts (MEFs) where *Oct4* and *Nanog* are silent and not occupied by mediator and cohesin. Moreover, the interaction frequency between the core promoter and enhancer sites of the *Nanog* gene was found to be decreased upon Cohesin knockdown, which is consistent with the idea that Cohesin stabilizes loops that are formed by bridging of two chromosome regions via Mediator (Kagey *et al*., 2010) (Figure 1-6).

In humans, there are also indications that in addition to keeping sister chromatids together proteins involved in sister chromatid cohesion may have other functions. Cornelia de Lange syndrome (CdLS), a multi-system developmental disorder, has been linked to mutations in genes encoding NIPBL/Delangin (the human Scc2 ortholog), Smc1A and Smc3 (Krantz et al. 2004; Deardorff et al. 2007). It is characterised by the limb and growth deficiencies, craniofacial anomalies and mild to severe mental deficiency. The observations that the defects are caused by a modest 25-30% reduction in the Nipbl protein, that the cells derived from some CdLS patients do not show defects in sister chromatid cohesion and segregation led to the proposal that CdLS is caused by misregulated gene expression.

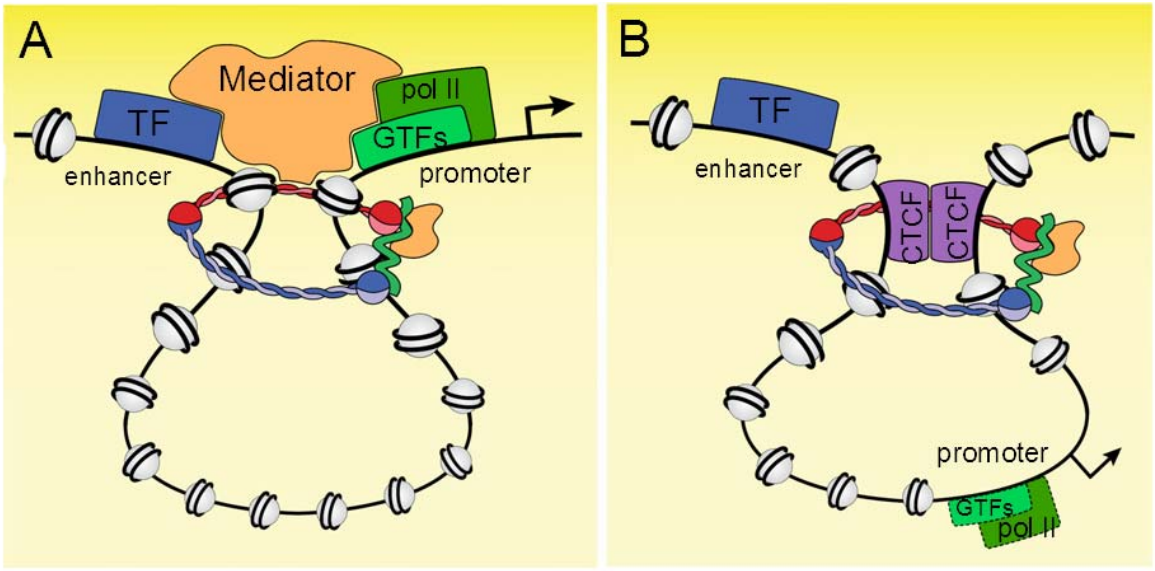

Figure 1-6: Models for cohesin`s function in Mediator- or CTCF-dependent chromatin loop formation

(A) DNA loop formation between enhancers and core promoters occurs as a result of the interaction between enhancer-bound transcription factors, Mediator and promoter bound RNA polymerase II. DNA loop formation is thought to be stabilized by Cohesin.

(B) CTCF and cohesin are thought to organize chromatin into loops in order to prevent promoter-enhancer interactions. (Adapted from Cuylen and Haering, 2010)

Mutations in the *ESCO2* (one of the human orthologs of Eco1) gene can cause Roberts/SC phocomelia (RBS/SC) syndrome, whose clinical features are not identical to but similar to those seen in CdLS patients (Vega *et al*., 2005; Schule et al., 2005). In contrast to CdLS, cells taken from RBS/SC syndrome patients show clear defects in chromosome segregation (reviewed in Dorsett, 2007). However, it is possible that these cohesion defects have an indirect effect on transcriptional regulation, and therefore lead to developmental defects.

1.5. Thesis objectives

The primary objective of this thesis was to develop a new way to cross-link inter-subunit cohesin interactions in order to characterise whether cohesin is topologically bound to DNA, when it does not form sister chromatid cohesion. The previously created cross-linkable cohesin molecule (Haering *et al*., 2008) was not suitable to test how "non-cohesive" cohesin interacts with chromatin, due to modifications making it cross-linkable (see Chapter 2). In order to overcome these problems, two new cross-linkable cohesin molecules were created that can be covalently circularized (see Chapter 3).

Chapter 2 – Covalent closure of cohesin`s ring: the need for new cross-linking methods

2.1. Introduction

2.1.1. Cohesin`s interaction with chromosomes

After the discovery that cohesin is a ring-shaped molecule necessary for sister chromatid cohesion, which is large enough to accommodate two 10nm chromatin fibres, various models have been proposed in order to explain how cohesin holds sister chromatids together (Figure 2-1). The fact that sister chromatid cohesion is destroyed by the targeted proteolytic cleavage of Scc1 or of both coiled coil regions of Smc3 (Uhlmann *et al*., 2000; Gruber *et al*., 2003; Oliveira *et al*., 2010; Tachibana-Konwalski *et al.,* 2010), suggests that cohesin might hold sister chromatids together by trapping them topologically inside its ring. There are several different "ring models" on how cohesin might hold sister DNAs together (Figure 2-1) (Campbell and Cohen-Fix, 2002; Milutinovich and Koshland, 2003; Nasmyth K., 2005; reviewed in Nasmyth and Haering, 2005). While the most widely accepted embrace model, the ring model, proposes that sister DNAs are trapped inside a single monomeric cohesin ring (Figure 2-1 A), the handcuff model postulates that sister DNAs are kept together through the two separate cohesin rings which are connected by topological intertwining (Figure 2-1 C), where each cohesin complex traps only one sister DNA.

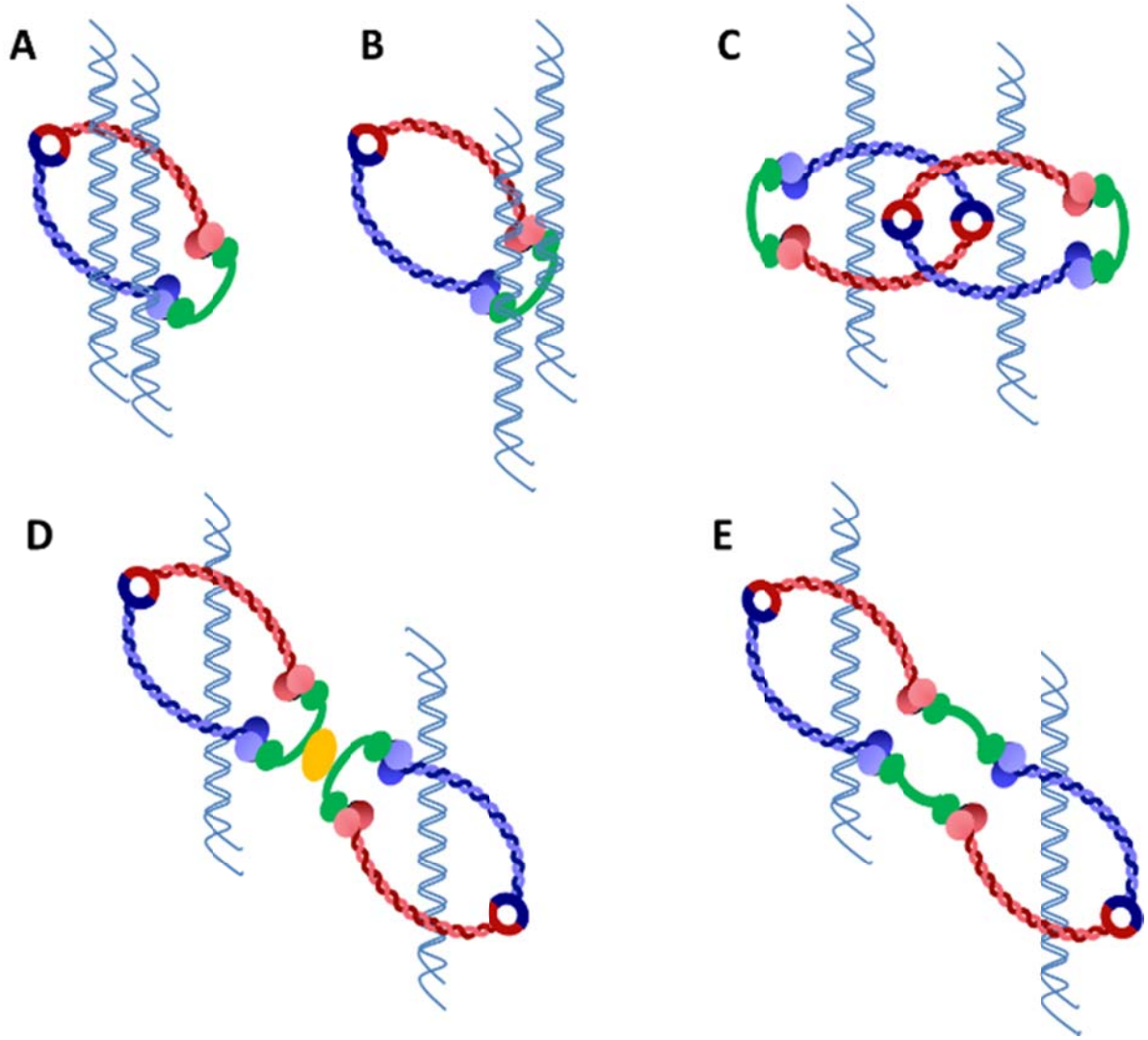

Figure 2-1: Models of how cohesin could hold sister chromatids together

(A) The Ring Model postulates that both sister chromatids are entrapped within the cohesin ring.

(B) A single cohesin ring connects the sister chromatids via physical interaction.

(C) The Handcuff Model proposes the topological interconnection of two cohesin rings, while each sister chromatid is entrapped within a cohesin molecule.

(D) Another version of the Handcuff Model envisages association of two cohesin rings by binding to a single Scc3 subunit.

(E) A dimeric cohesin ring entraps the sister chromatids topologically.

This figure was modified from Nasmyth and Haering, 2005.

Another model, derived from the handcuff model, envisages that two rings are associated physically with each other via binding to a single Scc3 subunit (Figure 2-1 D). Lastly, an alternative version of the ring model proposes that sister chromatids are encircled by a large dimeric/oligomeric cohesin ring encircling the sister chromatids (Figure 2-1 E). It has been shown that when Scc1 is purified from yeast strains expressing two differently tagged versions of Smc1 or of Smc3, Scc1 was observed to come along with only one of the tagged proteins (Haering *et al*., 2002). Moreover, electron micrographs of soluble cohesin molecules visualizing the cohesin holocomplexes (Anderson *et al*., 2002) has indicated that soluble and chromosome bound cohesin form monomeric rings, arguing against the presence of dimeric/oligomeric cohesin structure *in vivo*.

Both the embrace and the handcuff models propose that cohesin holds chromatin in a topological manner rather than physically binding to DNA or nucleosomes. In order to distinguish between the topological and physical binding modes (Figure 2-1 A and B), an elegant method has been developed by the Nasmyth laboratory (Ivanov and Nasmyth, 2007). Until recently, sister chromatid cohesion has only been detected using cytological methods in living cells due to the absence of an assay by which cohesion between sister DNA molecules can be measured in a test tube. Using an *in vitro* physical assay, it is now possible to detect cohesion between the sister DNAs of circular minichromosomes by employing velocity gradient sedimentation followed by agarose-gel electrophoresis and Southern blotting (Ivanov and Nasmyth, 2007). This method can be used to distinguish dimeric minichromosomes (dimers), which are formed *in vivo* during S-phase and held together by cohesin, from non-cohesed monomeric ones, since the dimers sediment more rapidly and electrophorese more slowly (Figure 2-2 A and B).

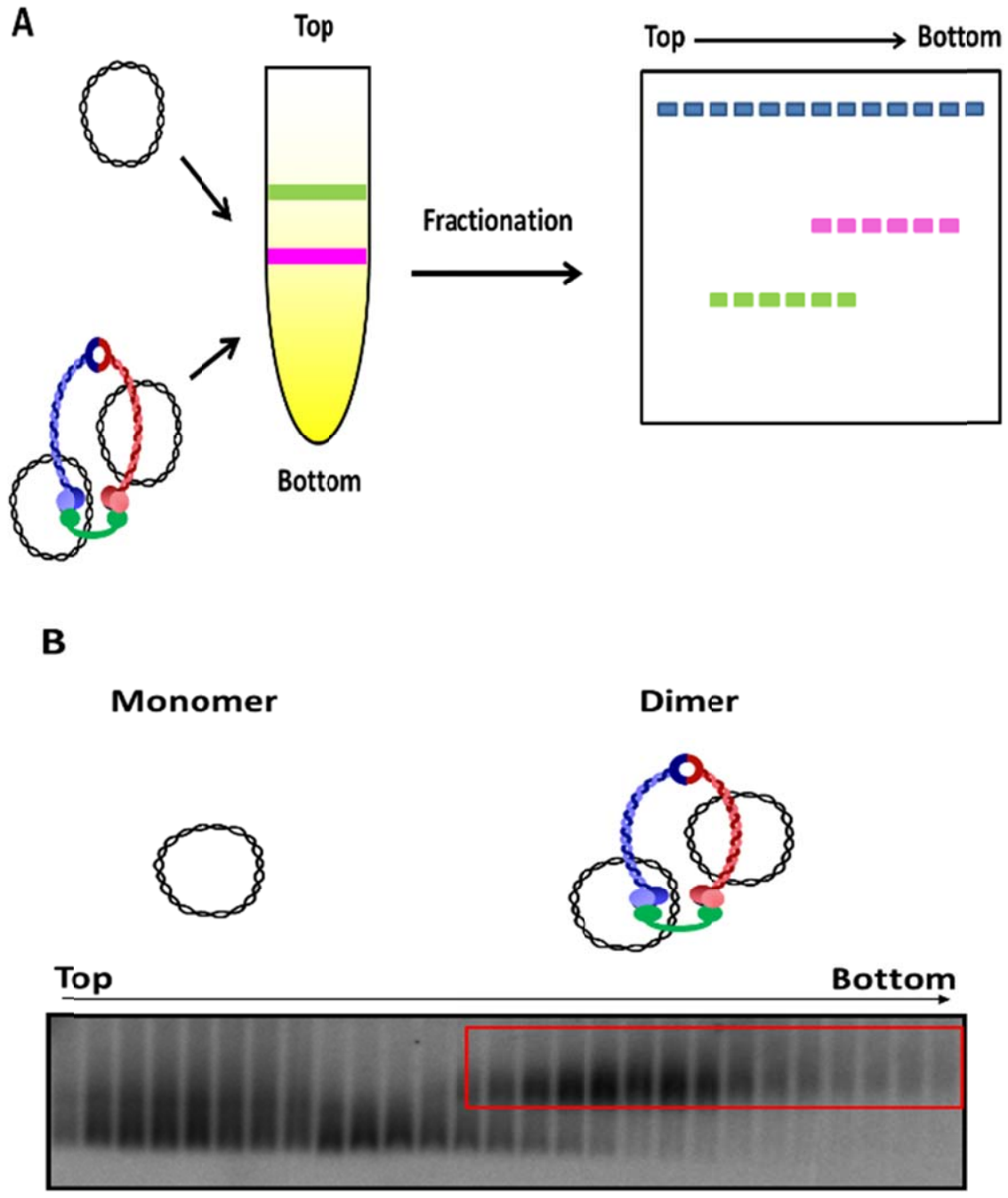

Figure 2-2: The minichromosomal assay for cohesion

(A) Schematic drawing of the sucrose gradient sedimentation and gel electrophoresis to purify small circular minichromosomes. This figure is modified from Ivanov and Nasmyth, 2007.

(B) A Southern blot showing the detection of minichromosomal DNA. Dimers are marked with a red box.

Through the utilization of this assay, it has been shown that, insertion of TEV-protease cleavage sites into the Scc1 and activation of TEV-protease releases cohesin from small mini-chromosomes, namely converts the dimeric minichromosomes to monomeric forms. Moreover, cohesin has been shown to dissociate from DNA by linearizing the mini-chromosomes supporting the idea that cohesin should be able to slide along chromosomes if it interacts with them topologically (Ivanov and Nasmyth, 2005).

Experiments performed in the Nasmyth laboratory provided the final proof for a topological mechanism for sister chromatid cohesion. The notion that cohesin holds sister minichromosomes together in a topological manner made a key prediction that if the three cohesin subunits (Smc1, Smc3, Scc1) were chemically cross-linked, then sister DNAs would be trapped inside a covalently closed cohesin ring (Haering *et al*., 2008). After purification of cohesed dimeric minichromosomes and cross-linking of the cohesin molecule, the sister DNAs should become resistant to denaturing conditions and still migrate as dimers during gel electrophoresis even after protein denaturation. Chemical circularisation was achieved by fusing Smc3`s C-terminus to Scc1`s N- terminus via a flexible linker containing TEV-cleavage sites and by introducing engineered cysteine residues into the two other interfaces (Smc1/Smc3 and Smc1/Scc1) that can be crosslinked by the thiol-reactive cross-linkers dibromobimabe (bBBr) and bis-maleimidoethane (BMOE) (Haering *et al*., 2008). As predicted by the embrace-/ring model, cohesed dimeric minichromosomes with covalently circularized cohesin rings were detected after being treated with harsh protein denaturants such as SDS (sodium dodecyl sulfate). Proteolytic cleavage of the polypeptide linker connecting Smc3 to Scc1 by TEV-protease verified that these dimers are actually composed of monomeric DNAs that are held together by covalently circularized cohesin complexes. Taken together, these experiments are consistent with the predictions of the embrace model

and confirm that cohesin indeed uses a topological mechanism to provide cohesion of the sister DNA molecules.

2.1.2. Does 'non-cohesive' cohesin interact with DNA topologically?

The cross-linking experiments raise a new possibility that cohesin may also function as a "concatenase" which also captures individual chromatin fibres. It is still unknown whether cohesin complexes that associate with chromatin but are not involved in the establishment of sister chromatid cohesion entrap DNA topologically. Cohesin is known to be capable of binding to chromatin in at least two different ways: one in which cohesin encircles DNAs and holds sister chromatids together and another in which it associates less tightly with individual chromatids, and is not "cohesive" (reviewed in Nasmyth and Haering, 2005). Experiments performed in mammalian cells using fluorescence recovery after photobleaching (FRAP) and quantitative live-cell imaging have identified three different cohesin populations during the cell cycle, which is based on the measurements of cohesin`s residence time on DNA (Figure 2-3) (Gerlich *et al*., 2006.) Interestingly, while the mean residence time of chromosomal cohesin is less than 25 minutes both in G1- and G2- cells, a second population has been detected in G2- cells whose residence time is much longer (6 hours). This population is thought to be composed of cohesin molecules that are stably associated with sister chromatids starting from DNA replication and persisted until metaphase, providing cohesion. Consistently, it has been observed in an unperturbed cell cycle in budding yeast that after S-phase there is no exchange of cohesion-mediating cohesin complexes, implying the presence of a similar cohesin population in yeast (Uhlmann and Nasmyth, 1998; Haering et al., 2004). The second pool is made up of a large fraction of cohesin complexes dynamically bound to DNA, which cycles on and off the chromatin many times throughout the entire cell cycle, but

does not establish cohesion. Lastly, a third pool identified consisting of soluble and unbound cohesin molecules (Gerlich *et al*., 2006) (Figure 2-3).

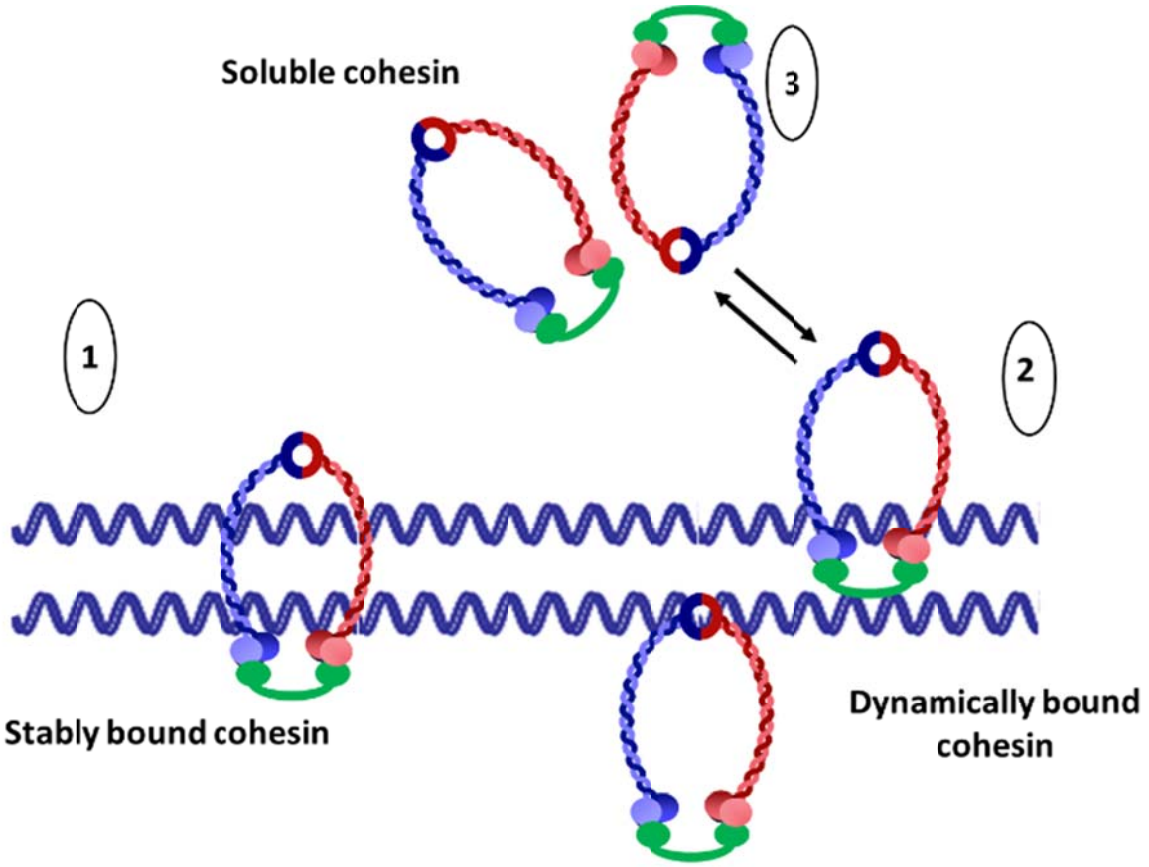

Figure 2-3: Model for possible dynamic turnover of cohesin complexes

Three pools of cohesin exist, one stably bound to sister chromatids and forming cohesion (1), one bound DNA but not involved in sister chromatid cohesion (2), and one soluble and unbound (3). Reproduced and modified from Nasmyth and Haering, 2005.

The mode of cohesin-DNA interaction in the dynamic cohesin pool is unknown. Understanding how these 'non-cohesive' cohesin molecules are associated with DNA fibres is important for two main reasons. Firstly, in budding yeast, most Scc1 is re-synthesised in late G1 after its destruction by separase cleavage at anaphase. This then leads to the immediate formation of cohesin "trimer", which subsequently associates with the chromatin, which is not yet replicated. At this stage, cohesin rings associated with unreplicated chromatin may be converted at/by replication forks into rings that entrap sister DNAs, without the rings dissociating at any stage from the chromosomes during the conversion. This could happen either due to replication fork passage through rings (Figure 2-4A) or by transient ring opening without dissociation from the chromatin template (Figure 2-4B) (Haering *et al*., 2002; Lengronne *et al*., 2006). In either case, understanding the nature of cohesin`s association with chromatin ahead of replication forks can be helpful in order to explain how cohesion is established during DNA replication.

Secondly, the binding of cohesin to unreplicated chromatin in metazoans, where cohesin is believed to play a key role in regulating gene expression, is even more widespread than in yeast. Understanding how cohesin binds unreplicated chromatin may therefore bring insight into the mechanisms by which cohesin complex promotes its non-canonical functions. In Xenopus and human cells, cohesin is already loaded onto unreplicated DNA in telophase, a time where sister chromatid cohesion does not yet exist (Losada et al. 1998; Sumara et al. 2000; Waizenegger et al. 2000). Moreover, cohesin and the cohesin associated protein Pds5B are also expressed in postmitotic cells such as neurons, which normally do not replicate their DNA again and will therefore never establish sister chromatid cohesion (Zhang *et al.,* 2007; Wendt *et al*., 2008; Pauli *et al*., 2008).

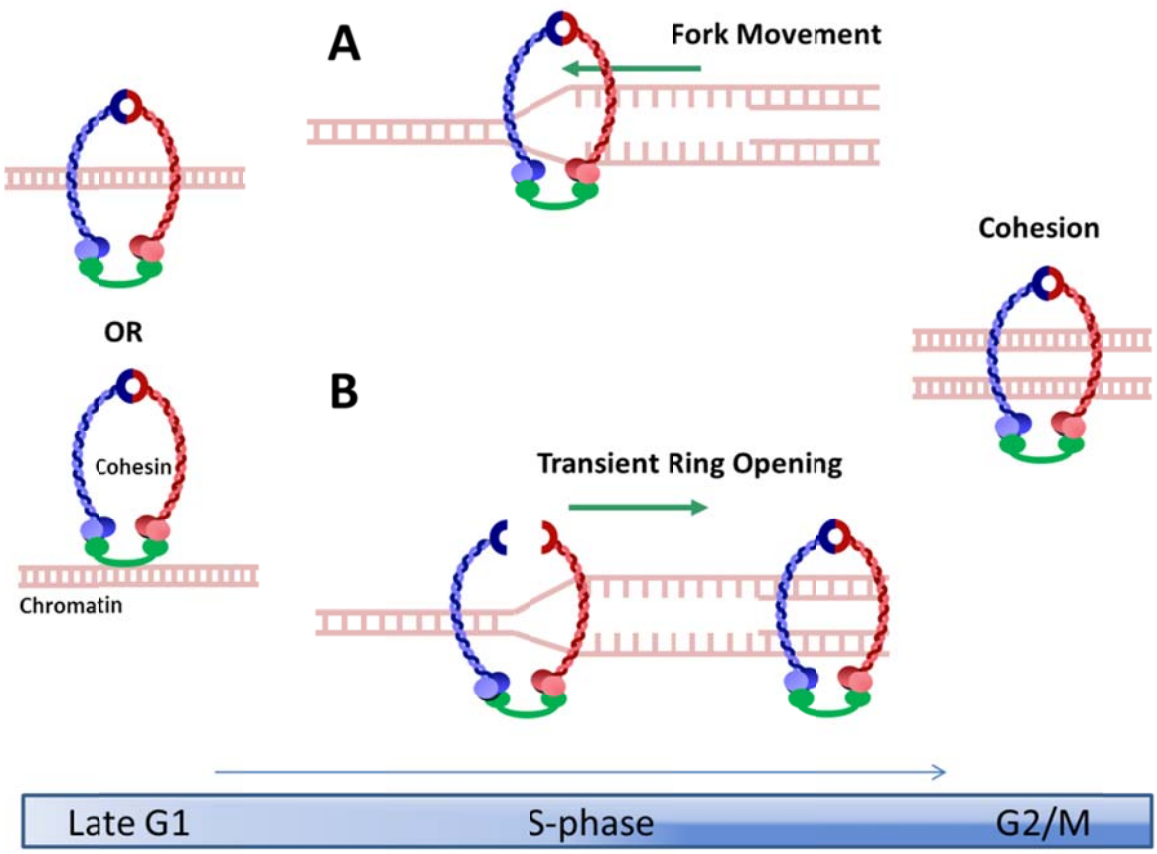

Figure 2-4: Models of cohesion establishment during DNA replication

(A) The Replication fork passes through the cohesin ring.

(B) Cohesin ring opens and closes without being released from the DNA during fork passage.

These observations indicate that in multicellular organisms cohesin associated with the unreplicated chromatin of post mitotic cells performs functions on DNA that are distinct from cohesin's role in sister chromatid cohesion and has been thought to regulate transcription (Peters *et al*., 2008). It is still unclear whether cohesin`s non-canonical functions also require the topological embracement of DNA inside its ring. Cohesin may regulate gene expression, by playing a role in the formation and stability of DNA loops, which are thought to occur between the enhancers and core promoters of active genes (Kagey et al., 2010). Cohesin could facilitate the "pairing" interactions between distant enhancers and promoters in a manner similar to the way it holds sister chromatids together. Whether this is indeed the case is currently unknown.

2.1.3. Experimental strategy

At the time when this study was started, my initial aim was to investigate whether "non-cohesive" cohesin interacts with the DNA topologically in budding yeast. To characterize this, I needed a situation where cohesin is already loaded onto chromosomes, but either DNA is not replicated or sister chromatid cohesion is not established. Cohesin can be accredited as "non-cohesive" before DNA replication during the cell cycle. Cohesin is known to associate with the DNA in late G1 (Michaelis et al., 1997; Ciosk et al., 2000), where it is either physically or topologically bound to the DNA, which is not yet replicated. Even though budding yeast has a long G1-phase and it is approximately known when cohesin associates with unreplicated DNA and when replication starts, the time frame between loading of cohesin and initiation of DNA replication is not long enough to collect cells, perform necessary treatments and cell lysis. Cohesin can also remain "non-cohesive" even after DNA replication, if cohesion establishment is impaired, e.g. when its Smc3 subunit is not acetylated by Eco1 (Ben-Shahar *et al*., 2008; Unal *et al*., 2008; Zhang *et al*., 2008; Rowland

et al., 2009). In this case, although cohesin associates with chromatin and DNA replication takes place, no sister chromatid cohesion is generated. Because there is a short time frame between G1-and S-phase, it is difficult to analyse the physical nature of cohesin`s interaction with DNA before replication. I therefore investigated how "non-cohesive" cohesin associates with the chromatin after DNA replication when there is no sister chromatid cohesion. Because in the temperature-sensitive (ts) allele of *ECO1* mutants where sister chromatid cohesion cannot be established, cohesin can still associate with DNA even when not holding sister chromatids together (Toth *et al*., 1999; Skibbens *et al*., 1999; Ivanov and Nasmyth, 2005), I decided to use *eco1* ts mutants in order to create the condition I need.

I then needed an assay to study whether cohesin`s association with chromatin involve trapping of chromatin fibers. Before this study had started, a physical assay using sucrose gradients and gel electrophoresis was already established to purify and detect cohesed sister chromatids of small minichromosomes from yeast (Figure 2-2 A and B) (Ivanov and Nasmyth, 2007). Utilization of this assay together with the usage of the cross-linkable cohesin ring, whose Smc1/Smc3, Smc1/Scc1, and Smc3/Scc1 interfaces can be covalently cross-linked, allowed the demonstration that sister DNAs of a 2.3kb minichromosomes are trapped inside a covalently circularized cohesin ring (Haering *et al*., 2008).

Through creating a chemically cross-linkable cohesin ring in the *eco1* ts mutant background, purifying small circular minichromosomes and covalently sealing the cohesin ring, I aimed to obtain a DNA–protein complex consisting of a circular minichromosome associated with a modified cohesin complex which is resistant to denaturing conditions. Employment of 2D gel electrophoresis in the absence or presence of proteinase K would then help me to identify whether circularized cohesin topologically holds DNA in the absence of Eco1. Denatured and cross-linked samples are first resolved on an agarose gel (the first dimension), and then electrophoresed perpendicularly through a thin zone of agarose or agarose containing

proteinase K into a second gel (the second dimension). Given that proteinase K should digest any proteins before DNAs enter the gel, DNA species that run as dimers in the first dimension should run as monomers in the second dimension if they are held together by cohesin (Haering *et al*., 2008). If there is a topological association between cohesin and unreplicated-monomeric DNA molecules, this monomeric DNA-cohesin complex should initially considerably migrate slower than monomeric supercoils in the first dimension and run as monomeric supercoils in the second dimension. In the absence of proteinase K each of the DNA species should behave similar in the first and the second dimensions, lying on the diagonal. However, if there is no topological association between cohesin rings and the unreplicated-monomeric DNA molecules, then upon covalent closure of the cohesin ring followed by the destruction of cohesin's integrity by proteinase K, the migration profiles in the absence and in the presence of proteinase K should be identical.

2.2. Results

2.2.1. The physical nature of sister chromatid cohesion in the absence of functional Eco1 protein

There are two different previously described temperature-sensitive *ECO1* alleles, *eco1(G211D)* and *eco1(G211H)*, in our yeast strain collection (Toth *et al*., 1999; Ivanov *et al*., 2002). Although both strains were dead at the restrictive temperature of 37 ^{0}C (data not shown), in order to decide on the allele that will be used, I compared their ability to inactivate Eco1 and prevent the formation of sister chromatid cohesion in just one cell cycle.

The physical nature of sister chromatid cohesion in wild type and *eco1* ts mutant cells was characterized using sucrose gradient sedimentation and gel electrophoresis to separate

cohesed circular minichromosomes from non-cohesed ones. Yeast strains containing 2.3kb circular minichromosomes in an *ECO1* wild type and *eco1* ts mutant background were synchronized in G1-phase with α-factor at the permissive temperature of 23 ^{0}C for 90 min. They were then shifted to the the non-permissive temperature of 37 ^{0}C for 60 min, in order to inactivate ts Eco1 protein before DNA replication, and finally transferred to fresh medium at 37 ^{0}C lacking α-factor but containing nocodazole to prevent mitosis. After 90 min, when all cells had undergone DNA replication and most had arrested in a pseudomitotic state, cells were harvested (Figure 2-5 A). The cleared lysates were obtained from spheroplasted cells and purified by sucrose gradient centrifugation. Fractions from the sucrose gradients were then electrophoresed in an agarose gel and visualised by Southern blotting (Figure 2-6 B). Wild-type cells produced a cohesion pattern, with 45% dimeric minichromosomes. Although no dimeric forms (1% of the total signal) were detected in *eco1(G211H)* allele, a small dimeric population (7-8% of the total signal) was still observed in *eco1(G211D)* cells (Figure 2-5 C). Western blotting using an acetyl-lysine specific antibody has showed that Smc3 acetylation is greatly reduced in *eco1(G211D)* cells even at 23 ^{0}C, and declines further upon incubation at 37 ^{0}C (Rowland *et al*., 2009), but a very slight band, indicative of Smc3 acetylation, can still be detected at 37 ^{0}C. This basal Smc3 acetylation might account for the small dimeric population that I detect in my experiment. I therefore decided to use the *eco1(G211H)* allele for the rest of the experiments.

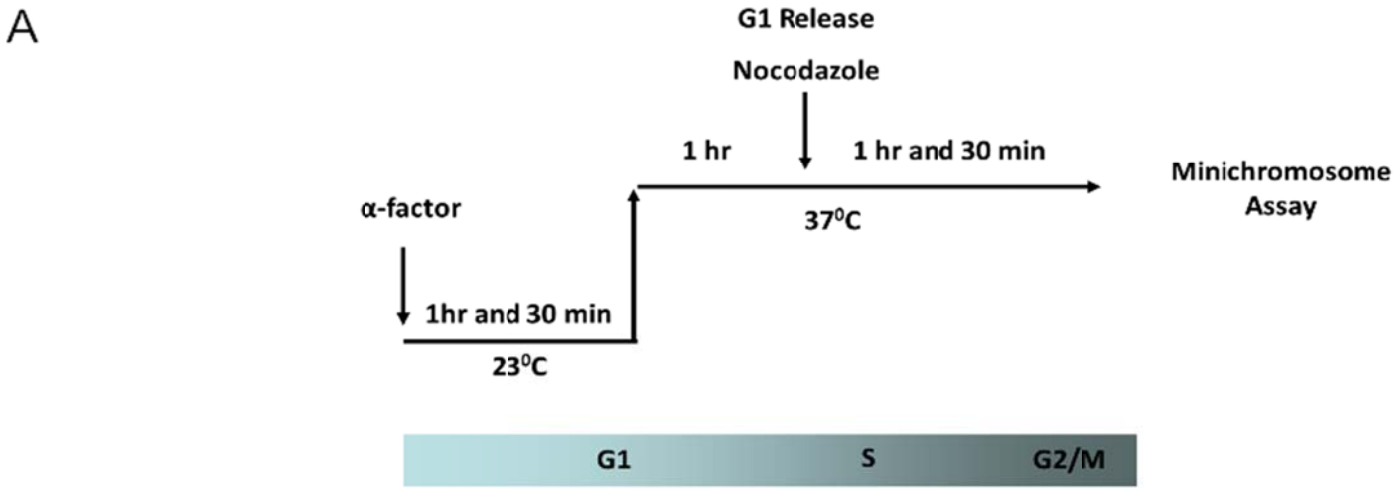
A
G1 Release
Nocodazole
1 hr
1 hr and 30 min
Minichromosome Assay
α-factor
37⁰C
1hr and 30 min
23⁰C
G1
S
G2/M

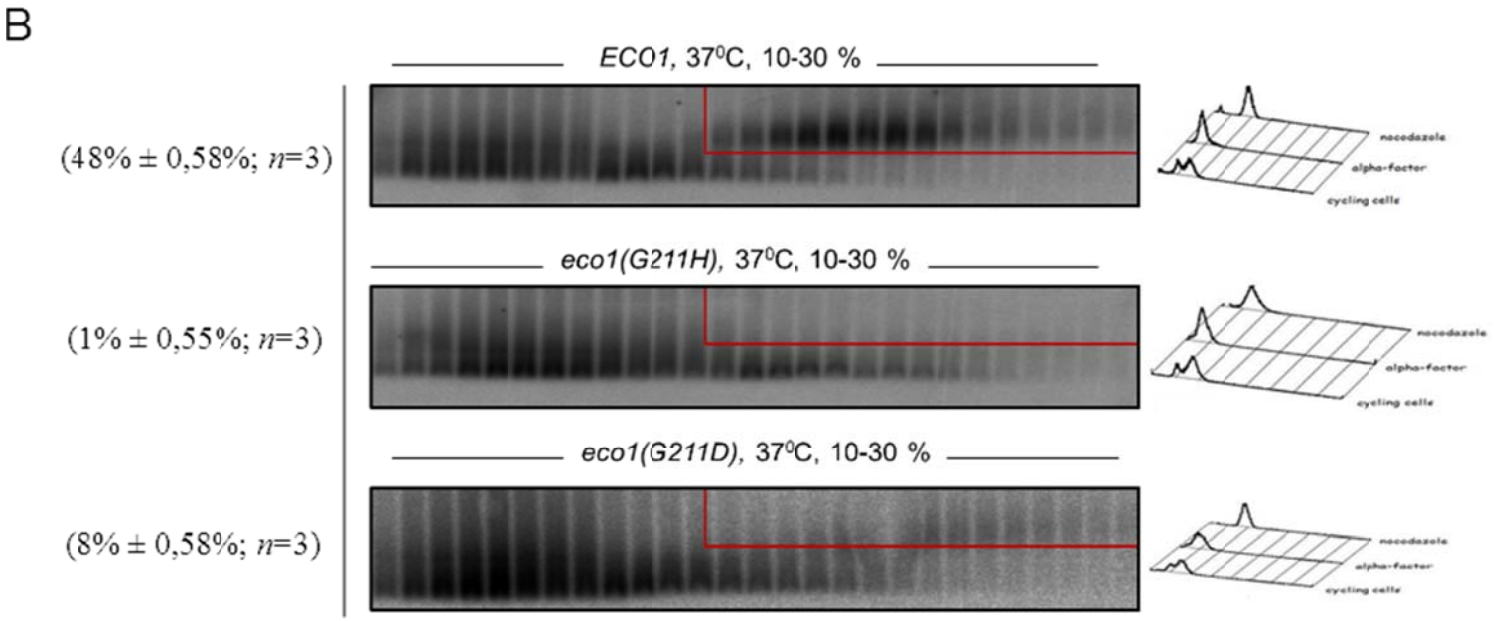
B
ECO1, 37⁰C, 10-30 %
(48% ± 0,58%; n=3)
eco1(G211H), 37⁰C, 10-30 %
(1% ± 0,55%; n=3)
eco1(G211D), 37⁰C, 10-30 %
(8% ± 0,58%; n=3)
nocodazole
alpha-factor
cycling cells

Figure 2-5: Measuring sister chromatid cohesion between circular sister minichromosomes in temperature sensitive *eco1* mutants.

(A) Scheme portraying the experimental setup: Exponentially growing cultures of K15103 (*Mat a, ECO1, 2.3kb TRP1-Cen4-ARS1 minichromosome*), and K14727 (*Mat a, eco1(G211H), 2.3kb TRP1-Cen4-ARS1 minichromosome*) and K16107 (*Mat a, eco1(G211D), 2.3kb TRP1-Cen4-ARS1 minichromosome*) strains were arrested in G1-phase with alpha factor at 23 ^{o}C, and released into nocodazole containing media at 37 ^{o}C.

(B) Cleared lysates were sedimented in a 10-30% sucrose gradient at 18krpm for 15hr in a Beckman SW41 rotor, followed by fractionation and gel electrophoresis on a 0.8% agarose gel at 65V for 8hr at 4 ^{o}C. FACS analysis of cellular DNA content shows that all strains had undergone DNA replication at 37 ^{o}C. The percentages of minichromosomal DNA present in dimeric fractions are shown in brackets. Data is shown as a mean of dimer percentage ± S.D. (standard deviation), 'n' is number of experiments.

2.2.2. Dynamics of cohesin binding to chromosomes in the absence of functional Eco1 protein

Given that no sister chromatid cohesion is formed in *eco1(G211H)* cells, I then wanted to check that the loss of sister chromatid cohesion in the absence of Eco1 was not due to cohesin's inability to associate with the chromosomes. The amount of cohesin bound to the chromosomes in wild type and mutant cells was assessed using chromatin immunoprecipitation (ChIP) followed by quantitative PCR (qPCR). The dynamics of cohesin's association with chromosomes were measured by ChIP-qPCR at six chromosomal loci, which were chosen according to a map of cohesin binding sites along *S. cerevisiae* chromosome VI (Lengronne *et al*., 2004). Site 1 is a low cohesin site and is 35kb away from the centromere, site 2 is the outer arm and is 50 kb away from the centromere, site 3 is the inner arm and is 25kb away from the centromere, site 4 is the outer pericentromere and is 15kb away from the centromere, site 5 is the inner pericentromere and is 2.5kb away from the centromere, and site 6 is the core centromere and is within the centromere.

The levels of cohesin binding at these six chromosomal sites were analysed in the presence or absence of functional Eco1 using the temperature sensitive allele *eco1(G211H)*. Yeast strains expressing Scc1-PK9 in an *ECO1* wild type and *eco1(G211H)* mutant background were grown at the permissive temperature of 23 ^{o}C in YEPD and arrested with α-factor in G1 phase. Cells were then released into YEPD media at the non-permissive temperature of 37 ^{o}C. ChIP and FACS samples were taken every 5 minutes for the first 30 minutes after release and every 15 minutes for another hour and 45 minutes. The ChIP time points corresponding to a particular site were run together in the same qPCR run.

The FACS profiles show that at 37 ^{o}C the cells from the *ECO1* and the *eco1(G211H)* go through S-phase at approximately 30 to 45 minutes post release, indicating that both the mutant and wild type cells have similar cell cycle kinetics (Figure 2-6 A).

In wild-type cells, the loading dynamics of cohesin correlates with S-phase progression revealed by FACS (Figure 2-6 B). Upon release, the loading of cohesin starts at approximately between 10-15 minutes for the centromere, outer arm, inner and outer pericentromeres, and 15-20 minutes for the inner arm. When the S phase starts (25 min after release), the percentage IP results peak at 25 minutes for all the sites examined. Cohesin levels start to drop by 30 minutes after release from centromere and inner pericentromere, and almost all cohesin has gone by 100 minutes. Cohesin removal from the other four sites starts also at 30 minutes post release, and nearly all cohesin has gone by 90 minutes. Considering anaphase should start at 105 minutes, cohesin is dissociated from all six sites before anaphase starts.

The percentage IP results for both *ECO1* and *eco1(G211H)* strains show peaks with similar cyclical kinetics for all six sites (Figure 2-6 B). Cohesin is loaded in G1, peaks in S phase, and starts to drop before anaphase. The centromere, inner and outer pericentromeres exhibit the highest percentages (peak at 25 minutes), the earliest loading (15 minutes), and the earliest dissociation (30 minutes). Although the amount of cohesin associated with centromeric and inner pericentromeric regions in *eco1(G211H)* strain are almost indistinguishable from the wild type throughout the whole cell cycle, the arm sites and the outer pericentromere have lower cohesin levels (approximately 50% less compared to the wild-type) in *eco1(G211H)* strain. Interestingly, in the absence of Eco1, as it is moved further away from the centromere, the amount of cohesin being loaded onto chromosomes is reduced compared to the wild-type (Figure 2-6 B).

Despite 50% decrease in the cohesin amount associated with DNA in *eco1(G211D)* cells as cohesin moves away from the centromere, they have the same amount of the cohesin at core centromeric and inner pericentromeric regions compared to the wild type. Since the minichromosome that was used in the physical assay has only core centromeric sequence, absence of dimeric minichromosomes in *eco1(G211D)* cells cannot be due to the lack of cohesin molecules associated with minichromosomes, but is rather due to their inability to form sister chromatid cohesion, namely the loss of Smc3 acetylation.

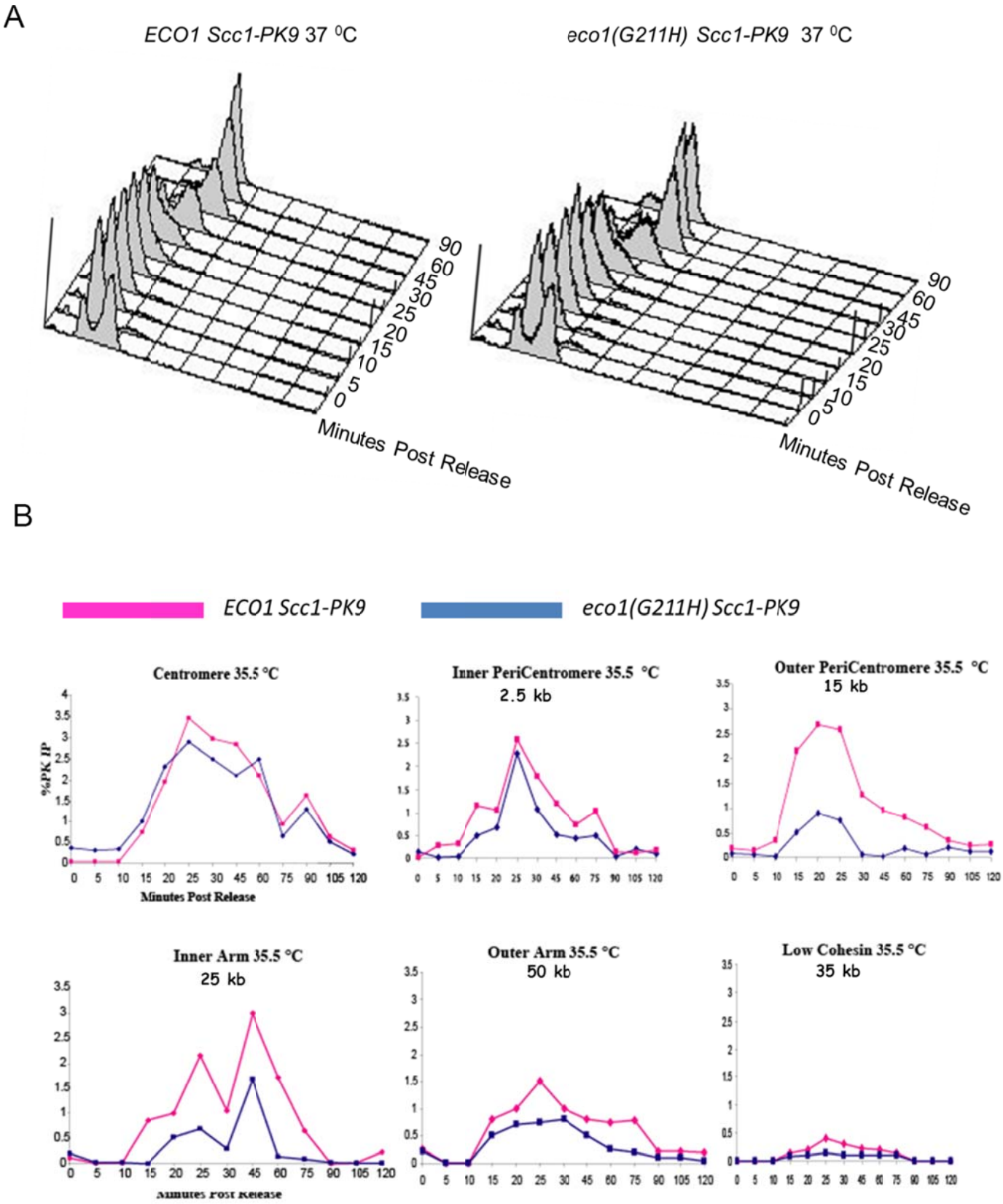
A
ECO1 Scc1-PK9 37 °C
eco1(G211H) Scc1-PK9 37 °C
90
60
45
30
25
20
15
10
5
0
Minutes Post Release
B
ECO1 Scc1-PK9
eco1(G211H) Scc1-PK9
Centromere 35.5 °C
%PK IP
Minutes Post Release
Inner PeriCentromere 35.5 °C
2.5 kb
Outer PeriCentromere 35.5 °C
15 kb
Inner Arm 35.5 °C
25 kb
Outer Arm 35.5 °C
50 kb
Low Cohesin 35.5 °C
35 kb

Figure 2-6

Figure 2-6: Cohesin Loading Dynamics in ts *eco1(G211H)* at 37°C.

Cells of strains K16107 (*MAT a, eco1(G211H), SCC1-PK9 cells)* and K14601 *(MAT a, ECO1, SCC1-PK9*) cells grown in YEPD media at 23°C were arrested with a-factor, and released into YEPD at 37°C. FACS and ChIP samples were taken every five minutes for the first 30 minutes after release and then every 15 minutes for an additional hour and 30 minutes.

(A) FACS analysis of the time-points for the *ECO1* wild-type (left) or *eco1 (G211D)* mutant strain (right) at 37°C. **(B)** The percentages of Scc1-PK9 IP for six cohesin sites were determined by ChIP/qPCR for time-points of the α-factor release timecourse and plotted against minutes after release at the restrictive temperature of 37°C.

2.2.3. Generation of a chemically circularized cohesin ring in the temperature sensitive allele of *Eco1* background

Having shown by mini-chromosomal/physical assay that no sister chromatid cohesion is formed in the *eco1(G211H)* mutants (Figure 2-5) and by ChIP-qPCR that at centromeric and inner pericentromerics regions *eco1(G211H)* mutant has no cohesin loading defect (Figure 2-6), I then decided to create a yeast strain that contains the cross-linkable version of cohesin ring in the *eco1(G211H)* mutant background. Generation of such strain would then help me to investigate how cohesin associates with DNA when there is no sister chromatid cohesion.

During the construction process of the cross-linkable cohesin complex, Smc1/Smc3 and Smc1/Scc1 interfaces of the cohesin ring were engineered to permit covalent connections between the inserted cysteine residues which were designed according to the available crystal structures (Haering *et al*., 2008). Because no structural information is available for interface between the N-terminal domain of Scc1 and the ATPase head of Smc3, this interface was connected by a long flexible linker containing triple target sequences for the TEV protease expressing Smc3 and Scc1 as a translational fusion (Gruber *et al*., 2006; Haering *et al*., 2008). Although this fusion provides sufficient cohesion for yeast cells to proliferate, it has a slight growth defect at both permissive (25 ^{o}C) and restrictive temperature (37 ^{o}C) (Gruber *et al*., 2006; Haering *et al*., 2008). However, the quantifiable effect of the fusion on sister-chromatid cohesion was measured when evaluated by the minichromosomal assay. Cells containing a 2.3kb minichromosome were arrested in G2/M phase by the addition of nocodazole. Clear lysates were sedimented, separated and analysed as described previously. Compared to the wild type strain which contains 45% cohesed minichromosomes (dimers) when arrested in G2/M phase, strains bearing the fusion protein have only 25% dimers,

indicating that fusing Smc3 to Scc1 via a TEV linker hinders entrapment or concatenation of sister DNAs by cohesin rings (Figure 2-7).

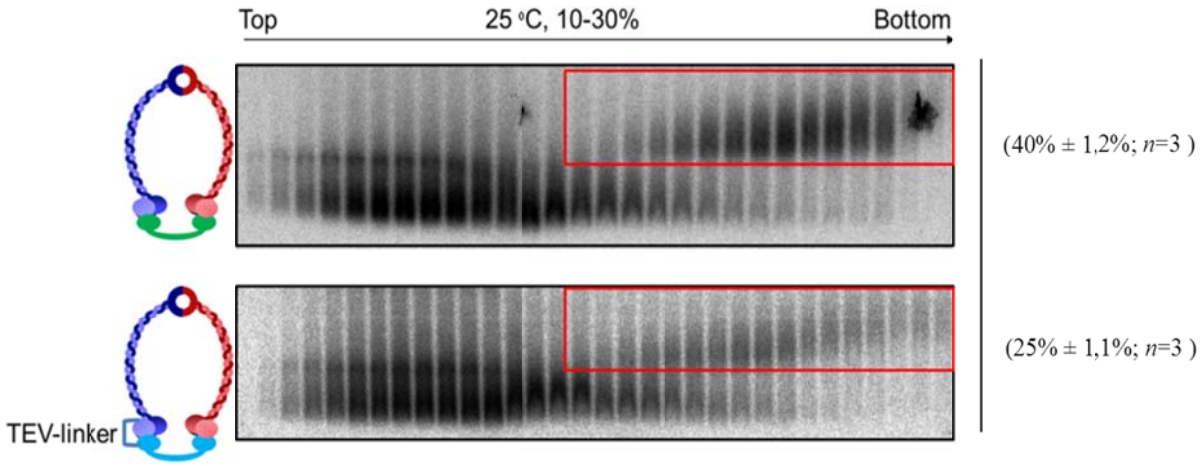

Figure 2-7: Fusing Smc3 to Scc1 via a TEV linker decreased the levels of dimeric minichromosomes. Clear lysates prepared from strains K15103 (*Mat a, 2.3kb TRP1-Cen4-ARS1)* and K19139 (*Mat a, ura3::Scc1P-Smc3-TEV3-Scc1-HA6::URA3, smc3::HIS3, scc1::KanMx, 2.3kb TRP1-Cen4-ARS1*) were purified by sucrose gradient centrifugation, followed by fractionation and visualised by Southern blotting. The dimeric population of each strain is represented in a red box. Quantification of the dimers, expressed as a percentage of the total signal (shown in brackets), revealed that the presence of the Smc3-Scc1 fusion protein roughly halved the fraction of dimeric minichromosomes.

Surprisingly, when *eco1(G211H)* mutant was crossed into a strain containing Smc3-Scc1 fusion protein, a slow growth was observed at the restrictive temperature when Eco1 is inactivated, suggesting that the fusion can bypass the requirement for Eco1 for unknown reasons (Figure 2-8). As expected, while *eco1(G211H)* mutant cells are able to proliferate at 25 ^{o}C, they fail to do so at the non-permissive temperature of 37 ^{o}C cells and viability is only restored when wild-type *ECO1* expression is induced (data not shown).

Having found out that the presence of Smc3-Scc1 fusion enables cells to grow at 37 ^{o}C in *eco1(G211H)* mutant background, it was investigated whether it can still permit cell proliferation when the *ECO1* gene is deleted (*Δeco1*). Because *Δeco1* cells are dead, the Smc3-Scc1 fusion was crossed with a strain in which *RAD61* and *ECO1* genes are both deleted. It has been shown that in the absence of both Eco1 and Rad61 proteins, cohesion can still be established (Rowland *et al*., 2009). Tetrad dissections were performed on heterozygous *Δrad61Δeco1/ (Smc3-TEV-Scc1, Δsmc3Δscc1)* strain. Spores that carry the *Smc3-TEV-Scc1* along with the deletion of *ECO1* were viable (Figure 2-8B, encircled spores), verifying that the Smc3-Scc1 fusion protein allows cells to build cohesion in the absence of Eco1 activity (M.B. Roig, unpublished data).

I then measured the ability of the Smc3-Scc1 fusion strain to form dimeric minichromosomes in the presence or absence of Eco1 using differential sedimentation velocity and gel electrophoresis. Clear lysates were prepared from cells containing a 2.3kb minichromosome. Analysis of the gradient fractions extracted from cultures arrested in metaphase showed that in the presence of Eco1, strains bearing the fusion protein have only 25% dimers (Figure 2-9) which is indicative of the underlying cohesion defects, compared to the wild type strain which contains 45% cohesed minichromosomes (dimers). When Eco1 is absent, the Smc3-Scc1 fusion strain is able to form dimeric minichromosomes, with 15% dimeric populations (Figure 2-9) as opposed to 0% in *Δeco1* alone. This result indicates that the ability of cells

lacking Eco1 to form cohesin mediated minichromosome dimers is restored by the presence of Smc3-Scc1 fusion protein, albeit not to wild-type levels.

As mentioned above, the interface between the ATPase head of Smc3 and the N-terminal of Scc1 was connected by expressing Smc3 and Scc1 as a fusion protein, using a long flexible linker containing triple target sequences for the TEV protease (Haering *et al*., 2008). If connecting the C-terminus of Smc3 to the N-terminus Scc1 via a linker containing TEV protease cleavage sites enabled cells to form cohesion in the absence of Eco1, cleavage of this linker would then cause a loss in the viability of the cells by restoring the requirement of Eco1 for viability. Induction of TEV protease expression was achieved from the *GAL1-10* promoter by the addition of galactose. Strains that expressed Smc3-Scc1 fusion in the absence of Eco1 were unable to grow at 30 ^{o}C after the cleavage of the TEV linker between Smc3 and Scc1, verifying that linking Smc3 to Scc1 bypasses the requirement of Eco1 activity and permits cells to build cohesion, albeit inefficiently (Figure 2-10, M.B. Roig, unpublished data). Taken all together, these results indicate that the presence of fusion protein rescues the lethality caused by the absence of Eco1.

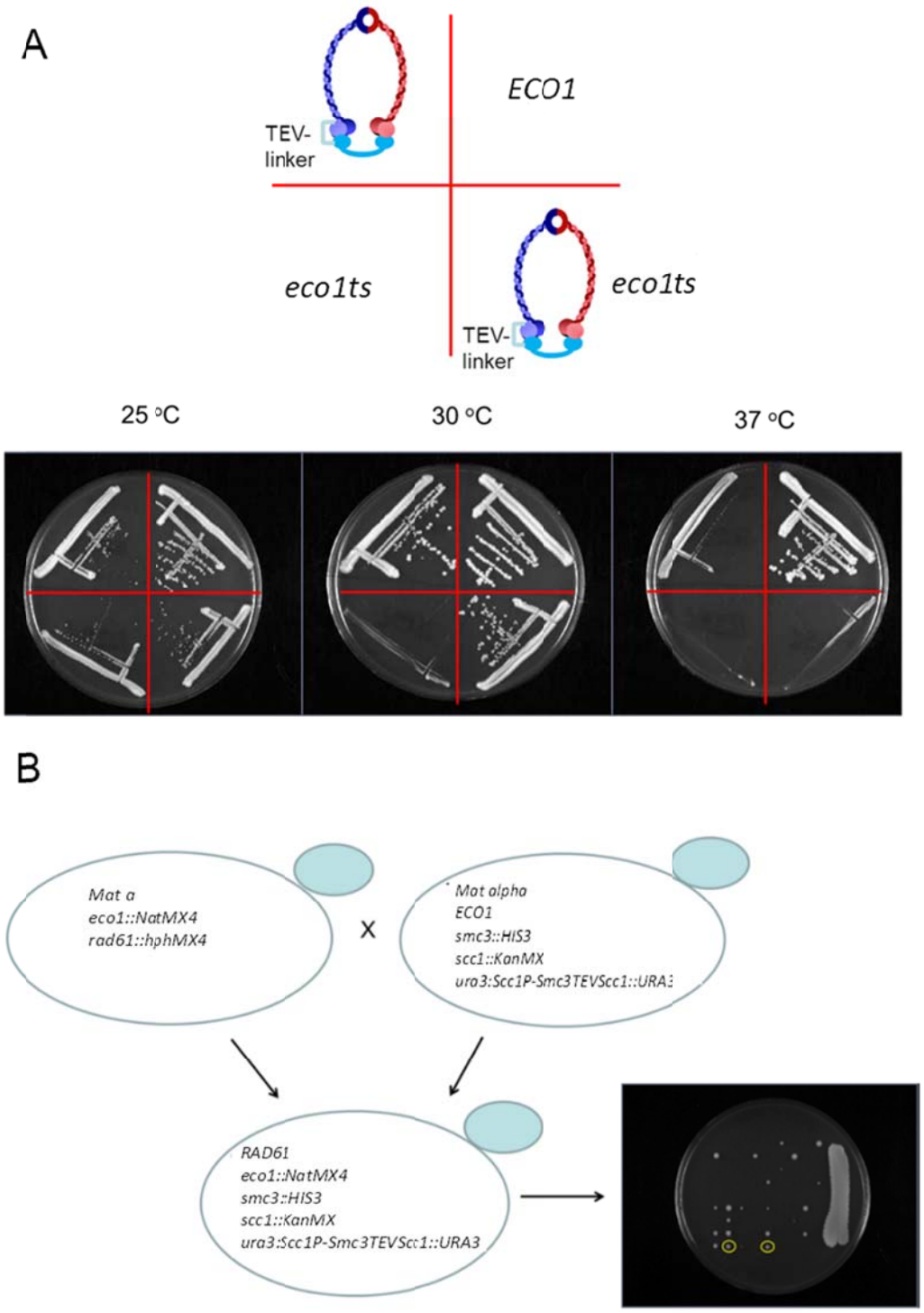
A
ECO1
TEV-
linker
eco1ts
eco1ts
TEV-
linker
25 °C
30 °C
37 °C
B
Mat a
eco1::NatMX4
rad61::hphMX4
X
Mat alpha
ECO1
smc3::HIS3
scc1::KanMX
ura3:Scc1P-Smc3TEVScc1::URA3
RAD61
eco1::NatMX4
smc3::HIS3
scc1::KanMX
ura3:Scc1P-Smc3TEVScc1::URA3

Figure 2-8

Figure 2-8: Connection of Scc1 to Smc3 permit growth in the absence of Eco1.

(A) Linking Scc1`s N terminus with Smc3`s head suppressed the lethality caused by *eco1 (G211H)* at the restrictive temperatures of 30 ^{o}C and 37 ^{o}C. Strains K699 *(Mat a, ECO1),* K16292 *(Mat a, smc3::HIS3, scc1::KanMx, ura3::Scc1P-Smc3-TEV3-Scc1::URA3),* K16456 *(Mat a, smc3::HIS3, scc1::KanMx, ura3::Scc1P-Smc3-TEV3-Scc1::URA3, eco1 (G211H)),* and K14727 *(Mat a, eco1(G211H))* were streaked onto YEPD plates and grown at 25^{o}C, 30 ^{o}C and 37 ^{o}C. Strains expressing Smc3-Scc1 fusion protein alone are viable, even though they have a growth defect at 37 ^{o}C (Experiment performed by Dr Maurici Brunet Roig).

(B) Linking Scc1`s N terminus with Smc3`s head permits growth when the *ECO1* is deleted (*Δeco1*). Strains K16431 (*Mat a, eco1::NatMx, rad61::HphMx*) and K16459 (*Mat a*, *smc3::HIS3, scc1::KanMx, ura3::Scc1P-Smc3-TEV3-Scc1::URA3* alpha). Genotypes of the encircled spores, which bear the deletion marker for *eco1Δ*, are shown (Experiment performed by Dr Maurici Brunet Roig).

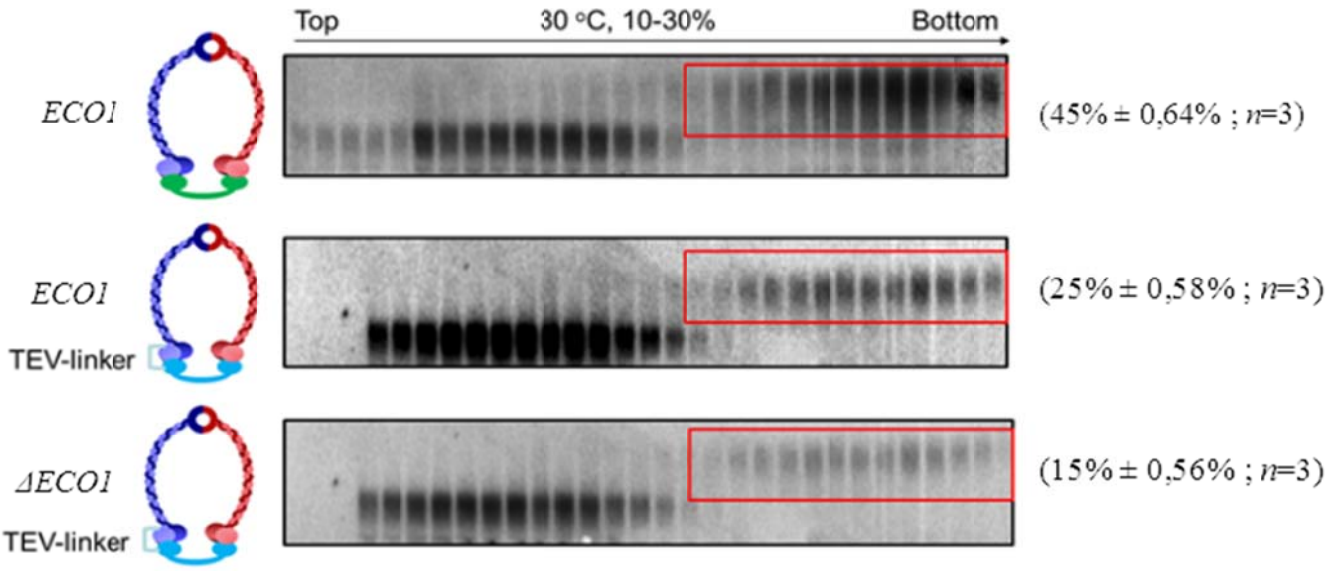

Figure 2-9: Presence of Smc3-Scc1 fusion permits cohesion between circular sister chromosomes in *eco1Δ*. The cells were arrested with nocodazole in a mitotic-like state. The clear lysates prepared from spheroplasted cells were sedimented in a sucrose gradient, followed by fractionation, agarose gel electrophoresis and Southern blotting. Dimers are marked with a red box. The percentages of minichromosome DNA present in dimer fractions for each strain are indicated.

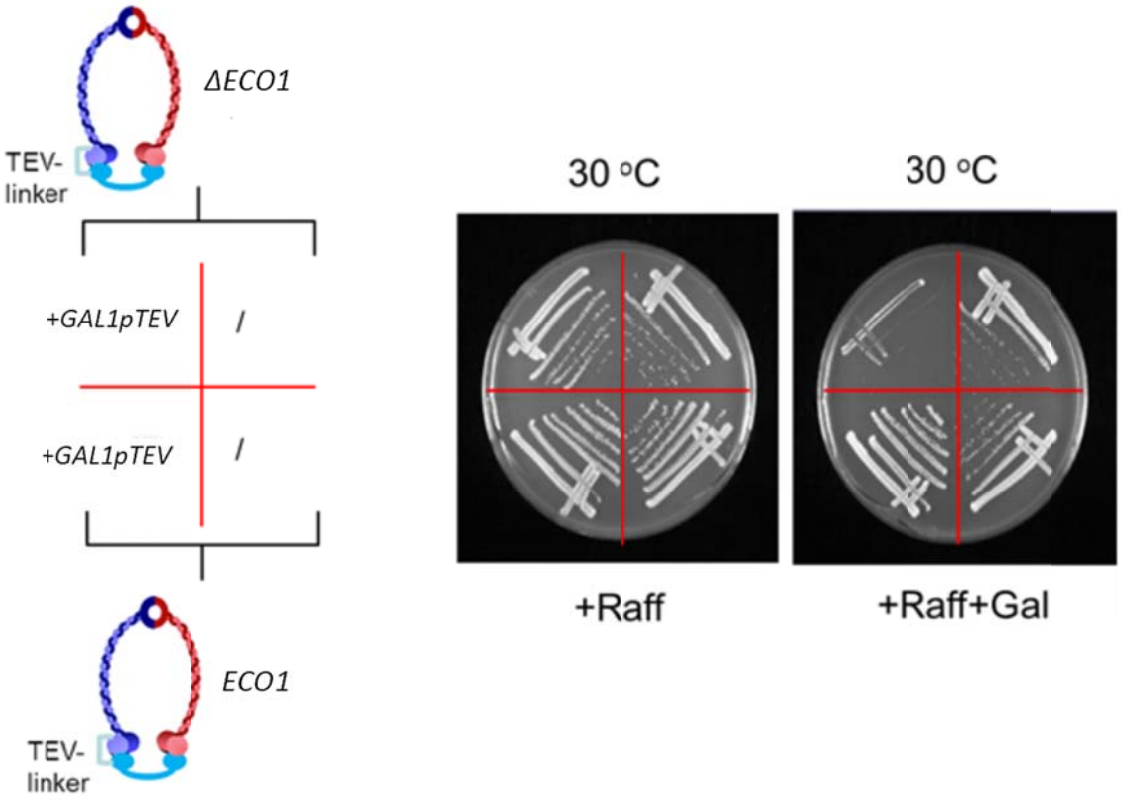

Figure 2-10: Cells are unable to grow in the absence of Eco1 after the TEV protease cleavage of the linker between Smc3 and Scc1. Strains, K16558 (*Mat a, smc3::HIS3, scc1::KanMx, ura3::Scc1P-Smc3-TEV3-Scc1::URA3, eco1::NatMx4, YEplac112-pGAL1-NLS-myc9-TEV protease-NLS-NLS*), K16560 (*Mat a, smc3::HIS3, scc1::KanMx, ura3::Scc1P-Smc3-TEV3-Scc1::URA3, eco1::NatMx4, YEplac112*), K16562 (*Mat a, smc3::HIS3, scc1::KanMx, ura3::Scc1P-Smc3-TEV3-Scc1::URA3, YEplac112),* K16564 (*Mat a, smc3::HIS3, scc1::KanMx, ura3::Scc1P-Smc3-TEV3-Scc1::URA3, YEplac112-pGAL1-NLS-myc9-TEV protease-NLS-NLS*) were streaked onto YEP+Raffinose and YEP+Raffinose+Galactose plates and incubated at 30°C for two days. Experiment performed by Dr Maurici Brunet Roig.

2.3. Discussion

The multi-subunit protein complex, cohesin, is required for the proper segregation of chromosomes during mitosis. The findings that cohesin complex forms a stable ring structure, and insertion of TEV protease cleavage sites into non-SMC subunit Scc1 or coiled-coil region of Smc3 distrupts the integrity of cohesin ring upon induction of TEV protease, have led to the proposal that cohesin holds sister chromatids together by trapping them inside its ring (Gruber *et al*., 2003; Haering *et al*., 2002). Recently, in order to test the Ring Model hypothesis, three cohesin ring subunits have been modified to create a covalently closed cohesin ring (Haering *et al*., 2008). As predicted by the Ring Model, it has been proven that in G2/M phase such chemically circularized cohesin rings still contain two circular DNAs even after protein denaturation indicating that cohesin is topologically associated with DNA.

These cross-linking experiments have raised a new possibility that cohesin may also capture individual chromatin fibres. Not much is known whether cohesin complexes associated with chromatin, but not involved in establishment of sister chromatid cohesion, trap DNA topologically. In order to investigate this, I made use of the temperature-sensitive *eco1(G211H)* mutant. Because in the absence of funtional Eco1 protein, it is possible to obtain a situation where DNA has replicated and cohesin has already loaded onto chromosomes, but no sister chromatid cohesion is established.

Through creating a chemically circularized cohesin ring in the *eco1(G211H)* mutant background, purifying small circular minichromosomes and covalently sealing the cohesin ring, I aimed at obtaining a DNA–protein complex consisting of a circular minichromosome associated to a modified cohesin complex which is resistant to denaturing conditions. Employment of 2D gel electrophoresis would then help us to analyze the nature of the interaction between protein and DNA within the complex.

However, before creating such cross-linkable strains in the *eco1* mutant background, it was crucial to check whether *eco1(G211H)* strain has a cohesin loading defect and confirm that it does not form cohesion. In the ChIP-qPCR experiment, cohesin is first maximally loaded at the centromere and then towards the end of S phase it slides out to the arm sites and outer pericentromere. As it starts to move away from the centromere, its loading kinetics slows down and density decreases. While the *ECO1* strain exhibits normal loading dynamics at all sites in terms of amount and kinetics, *eco1(G211H)* strain, despite having normal loading kinetics, shows a 2 fold decrease in amounts of cohesin loaded in the arm sites and the outer pericentromeric region.

In vertebrates, another protein called Sororin, which is a substrate of the anaphase-promoting complex, is necessary for sister chromatid cohesion during interphase (Rankin *et al*., 2005). Since Sororin-depleted cells are unable to generate normal amounts of stably chromatin-bound cohesin complexes, Sororin has been also considered to be required for stable binding of cohesin to chromatin (Schmitz *et al*., 2007). So far, Eco1 and Sororin are the only known proteins specifically required for cohesion establishment. Although it has not been addressed whether Eco1 and Sororin are collaborating to build cohesion, like Sororin, Eco1 could be also responsible for stabilizing cohesin-chromatin interactions. Therefore, without *ECO1* cohesin might be less stably associated with DNA, which can be an explanation for why I see less cohesin in the arm sites and outer pericentromere in *eco1(G211H)* cells. The ChIP-qPCR data indicate that in the absence of functional Eco1 cohesin is not loaded properly onto chromosomes. Although this loading defect is very severe at sites further from the centromere, cohesin loading seems not to be affected at centromeric and inner pericentromeric regions. Unless one would argue that the high levels of cohesin at the centromeres would not allow detection of small differences by ChIP-qPCR, these results suggest that centromeric loading is largely unaffected.

I also confirmed by minichromosomal assay that dimeric forms of minichromosomes are not present in cells that have replicated their DNA in the absence of the Eco1 protein. Dimeric minichromosomes are only formed when the loading of cohesin onto chromosomes is accompanied by the establishment of sister chromatid cohesion (Ivanov and Nasmyth, 2007). They are, however, absent from cells that have not replicated their DNA or from cells that have replicated their DNA in the absence of the Eco1 protein (Ivanov and Nasmyth, 2007). Cohesin is known to be associated with the monomers generated due to the inactivation of Eco1 in G2/M phase (Ivanov and Nasmyth, 2005). Therefore, monomeric forms observed in the absence of Eco1 in G2/M phase differ from the ones obtained due to an α-factor arrest in G1- phase, where cohesin is not yet loaded on the DNA (Ivanov and Nasmyth, 2005).

Having confirmed that *eco1(G211H)* mutants do not seem to have cohesin loading defects at core centromeric regions and do not form cohesion, I decided to proceed for creating cross-linkable cohesin ring strains in the *eco1(G211H)* mutant background. Surprisingly, it was found that the presence of Smc3-Scc1 fusion protein bypasses the lethality caused by the inactivation of Eco1 protein at the restrictive temperature (M.B. Roig, unpublished data), indicating that linking the N-terminus of Scc1 to Smc3`NBD is causing a conformational change, which might be required to convert non-cohesive cohesin bound to chromatin fibres into cohesion. Establishment of sister chromatid cohesion is regulated by Eco1 mediated-acetylation of Smc3`s NBD. The mechanistic consequences of Smc3 acetylation are still poorly understood. It is not known whether this modification assists cohesin rings to entrap DNA during S phase or stabilizes this state immediately after it has been established. Acetylation on Smc3`s NBD could also be a mark for other proteins, Scc3 or Pds5, to bind in order to keep cohesin rings closed and prevent their reopening.

The fact that the Smc3/Scc1 interface in the cross-linkable cohesin ring was connected by a translational fusion protein between Smc3 and Scc1, together with the finding that Smc3-

Scc1 fusion protein was partially functional and enabled cells to build cohesion in the absence of Eco1, abolished the experimental setup to test how "non-cohesive" cohesin interacts with chromatin. Therefore, instead of using Smc3-Scc1 fusion protein in the cross-linkable cohesin ring, I decided to close Smc3 NBD/Scc1 interface in a conditional and protein-denaturant resistant manner, thereby creating a new version of cross-linkable cohesin molecule (see Chapter 3).

Chapter 3 – Conditional cross-linking of Smc3/Scc1 interface and creation of a new cross-linkable cohesin ring

3.1. Introduction

Development of a setup, in which the covalent circularisation of cohesin complex can be induced, in combination with the mini-chromosome cohesion assay, which allows the purification of sister minichromosome DNA molecules (Ivanov and Nasmyth, 2007), has made important contributions to understand how cohesion is achieved (Haering *et al*., 2008). Although this system proved that cohesion is achieved via a topological mechanism, modification of this system is now required to understand the mechanism of "non-cohesive" cohesin association with individual chromatin fibres. In the current version of the cross-linkable cohesin molecule, successful covalent connections in Smc1/Smc3 and Smc1/C-Scc1 interfaces were achieved both in *in vivo* and *in vitro* experiments in budding yeast and the presence of four cysteine substitutions has been shown to have little or no effect on the viability of yeast strains (Haering *et al*., 2008). Due to the absence of any structural information regarding the Smc3/Scc1 interface, Smc3 was fused to Scc1 using a linker containing TEV protease cleavage sites, which therefore led to the generation of a cohesin ring where all three interfaces were covalently closed (Haering *et al*., 2008). Although the presence of Smc3-Scc1 fusion caused partial cohesion defect *in vivo* and halved the fraction of dimeric minichromosomes, it was still possible to perform the experiment to test the effect of covalent circularisation of cohesin on cohesion of the minichromosomes. However, the Smc3-Scc1 fusion protein makes the current version of cross-linkable cohesin molecule unsuitable to test how cohesin interacts with chromatin when cohesin does not form sister chromatid cohesion, due to the fact that it still permits growth in the absence of Eco1

(explained in Chapter 2). Therefore, instead of using a permanent connection between Scc1 and Smc3 in a cross-linkable cohesin ring, I decided to close Smc3 NBD/Scc1 interface conditionally, thereby creating a new version of cross-linkable cohesin molecule.

I tried two different methods to connect Scc1 to Smc3 in an inducible and protein-denaturant resistant manner. In my first attempt, I reasoned that if I were to fuse the C-terminus of Smc3 and the N-terminus of Scc1 to FRB and FKBP12 respectively, proteins that can form a complex upon addition of drug rapamycin, and design cysteine pairs based on the crystal structure of the ternary complex of FKP12/rapamycin/FRB in order to crosslink FRB and FKBP12 in a rapamycin dependent manner, I would then have a tool for conditional covalent connection of Smc3-Scc1 interface (Figure 3-1A). Upon isolation of minichromosomes from strains expressing Smc3-FRB, FKBP12-Scc1 and Smc1 proteins containing cysteine pairs at FRB/FKBP12, Smc1/3, and Smc1/Scc1 interfaces, the effect of cohesin circularisation by chemical cross-linkers in the presence of rapamycin could then be investigated by electrophoresis of DNAs after SDS denaturation (see Section 3.2.1.).

The second attempt of cross-linking the Smc3-Scc1 interface involves the usage of an unnatural photo-cross-linkable amino acid that can be induced to form covalent bonds with neighbouring proteins upon excitation at 350nm light. This approach allows the mapping of protein-protein interactions *in vivo*, and therefore would be useful to obtain an efficient cross-linking interaction between Smc3`s NBD and the N-terminal domain of Scc1, which should then allow me to generate a new version of covalently closed cohesin ring, whose Smc3/Scc1 interface is photo-cross-linked, whereas Smc1/Smc3 and Smc1/Scc1 interfaces are chemically cross-linked (see Section 3.2.2.).

3.2. Results

3.2.1. Conditional cross-linking of Smc3/Scc1 interface in a rapamycin-dependent way

3.2.1.1. Design of the cross-linkable residues

In order to close Smc3-Scc1 interface conditionally, I took advantage of the fact that the human proteins FKBP12 and FRAP are able to interact with each other strongly only in the presence of rapamycin (Figure 3-1B; Belshaw *et al*., 1996; Chen *et al*., 1995). Rapamycin (Sehgal *et al.,* 1975) is a potent immunosuppressive agent, which binds two proteins: the FK506-binding protein (FKBP12) and the FKBP-rapamycin-associated protein (FRAP) (reviewed by Schreiber, 1991) (Figure 3-1B). Rapamycin binds to FKBP12 with a very high affinity having a dissociation-constant (K_D) 0.4nM (Harding *et al.,* 1989; Siekierka *et al.,* 1989). Human FRAP is a 289kDa protein that binds FKBP12-rapamycin, and is required for G1 cell cycle progression (Brown *et al*., 1994; Sabatini *et al.,* 1994). Binding of FRAP to FKBP12-rapamycin is mediated by a small domain, the FKBP12-rapamycin-binding (FRB) domain, that can be expressed as an 11-kD soluble protein (Chen *et al*., 1995). Rapamycin alone cannot bind FRB efficiently, while rapamycin in complex with FKBP12 binds FRB to form a tight ternary complex of nanomolar dissociation constant (Banaszynski *et al*., 2005).

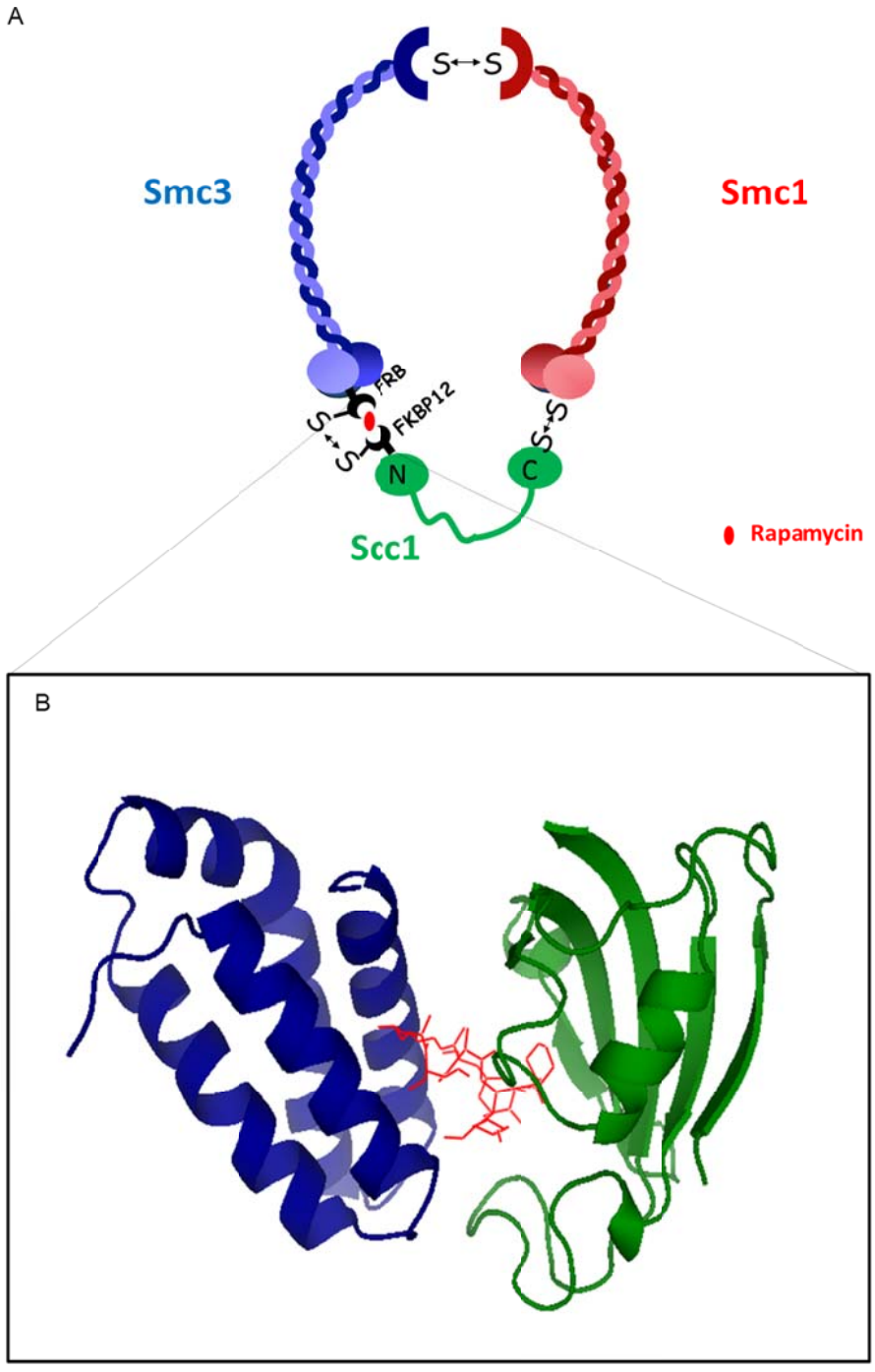

Figure 3-1

Figure 3-1: Creating a new cross-linkable cohesin whose Smc3/Scc1 interface is covalently connected in a rapamycin inducible manner.

(A) Scheme showing a modified version of cohesin ring: cysteine containing FRB and FRBP12 proteins, which are fused to Smc3 and Scc1, respectively, are combined with the cysteine mutations between the Smc1-Smc3 hinges and Scc1-Smc1 head regions in order to create a new cross-linkable cohesin.

(B) Crystal structure showing the ternary complex of human FKBP12, rapamycin, and the FKBP12-rapamycin binding (FRB) domain of human FRAP. In blue is depicted FRB, in red rapamycin, and in green FKBP12 (Choi *et al*., 1996; Liang *et al*., 1999).

The crystal structure of the ternary complex of human FKBP12, rapamycin, and the FKBP12-rapamycin binding (FRB) domain of human FRAP (Choi *et al*., 1996; Liang *et al*., 1999) helped us to identify residues that are close enough to form disulphide bridges when mutated to cysteines. Rapamycin is located at the center of the ternary complex and uses different faces to interact with FKBP12 and FRB (Figure 3-2). FKBP12 contains a twisted β-sheet wrapped around a short α-helix. Rapamycin binds in a hydrophobic pocket formed between the β-sheet and α-helix. The FRB domain forms a four helix bundle and the four helices are connected by short loops. Rapamycin is bound to a hydrophobic cleft present in FRB near the crossing point of α1 and α4. The interactions between FRB and rapamycin are completely hydrophobic (Choi *et al*., 1996; Liang *et al*., 1999). Although rapamycin interacts extensively with both protein partners, interactions between FKBP12 and FRB are relatively limited. Two regions of the complex show interactions between the proteins: residues in the 40s loop of FKBP12 with α4 of FRB, and the 80s loop of FKBP12 with the α1-α2 region of FRB. Moreover, loop regions of FKBP12, especially the 40s loop and the 80s loop have been reported to be more flexible than other regions of FKBP12 (Liang *et al*., 1999). Among the residues that are not closely situated in the vicinity of the rapamycin binding pocket, three pairs of residues (G89-V2094; T85-R2042; D37-K2095) were chosen in the regions where FKBP12 - FRB interact with each other, that are very likely to form disulphide bridges when they are changed to cysteines according to their proximities calculated using molecular visualization software Pymol (Figure 3-2).

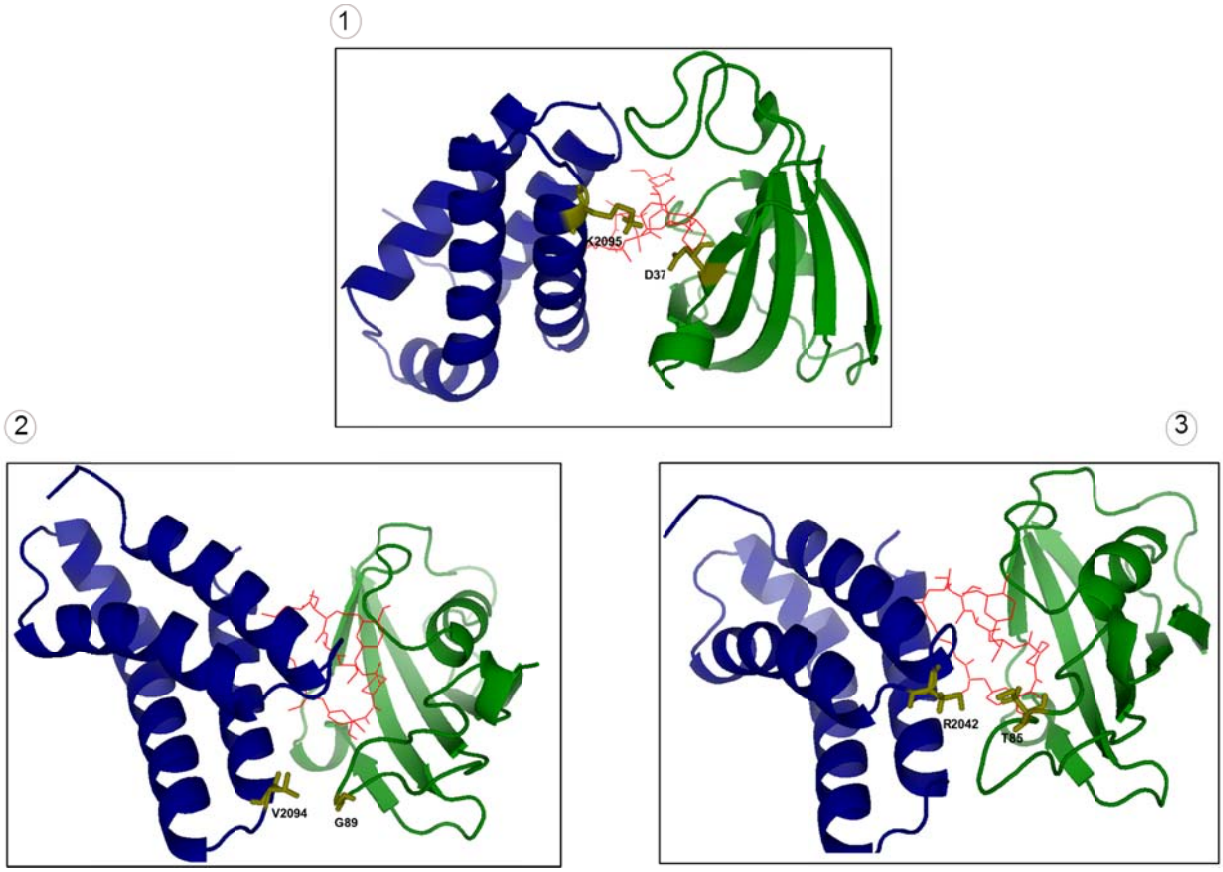

Figure 3-2: The pairs of residues selected for mutagenesis to cysteines in the ternary complex of FRB(blue), rapamycin(red) and FKBP12(green): residues selected for mutagenesis are highlighted in yellow: 1. K2095(FRB)-D37(FKBP12); 2. V2094(FRB)-G89(FKBP12); 3. R2042(FRB)-T85(FKBP12).

3.2.1.2. *In vitro* chemical cross-linking of the FKBP12 and FRB proteins

In order to test and optimize the induction of the covalent connection between the selected pairs, I separately expressed wild type and cysteine mutant FKBP12 and FRB proteins from *E.coli* (*Escherichia coli*) and purified to homogeneity either using affinity and size exclusion chromatography (Figure 3-3A and B). However, before optimizing the cross-linking conditions, it was important to first check whether the mutant FRB and FKBP12 proteins

bind each other and form a functional ternary complex in the presence of rapamycin in a pull-down assay using MBP-FRB. An equimolar mixture (each at 1μM) of GST-FKBP12 and rapamycin were pre-mixed in 1 ml of binding buffer. After incubation for 30 minutes at 4 ^{o}C, 1μM of purified MBP-FRB protein was added to the mixture together with anti-MBP (amylose) beads. As shown in Figure 3-4, while in the presence of rapamycin FKBP12 (T85C)-FRB(R2042C) and FKBP12(G89C)-FRB(V2094C) associated with each other, FKBP12 (D37C)-FRB (K2095C) failed to form a functional ternary complex. Since the residues of D37C in FKBP12 and K1095C in FRB are not situated in the vicinity of the rapamycin binding pocket, it is unlikely that proteins bearing these mutations are defective in rapamycin binding. Therefore, it is possible that mutations on these sites may perturb the tertiary structures of FRB and FKBP12, thereby preventing the formation of a FKBP12-rapamycin-FRB ternary complex.

After having identified the mutant protein combinations that were able to form functional ternary complexes, I next tested whether the mutated pairs of cysteine residues can be oxidised to form disulphide bridges. Homobifunctional cross-linkers were used in order to introduce covalent links between the two cysteine thiol groups, since they can span larger distances (Figure 3-5). Since two homobifunctional cross-linking agents, BMOE (bis-maleimidoethane) and bBBr (bibromobimane), were previously tested for their amenability in building covalent links between Smc3/Smc1 hinge and the Smc1/C-Scc1 globular heads (Haering *et al*., 2008), I first decided to use these chemicals to test whether they can form covalent bridges between FRB and FKBP12. BMOE and bBBr can cross-link the neighbouring cysteines within the range of 3-8 Å and 3-6 Å, respectively.

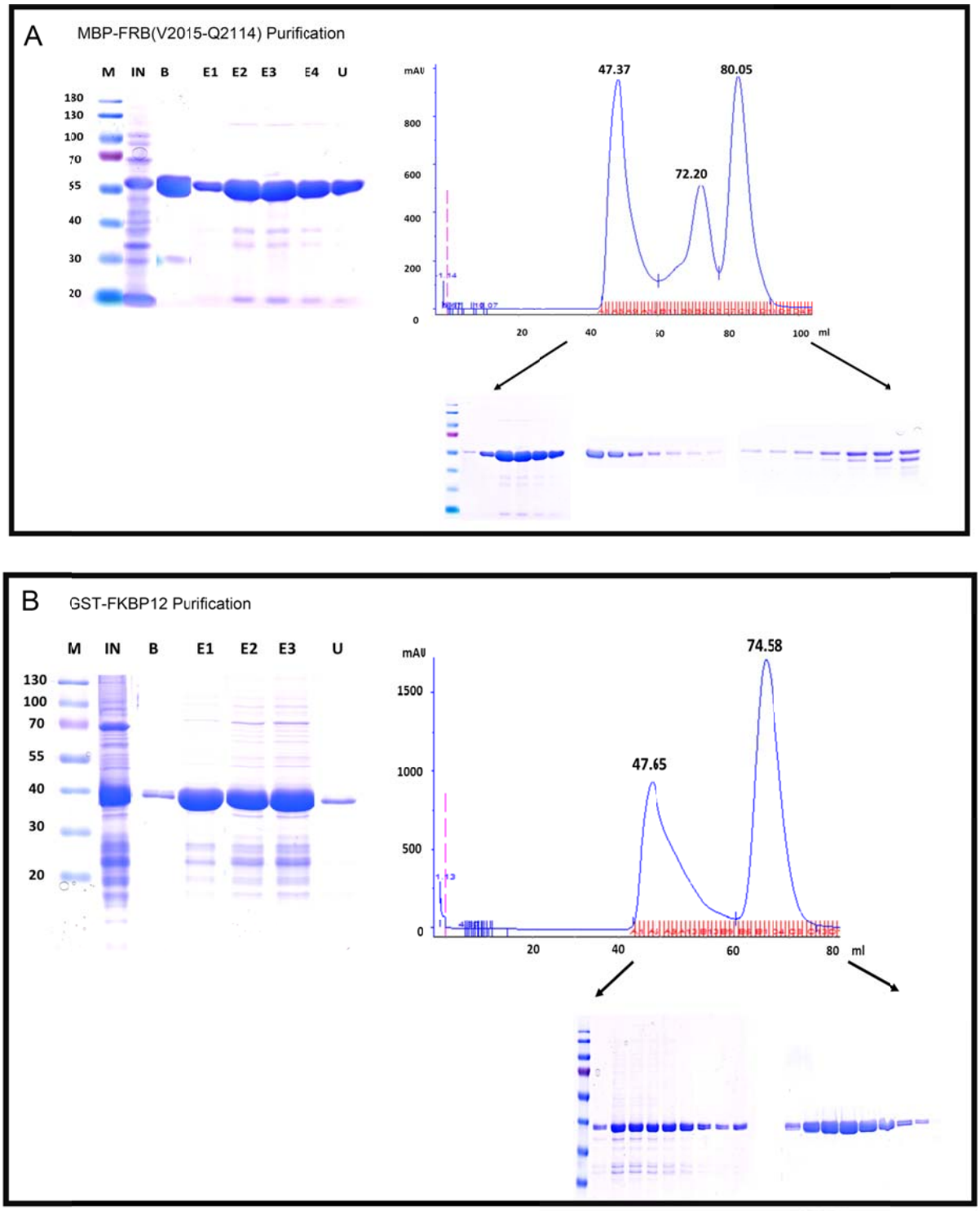
A
MBP-FRB(V2015-Q2114) Purification
M IN B E1 E2 E3 E4 U
130
130
100
70
55
40
30
20
mAU
800
600
400
200
0
47.37
80.05
72.20
20
40
60
80
100 ml
B
GST-FKBP12 Purification
M IN B E1 E2 E3 U
130
100
70
55
40
30
20
mAU
1500
1000
500
0
74.58
47.65
20
40
60
80 ml

Figure 3-3

Figure 3-3: Purification of GST-FKBP12 and MBP-FRB proteins

The wild type and mutant GST-FKBP12 and MBP-FRB fusion proteins were expressed and purified in two steps from *E. coli.* Two step purification for **(A)** MBP-FRB and **(B)** GST-FKBP12 fusion proteins. First step by affinity chromatography: **(A)** using amylose resin and protein eluted by 10mM maltose, **(B)** using glutathione sepharose beads and protein eluted by 10 mM glutathione. Upper lanes showing the intermediate fractions in the purification of MBP-FRB and μGST-FKBP12 as *Input (I), bound fraction (B), protein eluted (E1, E2, E3 and E4)* and *non-eluted protein (U).* Second step size-exclusion chromatography using Superdex 200 26/60 column. Peak fractions were collected and resolved on 12% SDS-PAGE. In case of MBP-FRB, three major peaks were observed at 44.37 ml, 72.20 ml, and 80.05 ml. Because the first and the third peaks contain degraded fragments, fractions from the second peak were pooled, concentrated and used for binding assays and cross-linking experiments. In case of GST-FKBP12, two major peaks observed at 47.65 ml and 74.58 ml. Because the first peak contains high molecular weight contaminants, the fractions from the second peak were pooled, concentrated and used for binding assays and cross-linking experiments.

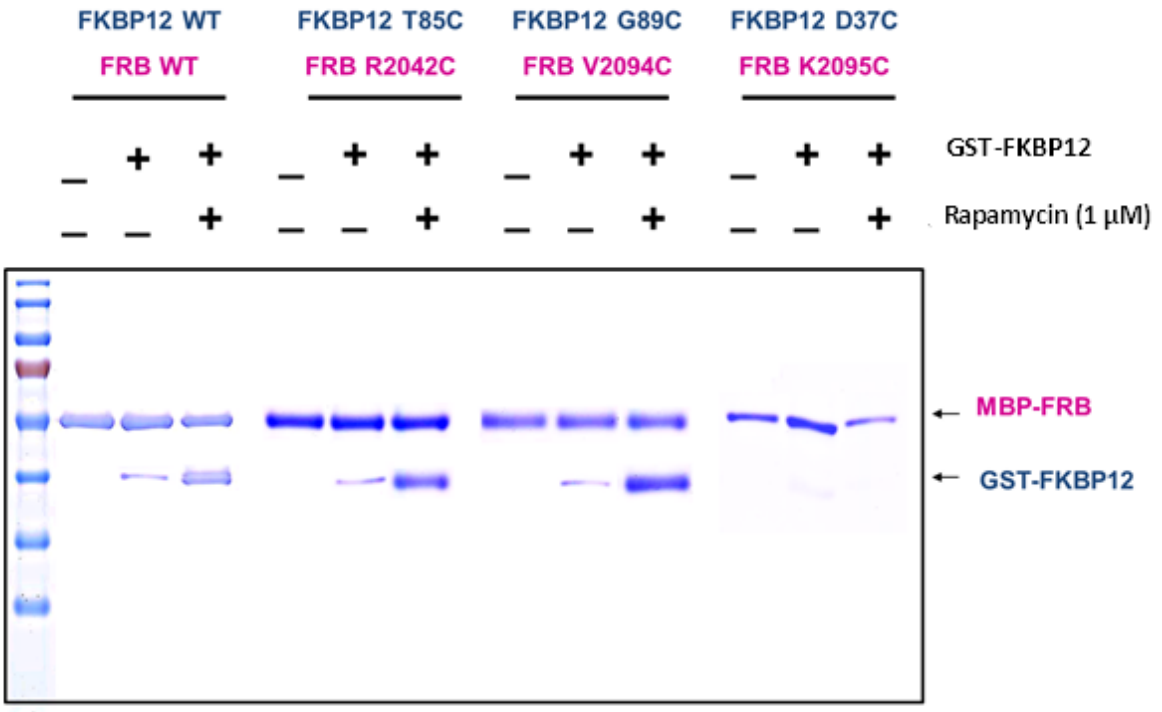

Figure 3-4: *In vitro* analysis to measure the FKBP12-rapamycin-FRB heterodimer formation

GST-FKBP12 and rapamycin were pre-mixed in 1 ml of binding buffer (100 mM NaCI, 50 mM Tris pH 7.5 with 1 mM DTT) at 1 µM each, followed by addition of 1 µM MBP-FRB protein and brief incubation on ice. Amylose resin (20 µl) was then added to the mixture and rocked at 4 ^{o}C for 1 hr. The matrix was subsequently washed three times in 1 ml of binding buffer and boiled in SDS sample buffer and loaded on a 12% SDS-PAGE gel.

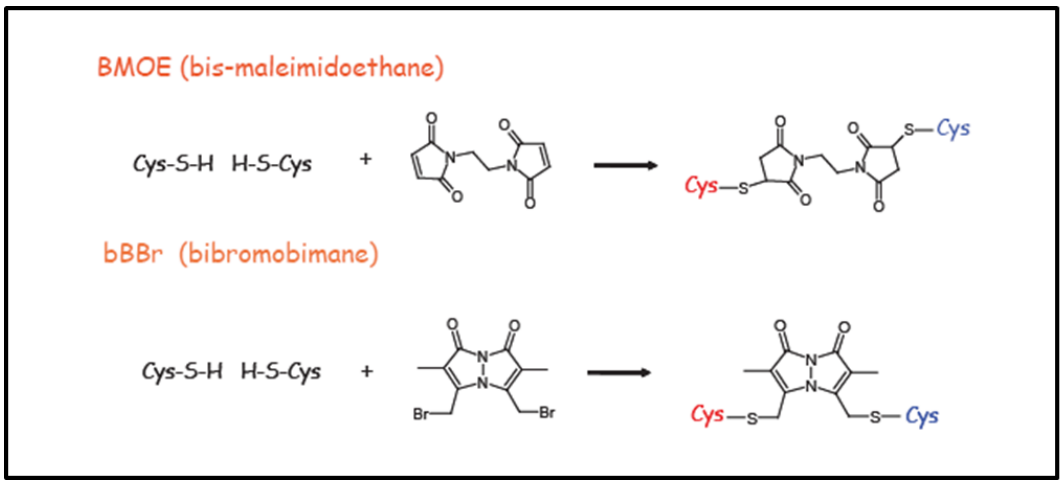

Figure 3-5: BMOE and bBBr can cross-link the neighbouring cysteines within the range of 3-8 Å and 3-6 Å, respectively.

Functional mutant FRKBP12/FRB complexes were incubated with various concentrations of the chemical cross-linkers (1-5mM) in the presence of 1mM rapamycin (data not shown). I found that in the presence of rapamycin the optimum cross-linker concentration for creating a covalent bridge for all the chosen pairs between FRB and FKBP12 was 1mM bBBr and 5mM BMOE. The best crosslinking efficiency that I obtained was 85%, which is in between the pair of FKBP12 (T85C) and FRB (R2042C). I also achieved 70% crosslinking between FKBP12 (G89C) and FRB (V2094C). The third pair, FKBP12 (D37C) and FRB (K2095C), gave 20% efficiency due to the fact that this pair is deficient in forming a functional ternary complex (Figure 3-6A). Cross-linking efficiency decreased significantly in the absence of rapamycin, indicating that formation of a functional ternary complex is essential for an efficient covalent connection (Figure 3-6B). Taken all together, using the crystal structure of FKBP12-rapamycin-FRB complex, I have identified two pairs of mutants that can be efficiently cross-linked with cross-linking agents, bBBr and BMOE, only in the presence of rapamycin *in vitro*.

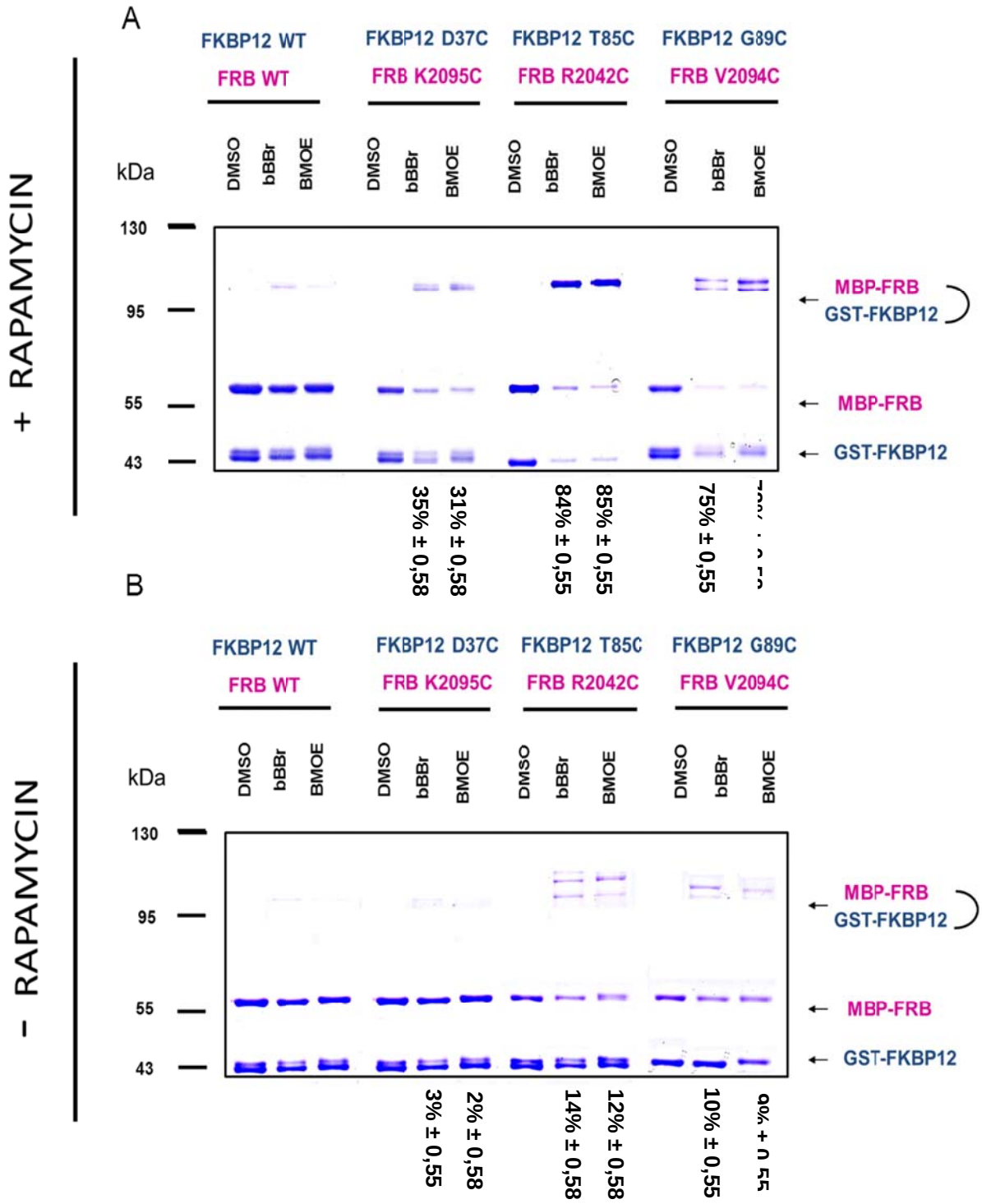

Figure 3-6: *In vitro* chemical cross-linking of FKBP12 and FRB proteins in the presence or absence of rapamycin. Wild-type or mutant FKBP12 and FRB proteins were incubated in the presence or absence of 1µM rapamycin for 1hr at 4 °C, and subjected to dialysis in order to remove the reducing agent DTT. Proteins in the presence **(A)** or absence **(B)** of 1 µM rapamycin were then incubated for 10 minutes with DMSO or final concentrations of 200mM bBBr or 1mM BMOE. Samples were boiled in SDS sample buffer, loaded on a 12% SDS-PAGE gel, and visualised by Coomassie blue staining. Values are means ± standard deviation combined from 3 replicates (n = 3).

3.2.1.3. Strains expressing Smc3-FRB and FKBP12-Scc1 do not have a cohesion defect.

Having established that purified FRB and FKBP12 proteins can be cross-linked *in vitro*, I next created a yeast strain where the C-terminus of Smc3 and the N-terminus of Scc1 are fused to FRB and FKBP12, respectively and transformed with a 2.3kb minichromosome. In order to test whether modifying the cohesin complex by introducing such fusions would affect the establishment and maintenance of sister chromatid cohesion, their ability to hold sister chromatids together was measured. Cells grown at 30 ^{o}C were arrested in a mitotic-like state through the addition of the microtubule depolymerising drug, nocodazole, clear lysates were extracted and subjected to sucrose gradient centrifugation followed by fractionation, agarose gel electrophoresis and Southern blotting. The detection, by Southern blot, of the minichromosomal DNA revealed that the modified cohesin complex containing the FKB12-Scc1 and Smc3-FRB fusion proteins showed a cohesion pattern similar to wild-type, with 40% of the fractionated minichromosomes in a dimeric form, suggesting that the modification introduced in the strain did not result in a defect in cohesion (Figure 3-7).

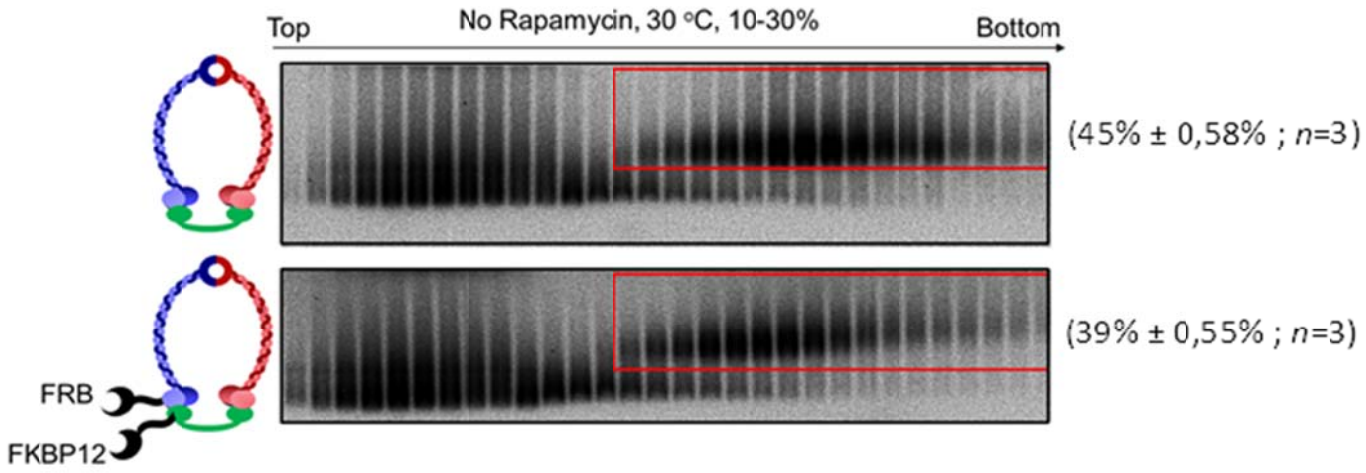

Figure 3-7: Presence of FKBP12-Scc1 and Smc3-FRB fusion proteins do not cause a reduction in the amount of dimeric minichromosomes.

Cell cultures bearing a 2.3kb minichromosome K15103 and K19145 (*Mat a, Smc3-GL-mFRB::HIS3, scc1::NatMx, ura3::FKBP12-GL-Scc1-PK6-Avitag::URA3, 2.3kb TRP1-Cen4-ARS1 minichromosome*) were grown in a nocodazole containing media at 30 ^{o}C. Clear lysates were sedimented in a 10-30% sucrose gradient at 18krpm for 15hr in a Beckman SW41 rotor, followed by fractionation and electrophoresis on a 0.8% agarose gel for 7.5hr at 4 ^{o}C. Dimeric populations are highlighted by a red box. Quantification of the dimeric population revealed that the abundance of dimeric minichromosomes is slightly decreased in the presence of FKBP12-Scc1 and Smc3-FRB as compared to the wild-type strain.

3.2.1.4. Cross-linking of FKBP12-Scc1 and Smc3-FRB proteins in yeast extracts

To test whether cysteine containing FBR and FKBP12 can also cross-link when they are fused to Smc3 and Scc1, clear lysates were prepared from yeast cells arrested in G2/M at 30 ^{o}C by nocodazole in order to minimize cleavage of Scc1 by separase. Wild-type or mutant FKBP12-Scc1 proteins were immunoprecipitated with PK-specific antibodies, and immunocomplexes were isolated by adsorption to protein A sepharose beads. Beads were washed extensively in reaction buffer (25mM NaPi pH7.4, 50mM NaCI, 10mM $MgSO_4$, 0.25% Triton X-100) to remove DTT, and other low molecular contaminants which are known to interfere with the chemicals required for the cross-linking reaction. Beads were then incubated with 100μg/ml rapamycin for 1hr in order to induce the heterodimerization of FKBP12 and FRB and the samples were then treated with DMSO, bBBr or BMOE. Immunocomplexes were recovered by incubation with elution buffer containing 1% SDS for 10min at 65 ^{o}C. The reaction was stopped with DTT. Samples were separated on a 3-8% Tris-Acetate gel and the detection of the PK6 epitope-tagged-FKBP12-Scc1 was performed using an anti-pk antibody (Figure 3-8). I managed to obtain covalently linked products for the two cysteine pairs that were shown to cross-link efficiently. The cross-linked species of the FKBP12-Scc1/Smc3-FRB heterodimer were specific to the presence of the cysteine pairs and to the treatment with the bBBr or BMOE. However, the measured efficiency of cross-linking was 30% for the FKBP12(T85C)-Scc1/Smc3-FRB(R2042C) combination (Figure 3-8) and 10% for the combination of FKBP12(G89C)-Scc1/Smc3-FRB(V2094C) (Figure 3-8). This result was rather surprising, since I was able to obtain 75-80% cross-linking efficiencies between the same cysteine pairs with the purified proteins *in vitro* (Figure 3-6). Moreover, my attempts to maximise the efficiency of cross-linking (i.e. changing the rapamycin or the cross-linker concentrations) also did not help (data not shown).

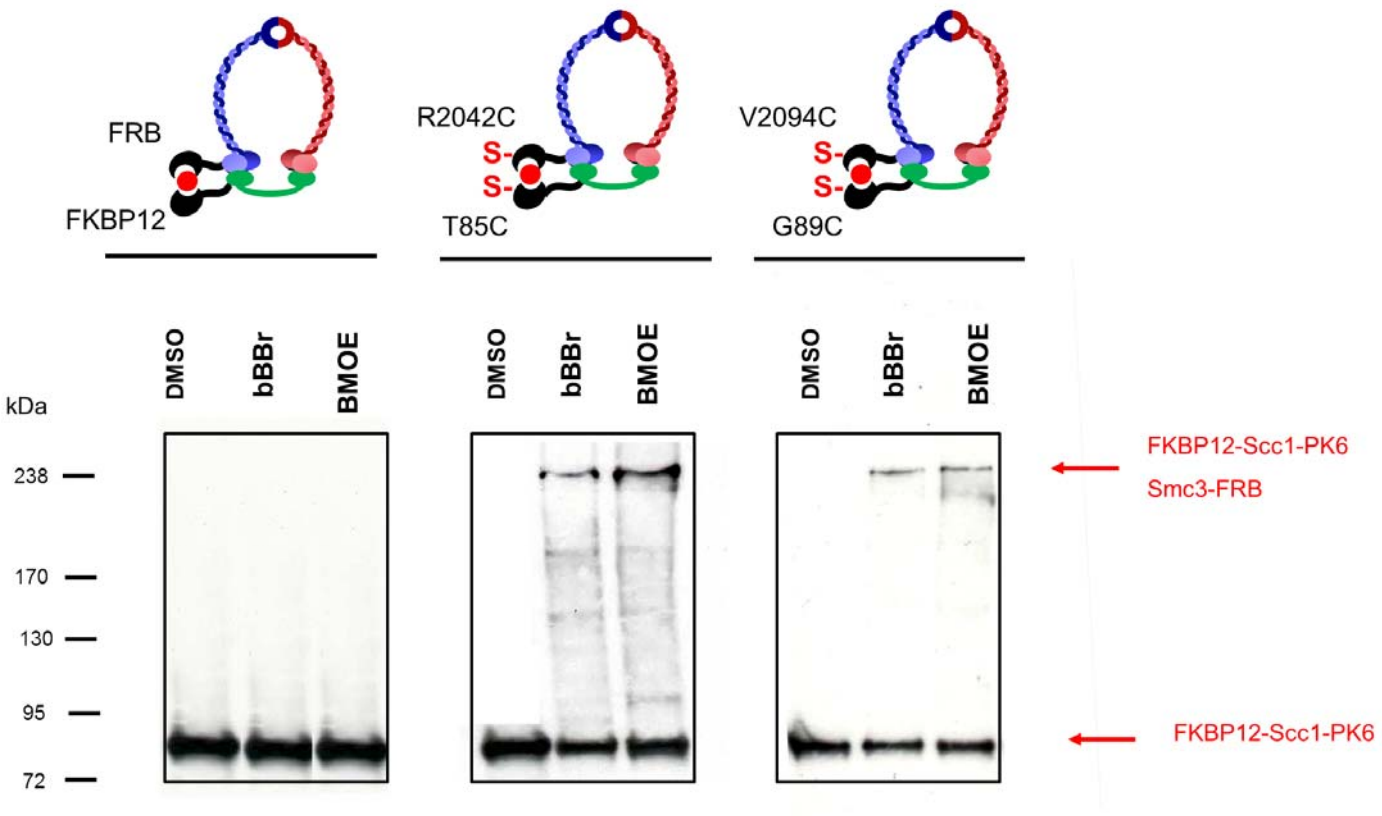

Figure 3-8: Testing the efficiency of chemical cross-linking between FKBP12-Scc1 and Smc3-FRB proteins in yeast extracts. Soluble extracts were prepared from nocodazole arrested yeast cells expressing either wild type, K19149*(Mat a, ura3::FKBP12-GL-Scc1-PK6-Avitag::URA3, Smc3-GL-mFRB::HIS3, scc1::NatMx, leu2:Smc1-myc9::LEU2, smc1::KanMx*), or cysteine substituted FKBP12-Scc1-PK6 and FRB-Smc3 proteins, K19151(*Mat a, ura3::FKBP12(T85C)-GL-Scc1-PK6-Avitag::URA3, Smc3-GL-mFRB(R2042C)::HIS3, scc1::NatMx, leu2:Smc1-myc9::LEU2, smc1::KanMx*) and K19172 *Mat a, ura3::FKBP12(G89C)-GL-Scc1-PK6-Avitag::URA3, Smc3-GL-mFRB(V2094C)::HIS3, scc1::NatMx, leu2:Smc1-myc9::LEU2, smc1::KanMx* as labelled in the figure. Scc1 was immunoprecipitated using anti-PK antibody in the presence of rapamycin and isolated immunocomplexes were then incubated with DMSO, bBBr or BMOE for 10min at 4^{o}C in the presence of rapamycin. Samples were boiled in SDS containing buffer for 10min and separated on a 3-8% Tris-Acetate gel followed by western blotting with anti-PK antibody.

In order to check whether addition of rapamycin inhibits the cross-linking reaction in yeast extracts, I tested its effect on cross-linking using the hinge regions of Smc1 and Smc3. *S.cerevisiae* Smc1-Smc3 hinge heterodimer has already been shown to be cross-linked at 60-70% efficiency with bBBr or BMOE (Haering *et al*., 2008). After nocodazole arrest and cell lysis, wild-type or cysteine containing Smc1-myc$_9$ proteins were immunoprecipitated with myc-specific antibodies and beads were incubated with 100µg/ml rapamycin for 1hr. Upon treatment with DMSO and bBBr, the cross-linking efficiency was analysed by western blot analysis. Compared to the untreated sample, crosslinking of hinge heterodimer was barely, if at all, affected by the presence of rapamycin (Figure 3-9), indicating that rapamycin does not interfere with the cross-linking chemicals that are used.

Although I was able to get covalently linked products *in vitro* with cross-linking efficiency around 75%, approximately only 30% of the material in yeast extracts was found to form disulphide bridges in the presence of rapamycin. Considering the fact that linking Smc3 to Scc1 via a TEV linker is equal to having a cross-linking with 100% efficiency, using FKBP12-FRB system to close this interface would approximately create four times less efficient cross-linkable cohesin molecule than the current version. Therefore, I decided to devise a new and more efficient way of cross-linking Smc3-Scc1 interface *in vivo* (see chapter 3.2.2).

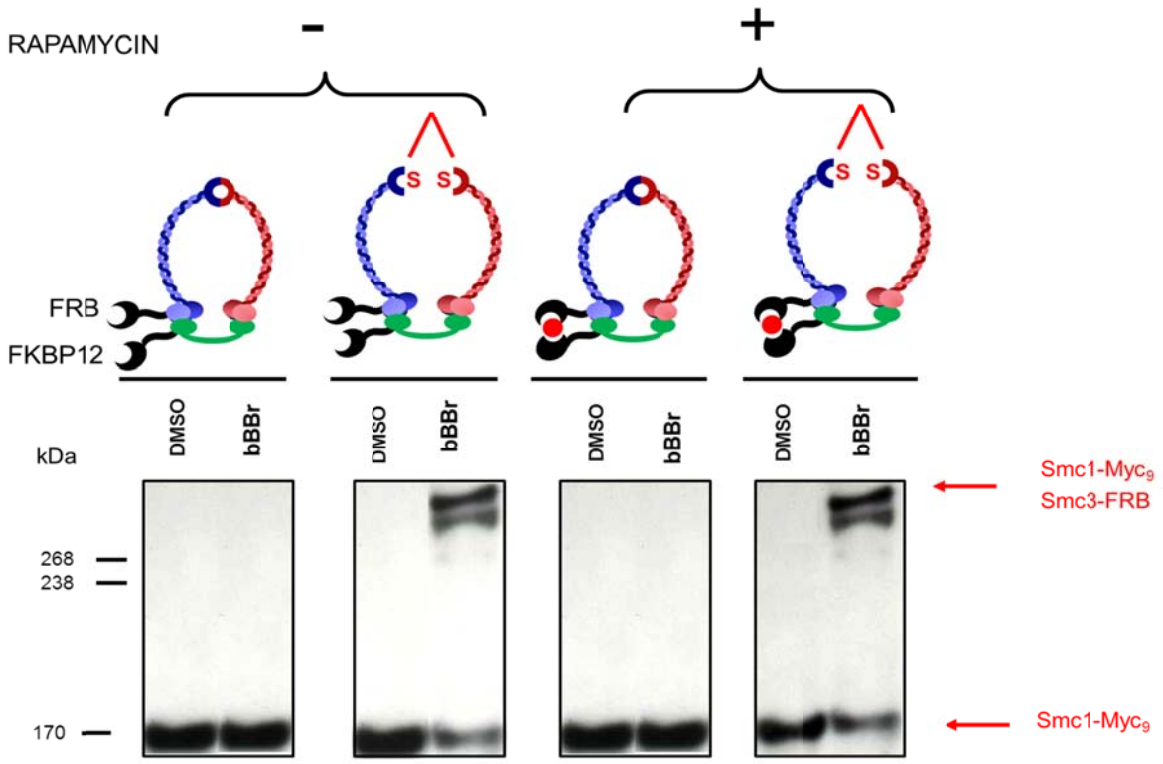

Figure 3-9: Presence of rapamycin does not interfere with the cross-linking reaction.

Clear extracts were prepared from nocodazole arrested yeast cells of K19147(*Mat a, ura3::FKBP12-GL-Scc1-PK6-Avitag::URA3, Smc3(E570C)-GL-mFRB::HIS3, scc1::NatMx, leu2:Smc1(K639C)-myc9::LEU2, smc1::KanMx*) and K19149. Smc1 and Smc3 hinge domains were either wild type or carrying E570C and K639C mutations in the yeast strains, as labelled in the figure. Smc1 was immunoprecipitated using anti-Myc antibody, and then incubated with DMSO, or bBBr for 10min at 4^{o}C in the presence of rapamycin. Samples were run on a 3-8% Tris-Acetate gel and the cross-links were detected by western blotting.

3.2.2. *In vivo* photo-cross-linking of Smc3/Scc1 interface

An alternative method to close Smc3-Scc1 interface covalently involves the usage of photo-chemical cross-linking by site-specific incorporation of a photo-cross-linkable unnatural amino acid at specific locations of Smc3`s NBD or the N-terminal domain of Scc1.

Expansion of the genetically encoded amino acids with unnatural amino acids with novel chemical, physical and biological properties has increased our ability to manipulate protein structure and function *in vivo* and *in vitro* (Wang *et al*., 2001; Chin *et al*., 2002; Chin *et al*., 2003). Development of the methodology, which allows incorporation of unnatural amino acids with a high translational fidelity into the proteins *in vivo,* has played a significant role in studying protein-protein interactions (Chin *et al*., 2002; Chin *et al*., 2003). Among the unnatural amino acids, benzophenone containing amino acids have been widely used to cross-link small molecules or peptides to proteins in order to identify and map protein-protein interactions (Dorman and Prestwich, 1994). An elegant tool has been developed for site-specific incorporation of the photo-cross-linking amino acid *ρ*BPA (*ρ*-benzoyl-l-phenylalanine) into proteins *in vivo* (Figure 3-10; Chin *et al*., 2002; Chin *et al*., 2003). *ρ*BPA, is similar to phenylalanine, containing an additional benzoyl group which can be activated upon excitation at 350-365nm (Figure 3-11). Having a benzophenone group makes *ρ*BPA particularly reactive with unactivated carbon-hydrogen bonds (C-H). Moreover, in contrast to other photo-cross-linking groups, benzophenones do not photodissociate and this allows repeated excitation by long-wavelength UV light and thereby efficient cross-linking yields (Kauer *et al*., 1986). *In vivo* incorporation of *ρ*BPA into proteins expressed in bacteria or yeast is carried out in response to the amber stop codon, TAG. Because the amber codon is the least used among the 64 unique genetic codons in *E.coli* and *S. cerevisiae*, it has been chosen as the most suitable candidate for the reassignment to an unnatural amino acid. The

use of an amber codon to encode an unnatural amino acid relies on an orthogonal aminoacyl tRNA synthetase-tRNA pair that does not interfere with the endogenous translational machinery and incorporates *ρ*BPA, but not any of the 20 common amino acids at the position encoded by the amber codon in the target gene (Figure 3-10; Chin *et al*., 2002; Chin *et al*., 2003). Upon excitation by 350 nm light, incorporated *ρ*BPA in the protein of interest is induced to form a covalent bond with neighbouring unactivated C-H bonds within approximately 6.5Å, thereby enabling one to covalently capture protein-protein interactions.

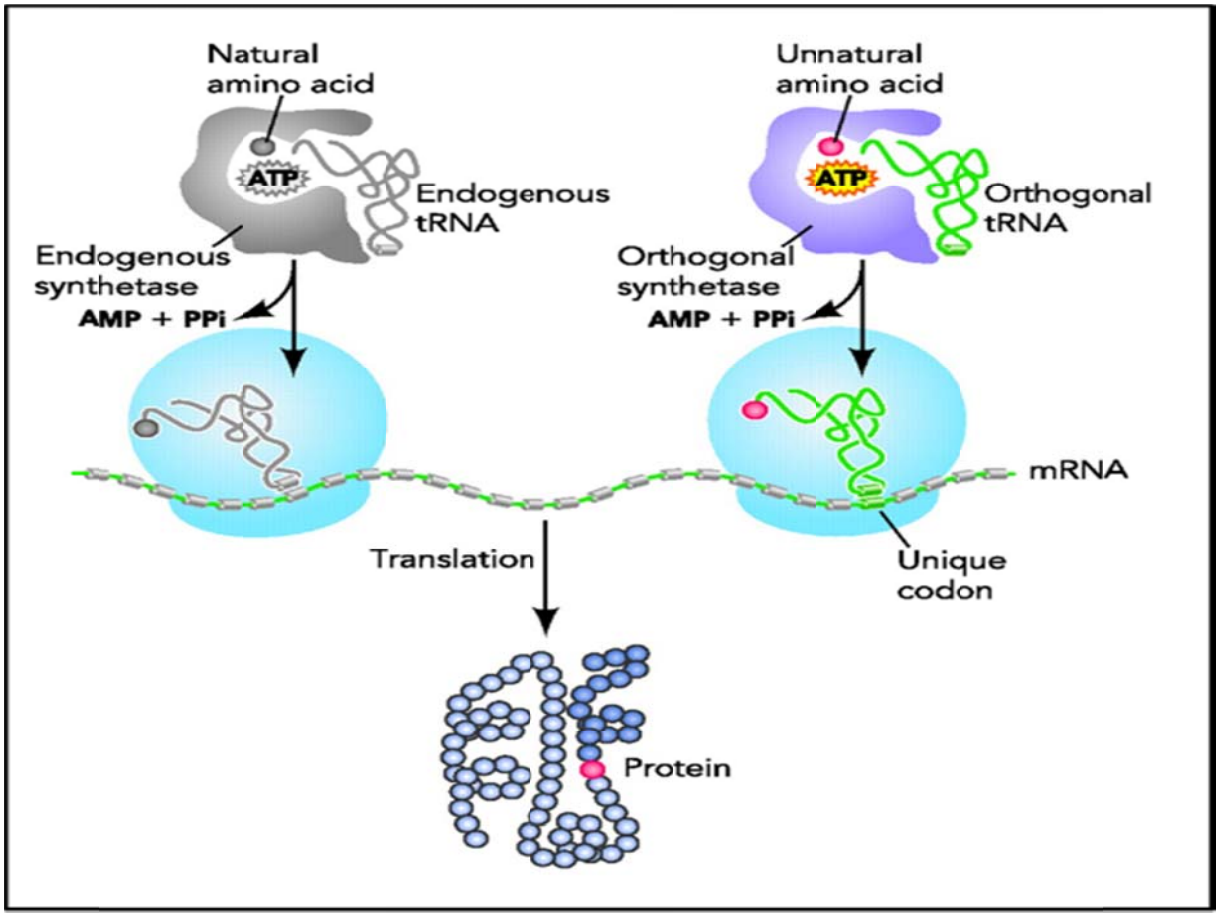

Figure 3-10: Various modifications can be site-specifically introduced into proteins in the format of an unnatural amino acid.

Unnatural amino acid (e.g., *ρ*BPA) can be incorporated into the protein of interest by a modified orthogonal pair, an orthogonal tRNA and an orthogonal aminoacyl-tRNA synthetase, that recognises the amber stop codon TAG (Adapted from Lin and Wang, 2008).

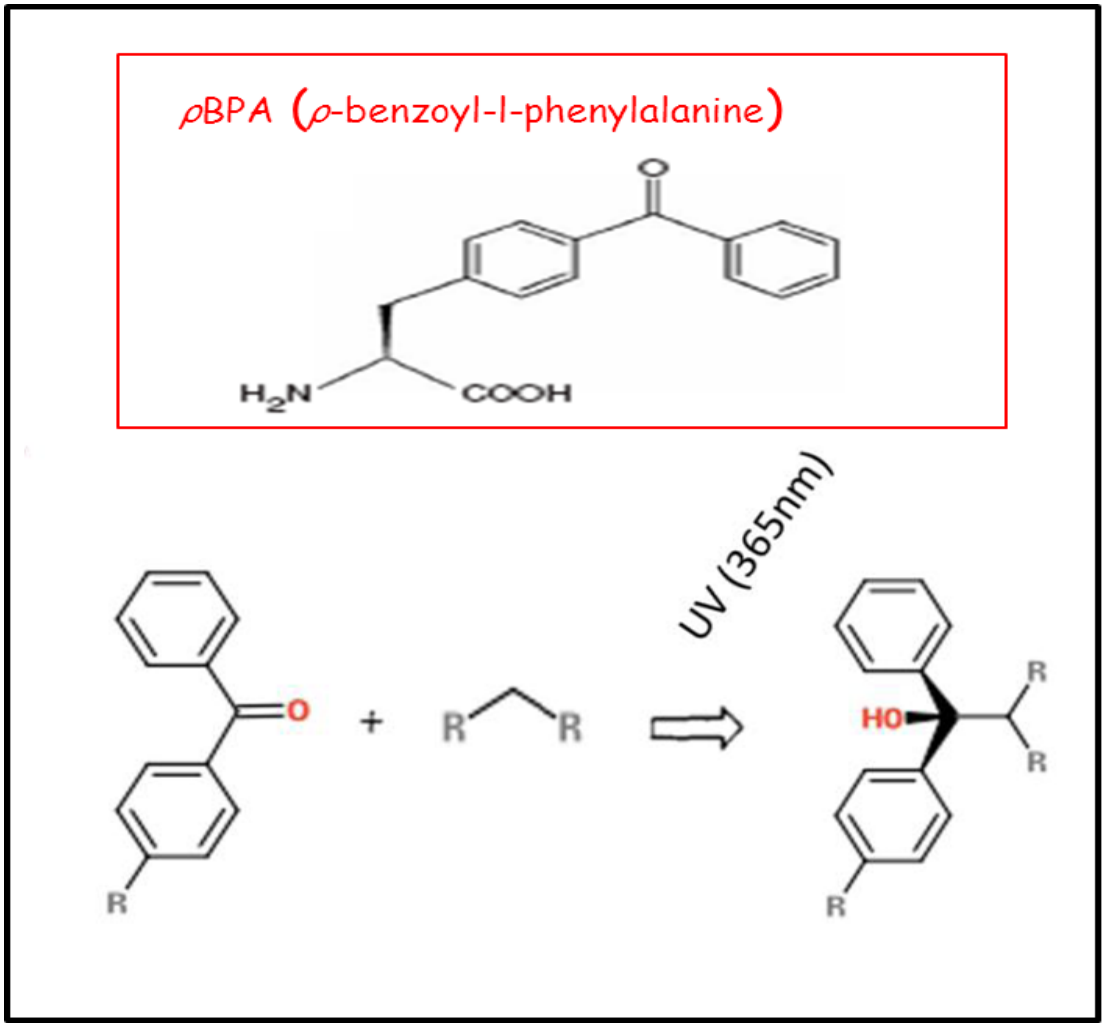

Figure 3-11: Photo-cross-linker *ρ*BPA covalently locks interacting proteins.

The Structure of *ρ*BPA is shown the red box. *ρ*BPA preferentially reacts with tertiary carbon centres, as shown (Chen et al., 2007).

3.2.2.3. Covalent connection of three cohesin subunits: Generation of a photo and chemically cross-linkable cohesin ring

To seal all three interaction points to generate a covalently closed cohesin ring, photo and chemically cross-linkable interfaces of cohesin were combined with each other (Figure 3-13). Two other interfaces, Smc1/Smc3 hinge region and the Scc1/Smc1 interface, have successfully shown to be covalently closed (Haering *et al*., 2008). I have therefore, created a yeast strain that has a *ρ*BPA -substitution in K185 of Smc3 protein, and E570C substitutions in the hinge, with A547C substitution in the C-terminal domain of Scc1, along with the Smc1 protein bearing the G22C and K639C substitutions in its hinge and head regions (Figure 3-13). It was first important to test whether the cohesin complex with the above modifications was functional. It was known that the Smc1 protein containing cysteine mutations in the hinge and the head domains was viable, having a phenotype similar to the wild-type strain (Haering *et al*., 2008). The strain bearing *SCC1(A547C)-PK$_6$::KanMX* was functional and behaved similar to the wild-type strain. The yeast strain that contained *SMC3(E570C, A181→Amber codon)-HA$_3$* on a 2μ plasmid can complement the *smc3* deletion, but showed a slower growth compared to the wild-type strain even at low temperature (25 ^{o}C) (data not shown). The strain that contained *SMC3(E570C, A181→Amber codon)-HA$_3$, ΔSmc3*, *SCC1(A547C)-PK$_6$::KanMX*, and *SMC1(G22C, K639C)-myc$_9$, ΔSmc1* was viable, but displayed a growth defect similar to the strain containing *SMC3(E570C, A181→Amber codon)-HA$_3$.*

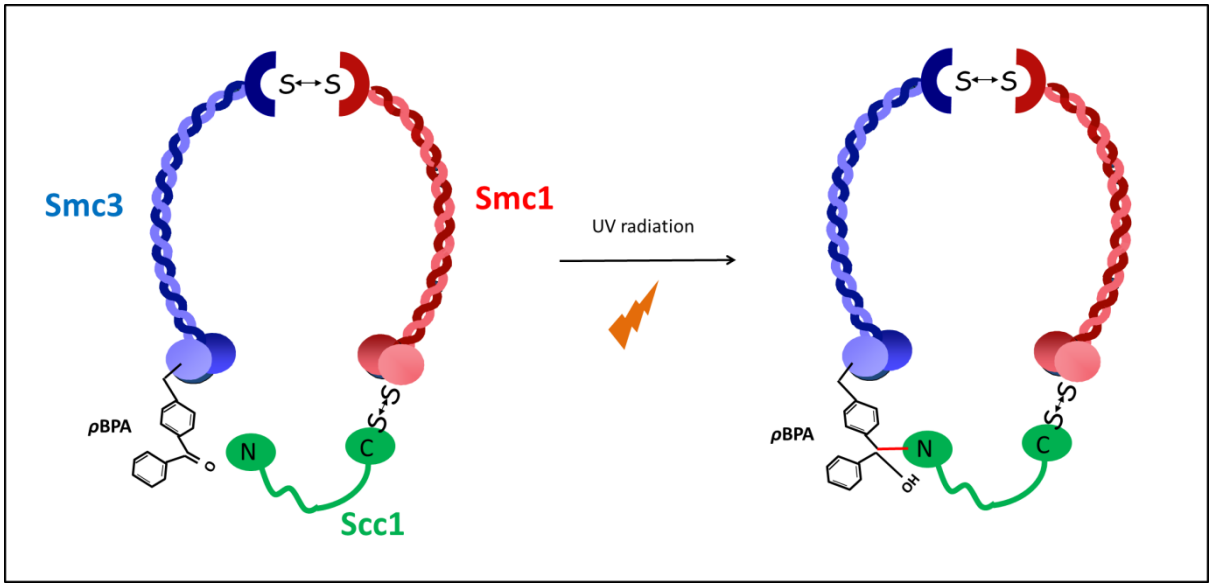

Figure 3-13: Generation of a photo and chemically cross-linkable cohesin ring

Scheme showing a modified version of cohesin ring: Smc3 with *ρ*BPA substituted either at position A181 or position K185 is combined with the cysteine mutations between the Smc1-Smc3 hinges and Scc1-Smc1 head regions in order to create a new cross-linkable cohesin. Subsequent to UV radiation, Smc3 becomes covalently cross-linked to Scc1 *in vivo*. After cell lysis, Smc1/Smc3 and Scc1/Smc1 interfaces are covalently connected by the incubation with chemical cross-linker, bBBr, which would then lead to the formation of a covalently circularized cohesin ring.

In order to test whether all three cohesin interfaces can be covalently closed, immunoprecipitations were performed from soluble extracts prepared from yeast cells. In order to minimise the cleavage of Scc1 by separase, cells grown in *ρ*BPA containing media were arrested in G2/M by the addition of nocodazole, and the culture was irradiated with UV light to activate the cross-linker. Cells were then collected by centrifugation and disrupted to generate whole-cell extracts. Wild-type or mutant Scc1-PK_6 proteins from irradiated and non-irradiated cells were immunoprecipitated by PK-specific antibody. In order to induce the formation of covalent links between both the Smc1/Smc3 hinge region and the C-Scc1/Smc1 globular domains, beads were incubated with either DMSO or bBBr, and cross-linking to Smc1 or Smc3 was detected by Western blotting. In the absence of *ρ*BPA and cysteine substitutions in Smc3, upon treatment with bBBr Scc1 with a cysteine substitution at position A547 cross-linked to Smc1, bearing a cysteine substitution at G22C, only in its head domain even under UV exposure (Figure 3-14, panel A). The multiple bands seen in the cross-linked product probably correspond to cleavage fragments of Scc1. When the cysteine pair in Scc1/Smc1 interface was combined with the cysteine pair in Smc3/Smc1, a cross-linking product was obtained having a molecular weight of 430 kDa, which is approximately equal to the total molecular weight of a “cohesin trimer”. This high-molecular-weight cross-linked product can also be considered as “linear cohesin” since the Smc3/Scc1 interface is not closed yet (Figure 3-14, panel B). When the cysteine pair in Scc1/Smc1 interface is combined with the Smc3 having only a *ρ*BPA substitution, upon treatment with bBBr and UV exposure, a covalently-linked product is produced having the same molecular weight as of the “linear cohesin” observed in panel B (Figure 3-14, panel C). When all cysteine and *ρ*BPA substituted cohesin subunits were integrated with each other, their cross-linking formed a high-molecular-weight product migrating slower than the “linear cohesin” in the gel after the treatments with bBBr and UV irradiation. The slow migration could be due to the full

circularisation of the cohesin ring, which would alter its shape causing it to migrate slightly slower than the "linear cohesin" in the gel (Figure 3-14, panel D). Given that equal amounts of sample were loaded, the efficiency of cross-link formation between the cohesin subunits was determined by the decrease in the intensity of Scc1-PK_6 band staining upon treatment with the chemical cross-linker or UV irradiation. As a result of the quantification, I detected 91% efficiency in the formation of "circularized cohesin" (Figure 3-14, panel D, last lane). Similar cross-linking results were also obtained when the chemical cross-linking was achieved by BMOE (data not shown).

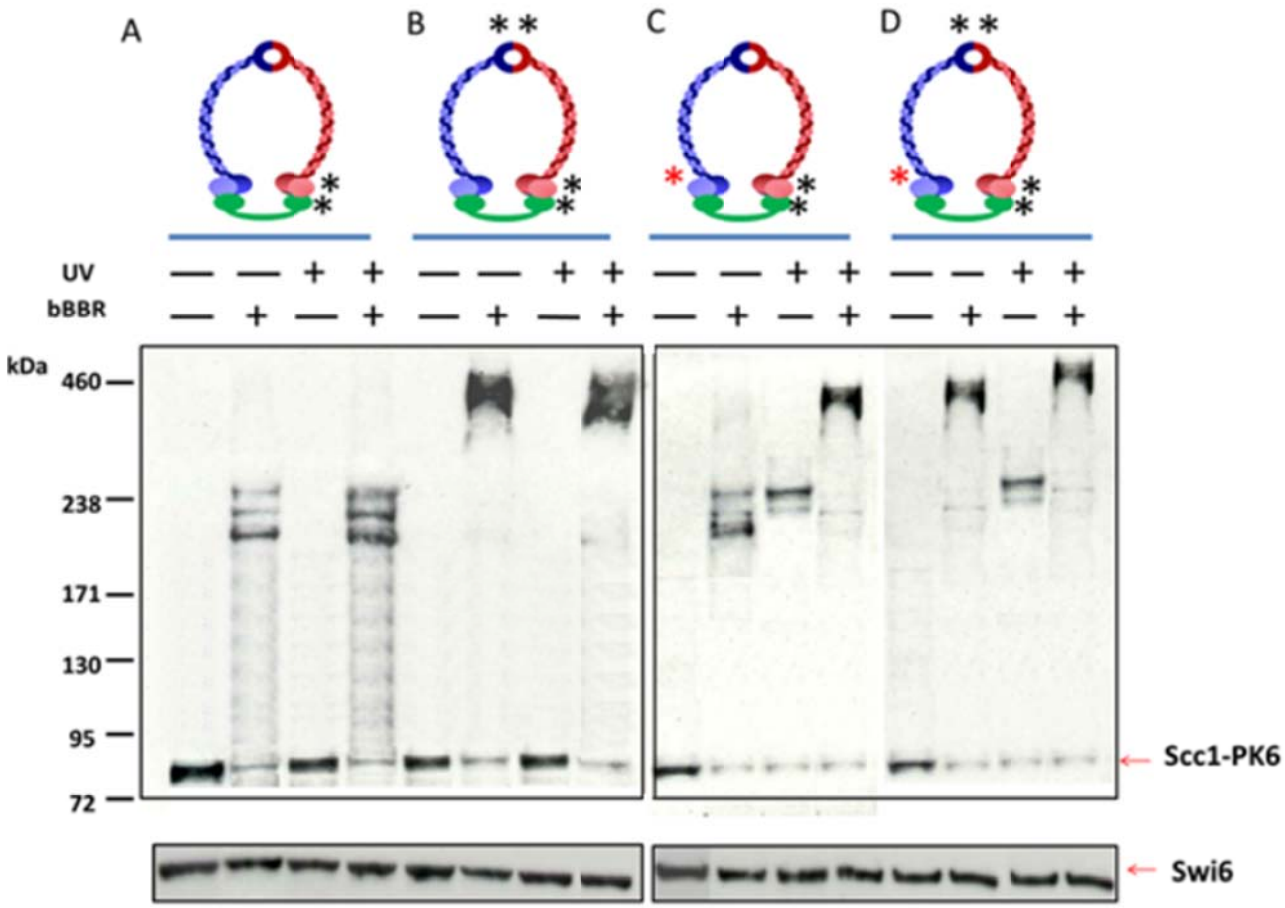

Figure 3-14

Figure 3-14: Inducing the covalent closure of the cohesin interfaces

Whole cell extracts were prepared from nocodazole arrested yeast cells (bearing the indicated modifications above (black asterisk stands for cysteine substitutions; red asterisks stands for *ρ*BPA substitutions)) grown in 2mM *ρ*BPA containing media treated with or without UV light at 365 nm for 15 minutes. Scc1-PK6 was immunoprecipitated using PK-specific antibody, and isolated immunocomplexes were then incubated with DMSO or 0.25mM bBBr for 10min at 4^{o}C. Samples were boiled in SDS containing buffer for 10 minutes and separated on a 3-8% Tris-Acetate gel. The efficiency of cross-linking was determined by quantification of the Western blot probed with an antibody against the PK epitope. Swi6 serves as a loading control.

Labelling: **A.** Scc1(A547C)-Smc1(G22C), K19163 (*Mat a, smc3::HIS3, smc1::NatMx, YEplac181-Smc3-HA3, pLH157(TRP+), Scc1(A547C)-PK6-Avitag::KanMx,leu2: Smc1(G22C)-myc9::hphNT1::leu2*); **B**. Scc1(A547C)-Smc1(G22C, K639C)-Smc3(E570C), K18654 (*Mat a, smc3::HIS3, smc1::NatMx, YEplac181-Smc3(E570C)-HA3, pLH157(TRP+), Scc1(A547C)-PK6-Avitag::KanMx,leu2: Smc1(G22C, K639C)-myc9::hphNT1::leu2*); **C.** Scc1(A547C)-Smc1(G22C)- Smc3(A181→Amber codon), K19159 (*Mat a, smc3::HIS3, smc1::NatMx, YEplac181-Smc3(A181→Amber codon)-HA3, pLH157(TRP+), Scc1(A547C)-PK6-Avitag::KanMx,leu2: Smc1(G22C)-myc9::hphNT1::leu2);***D.** Scc1(A547C)-Smc1(G22C, K639C)- Smc3(A181→Amber codon, E570C), K18656 (*Mat a, smc3::HIS3, smc1::NatMx, YEplac181-Smc3(E570C, A181→Amber codon)-HA3, pLH157(TRP+), Scc1(A547C)-PK6-Avitag::KanMx,leu2: Smc1(G22C, K639C)-myc9::hphNT1::leu2).*

3.2.2.4. Isolation of cohesed minichromosomes from the strain expressing a photo and chemically cross-linkable cohesin ring

To purify cohesin-associated circular minichromosomes, sucrose gradient centrifugation and gel electrophoresis were used, which allows the purification and resolution of cohesin-associated circular minichromosomes (Ivanov and Nasmyth, 2007; Figure 2.2). In order to investigate the effect on cohesin`s circularisation on sister chromatid cohesion, I had to test how modifying the cohesin complex, to create the photo and chemically cross-linkable version, would affect the establishment and maintenance of sister chromatid cohesion of small circular minichromosomes. I first examined whether treatment of cells with UV light would have an effect on the integrity of the dimeric minichromosomes. Although protein-protein cross-links can be efficiently obtained *in vivo* by exposing cells to UV light, DNA damage can be induced by UV radiation, which results in broken chromosomes (reviewed in Bakkenist and Kastan, 2004). Therefore, breakage in the minichromosomal DNA upon UV treatment could cause a decrease in the percentage of the dimeric minichromosomal DNA population.

A 3 kbp circular minichromosome (containing the auxotrophic marker uracil (*URA3*), an origin of replication (*ARS1*), and ~900bp long *CEN6* sequences) was introduced into a yeast strain, which contained a 2μ plasmid carrying either wild-type or *ρ*BPA-substituted *Smc3* gene over *smc3* deletion along with a second 2μ plasmid expressing the tRNA/tRNA synthetase. Cells were grown at 30 ^{o}C and arrested in G2/M phase in the presence of nocodazole. Subsequent to UV radiation, cellular extracts were prepared for the minichromosomal assay. Southern blot analysis of the gradient samples showed that cells

treated with UV light were able to maintain the cohesion of the 3 kbp minichromosome, having cohesion levels similar to the wild type (Figure 3-15, compare the first and the second panels). However, addition of the unnatural amino acid, *ρ*BPA, whose incorporation is essential for creating covalent bonds, into the growth medium changed the cohesion profile of the wild-type strain, resulting in a 20% decrease in the amount of dimer percentage. This therefore indicates that presence of *ρ*BPA causes toxicity to the cell growth (Figure 3-15, compare the first and the third panels). Finally, UV treatment of cells grown in *ρ*BPA containing media did not cause a dramatic change in the dimer percentage compared to the cells grown in *ρ*BPA containing media, but not treated with UV (Figure 3-15, compare the third and the fourth panels).

I next assayed the strain carrying the *ρ*BPA substitution at position A181 in Smc3 for its ability to provide cohesion to the 3kbp minichromosome. Analysis of the gradient fractions extracted from cells, which were grown in *ρ*BPA containing media at 30 ^{o}C and arrested in G2/M phase with nocodazole, showed that compared to the wild-type strain which contains 40% dimers, strains bearing the *ρ*BPA substitution at position A181 in Smc3 have only 21% dimers (Figure 3-16, compare the first and the second panels). The drastic reduction in the percentage of dimeric population indicates the underlying cohesion defects due to the presence of the *ρ*BPA substitution in Smc3, which might cause impairment in cohesin to perform its function. Similar results were also obtained with the strain carrying the *ρ*BPA substitution at position K185 in Smc3 (data not shown). Consistent with the previous experiments (see Figure 3-15), UV exposure did not lead to any change in the percentage of dimeric minichromosomes as cells exposed to UV exhibit the same amount of dimers (20%) as those that are not (Figure 3-16, compare the second and the third panels).

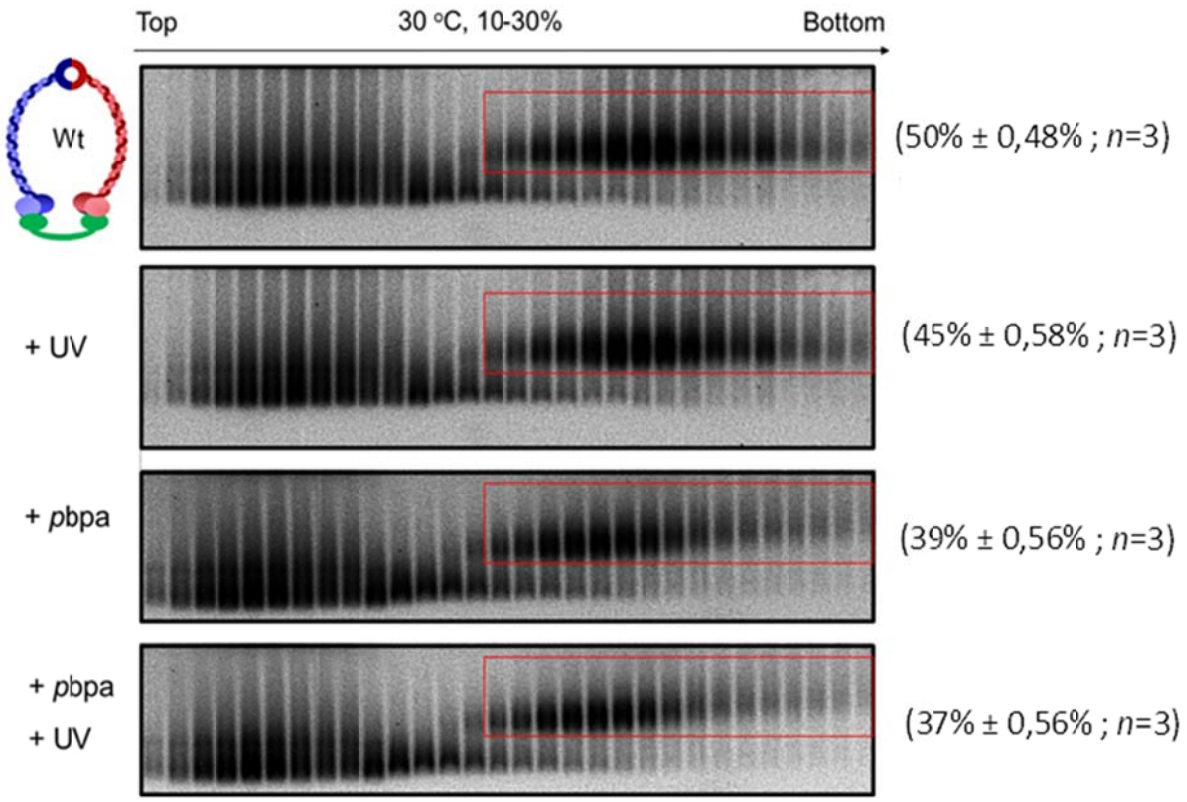

Figure 3-15: Presence of *ρ*BPA in the growth media but not exposure to UV light causes a reduction in the amount of dimeric minichromosomes

Cell culture of wild-type (wt) strains, K19165(*Mat a, smc3::HIS3, YEplac181-Smc3-HA3, pLH157(TRP+), Scc1-PK6::KanMx, 3kb URA3-Cen6-ARS1 minichromosome*), were grown at 30 °C with or without 2 mM *ρ*BPA containing media, arrested in G2/M-phase in the presence of nocodazole and treated with or without UV light at 365 nm for 15 minutes. Clear lysates were sedimented in a 10-30% sucrose gradient at 18krpm for 15h in a Beckman SW41 rotor, followed by fractionation and electrophoresis on a 0.8% agarose gel at 4°C for 8 h. Red boxes highlight the dimeric populations. The percentages of minichromosomal DNA present in dimeric fractions are shown in brackets. Data is shown as a mean of dimer percentage ± S.D. (standard deviation), 'n' is number of experiments.

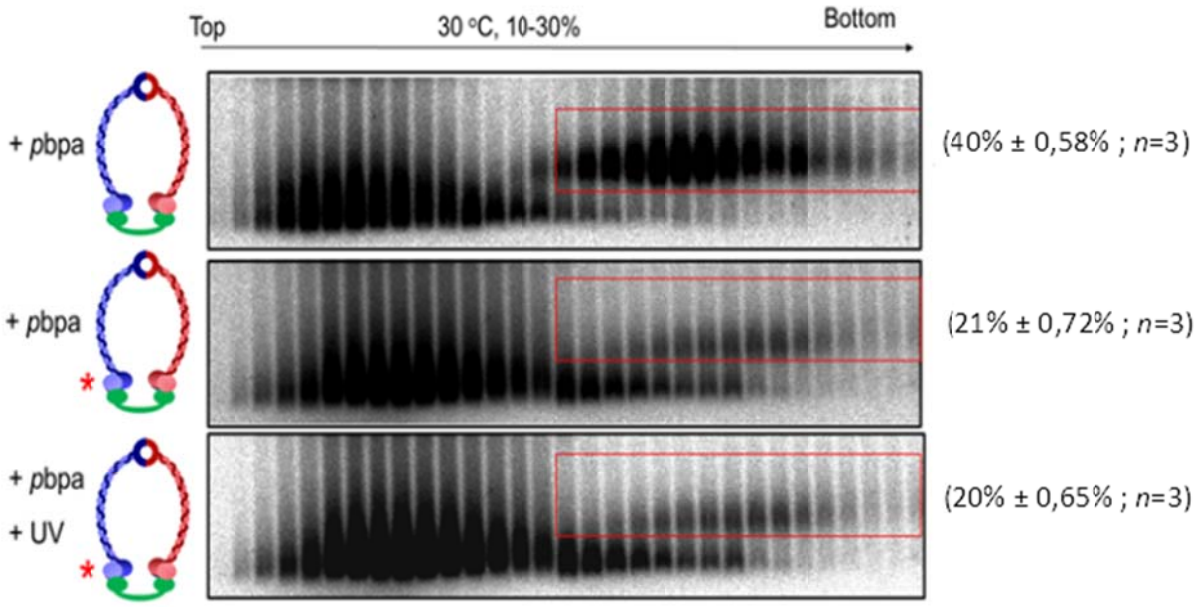

Figure 3-16: *ρ*BPA substitution at position A181 in Smc3 causes a decrease in the percentage of cohesed minichromosomes

Cell cultures of wild-type, K19165, and mutant, K19169 (labelled by a red asterisks) (*Mat a, smc3::HIS3, YEplac181-Smc3(A181→Amber codon)-HA3, pLH157(TRP+), Scc1-PK6::KanMx, 3kb URA3-Cen6-ARS1 minichromosome*) strains bearing the 3kbp minichromosome were grown at 30 °C in 2 mM *ρ*BPA containing media, arrested at G2/M-phase in the presence of nocodazole and treated with or without UV light at 365 nm for 15 minutes. The clear lysates were sedimented in a 10-30% sucrose gradient at 18krpm for 15h in a Beckman SW41 rotor, followed by fractionation and electrophoresis on a 0.8% agarose gel at 4°C for 8 h. Red boxes highlight the dimeric populations. The percentages of minichromosomal DNA present in dimeric fractions are shown in brackets.

The measured cohesion defect is mirrored in the observed sickness of the cells bearing the *ρ*BPA substitution at position A181 in Smc3 and it might reflect the importance of Smc3/Scc1 interface in processes more complex than the simple interaction of the two cohesin complex subunits, such as Smc3`s acetylation and cohesion establishment (Ben-Shahar *et al*., 2008; Rowland *et al*., 2009; Unal *et al*., 2008).

Even though the defect in cohesion might have decreased the chances to induce cohesin`s circularisation and to detect its effect on minichromosomal cohesion, I proceeded to test the effect of cohesin`s circularisation by photo and chemical cross-linking on sister minichromosome cohesion. As a positive control, I used the original version of the cross-linkable cohesin strains where Smc3 and Scc1 are fused via a TEV linker. Cells expressing the modified version of cohesin complexes were grown in *ρ*BPA containing media and arrested in G2/M-phase in the presence of nocodazole. Before the preparation of clear lysates, cells were irradiated for 15 minutes at 365nm. Clear lysates were then centrifuged through sucrose gradient and the fractions containing monomeric and dimeric minichromosomes were separated by agarose gel electrophoresis and detected by Southern blotting. While the presence of cysteine pairs caused minor cohesion defects (36-38% dimeric population) (Figure 3-17, first two panels), integration of photo and chemically cross-linkable interfaces of cohesin caused a 50% decrease in the dimer percentage (19% dimeric population), due to the presence of *ρ*BPA substitution in Smc3 (Figure 3-17, last two panels). Indeed, the cohesion defect caused by *ρ*BPA substitution in Smc3 seemed to be more than the cohesion defect caused by the presence of Smc3-Scc1 fusion protein, according to the quantifications of dimeric populations (Figure 3-18).

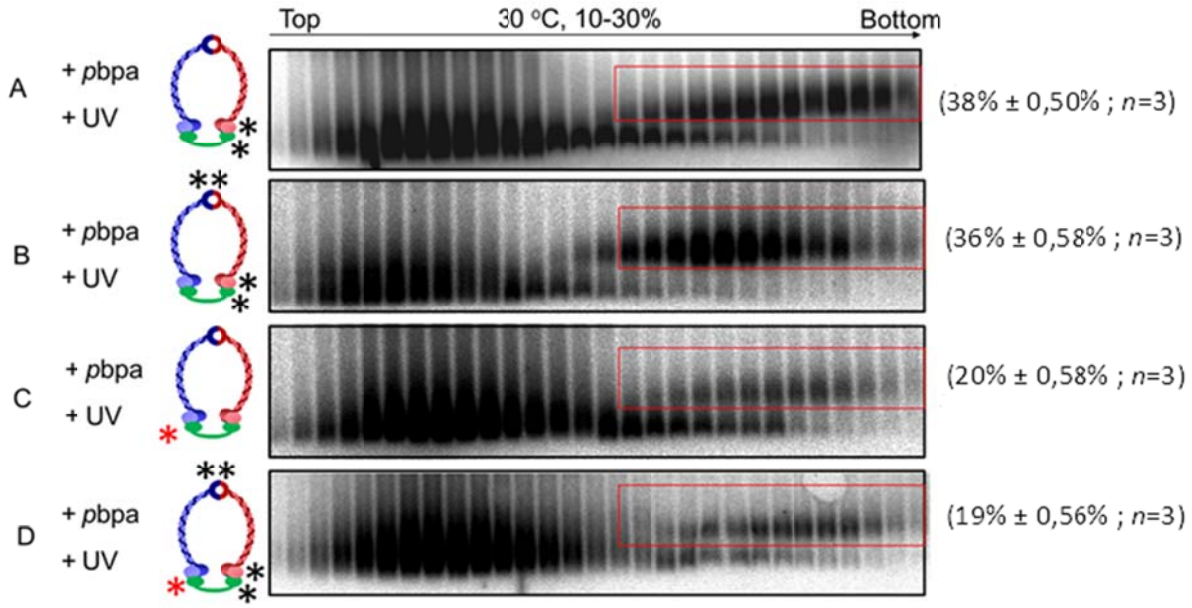

Figure 3-17: Modified cohesin complexes can build cohesion of the small minichromosomal DNA molecule.

Cells with the indicated modifications above (black asterisk stands for cysteine substitutions; red asterisks stands for *ρ*BPA substitutions) were grown at 30 °C in 2 mM *ρ*BPA containing media, arrested at G2/M-phase in the presence of nocodazole and treated with UV light at 365 nm for 15 minutes. The clear lysates were sedimented in a 10-30% sucrose gradient at 18krpm for 15h in a Beckman SW41 rotor, followed by fractionation and electrophoresis on a 0.8% agarose gel at 4°C for 8 h.

Labelling: **A.** Scc1(A547C)-Smc1(G22C), K19413 (*Mat a, smc3::HIS3, smc1::NatMx, YEplac181-Smc3-HA3, pLH157(TRP+), Scc1(A547C)-PK6-Avitag::KanMx,leu2: Smc1(G22C)-myc9::hphNT1::leu2, 3kb URA3-Cen6-ARS1 minichromosome*); **B**. Scc1(A547C)-Smc1(G22C, K639C)-Smc3(E570C), K19414 (*Mat a, smc3::HIS3, smc1::NatMx, YEplac181-Smc3(E570C)-HA3, pLH157(TRP+), Scc1(A547C)-PK6-Avitag::KanMx,leu2: Smc1(G22C, K639C)-myc9::hphNT1::leu2, 3kb URA3-Cen6-ARS1 minichromosome*); **C.** Scc1(A547C)-Smc1(G22C)- Smc3(A181→Amber codon), K19415 (*Mat a, smc3::HIS3, smc1::NatMx, YEplac181-Smc3(A181→Amber codon)-HA3, pLH157(TRP+), Scc1(A547C)-PK6-Avitag::KanMx,leu2: Smc1(G22C)-myc9::hphNT1::leu2, 3kb URA3-Cen6-ARS1 minichromosome);* **D.** Scc1(A547C)-Smc1(G22C, K639C)- Smc3(A181→Amber codon, E570C), K19416 (*Mat a, smc3::HIS3, smc1::NatMx, YEplac181-Smc3(E570C, A181→Amber codon)-HA3, pLH157(TRP+), Scc1(A547C)-PK6-Avitag::KanMx,leu2: Smc1(G22C, K639C)-myc9::hphNT1::leu2, 3kb URA3-Cen6-ARS1 minichromosome).* Red boxes highlight the dimeric populations.

To test the effect of cohesin`s circularisation, fractions containing dimeric minichromosomes were dialysed against reaction buffer (25mM NaPi pH7.4, 50mM NaCI, 10mM $MgSO_4$, 0.25% Triton X-100) to remove DTT, sucrose and other low-molecular-mass contaminants. The dialysed fractions were treated with 5 mM bBBr, 25 mM BMOE or DMSO. The crosslinking reaction was stopped by addition of DTT and samples were heated at 65°C in the presence of 1% SDS. The denatured samples were then electrophoresed in a 0.8% agarose gel and probed for the minichromosomal DNA by Southern Blotting (Figure 3-18, panel 2). Four different DNA species were observed in the dimeric fractions extracted from all strains. The most predominant and the fastest migrating band represented the supercoiled monomers. Despite being poorly resolved from each other, the next two bands corresponded to the nicked monomers and catenated-supercoiled DNAs. The fourth and the least abundant one was the slowing migrating form, corresponding to the supercoiled-nicked catenates.

When dimeric fractions extracted from the positive control strain (strain that expressed the original version of cross-linkable cohesin) were treated with either bBBr or BMOE, an additional form of DNA appeared that were resistant to SDS treatment. While the more abundant species migrated slightly slower than the supercoiled-supercoiled concatenated species, the second form was less abundant and migrated slightly slower than the supercoiled-nicked concatenated species (Figure 3-18, panel 2F). Importantly, this new form of DNA was absent in the fractions treated with DMSO**.** Irrespective of the chemical crosslinking agent used, the total fraction of the new species calculated from the Southern blot was 31%. In experiments conducted by Haering *et al.* (Haering *et al*., 2008), a very low abundant form of DNA was also noticed in the cross-linked dimeric fraction, which could correspond to monomeric supercoiled DNA entrapped by a chemically circularized cohesin. However, I was unable to detect this form of DNA in my experiments.

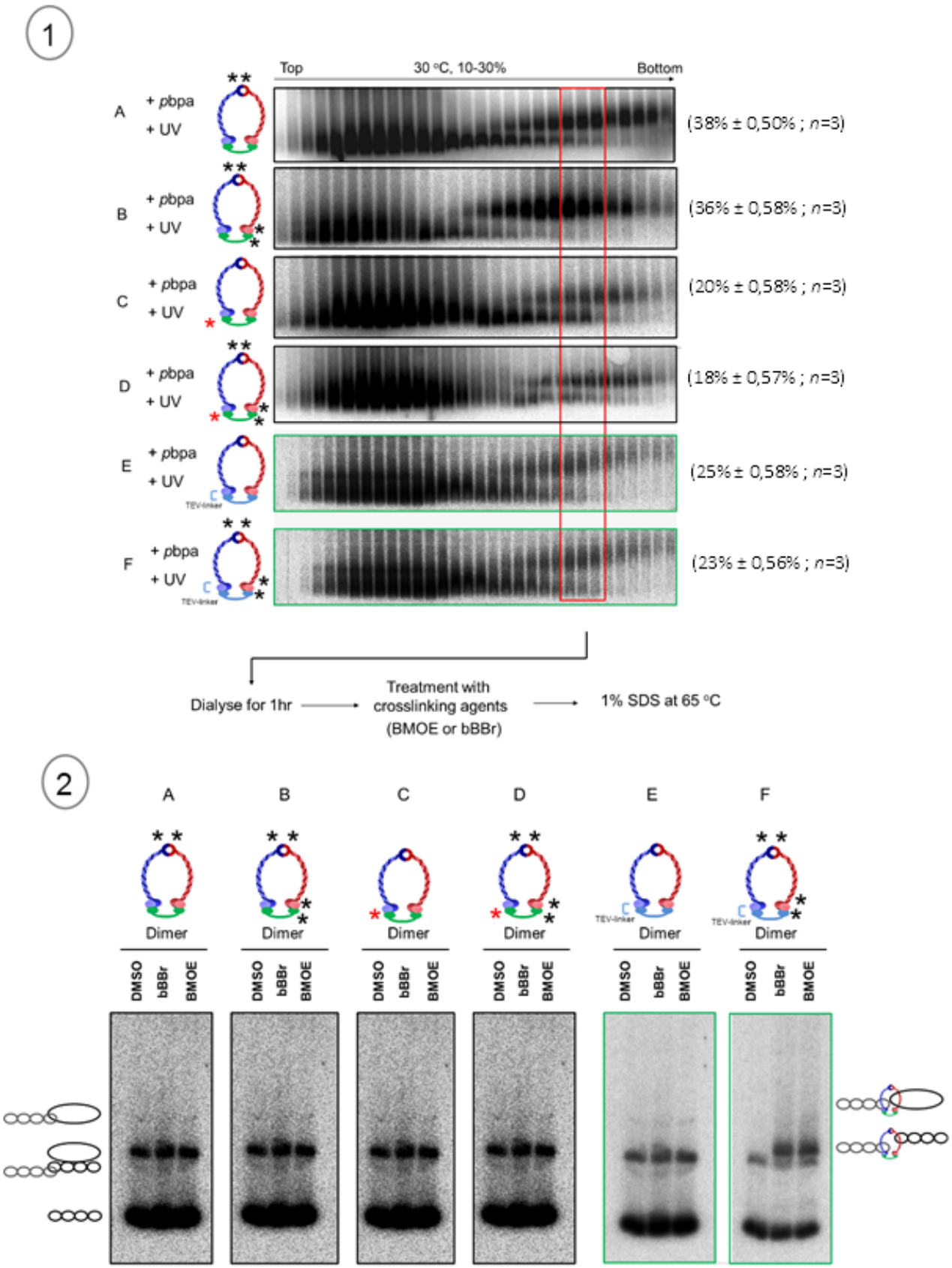
1
Top
30 °C, 10-30%
Bottom
A
+ pbpa
+ UV
(38% ± 0,50% ; n=3)
B
+ pbpa
+ UV
(36% ± 0,58% ; n=3)
C
+ pbpa
+ UV
(20% ± 0,58% ; n=3)
D
+ pbpa
+ UV
(18% ± 0,57% ; n=3)
E
+ pbpa
+ UV
(25% ± 0,58% ; n=3)
F
+ pbpa
+ UV
(23% ± 0,56% ; n=3)
TEV-linker
Dialyse for 1hr
Treatment with crosslinking agents (BMOE or bBBr)
1% SDS at 65 °C
2
A
B
C
D
E
F
Dimer
DMSO
bBBr
BMOE

Figure 3-18

Figure 3-18: Covalent circularisation of photo-and chemically-cross-linkable cohesin ring does not create SDS-resistant circular sister minichromosomes.

1. The dimeric and monomeric forms of the 3kbp mini-chromosome were detected in extracts from strains (A) K19413, (B) K19414, (C) K19415, (D) K14416, (E) K19417 (*Mat a, smc3::HIS3, smc1::NatMx, Scc1P-Smc3-TEV3-Scc1::KanMx, leu2: Smc1-myc9::hphNT1::leu2, 3kb URA3-Cen6-ARS1 minichromosome*) and (F) K19418 (*Mat a, smc3::HIS3, smc1::NatMx, Scc1P-Smc3(E570C)-TEV3-Scc1(A547C)::KanMx, leu2: Smc1(G22C, K639C)-myc9::hphNT1::leu2, 3kb URA3-Cen6-ARS1 minichromosome*). The cells were grown in 2mM *ρ*BPA containing media, arrested in G2/M with nocodazole, and irradiated with UV for 15 minutes at 365nm. The clear lysates prepared from spheroplasted cells were sedimented in a 10-30% sucrose gradient at 18krpm for 15h in a Beckman SW41 rotor, followed by fractionation and electrophoresis on a 0.8% agarose gel at 4^{o}C for 8 h. Presence of the minichromosomes were detected by Southern blotting. Southern blots were hybridized with a ^{32}P-labelled probe. The percentages of minichromosomal DNA present in dimeric fractions are shown in brackets. Data is shown as a mean of dimer percentage ± S.D. (standard deviation), 'n' is number of experiments.

2. 3 fractions from each dimeric population (indicated by red box) of the 3kbp plasmid purified from the indicated strains were pooled together, dialysed against the reaction buffer for 1hr at 4°C and then treated with DMSO or with 5mM bBBr or 25 mM BMOE for 10 min at 4°C. Crosslinking reactions were then stopped by the addition of DTT and samples were denatured with 1% SDS at 65^{o}C.

Suprisingly however, covalent circularisation of cohesin in dimer fractions extracted from the strain expressing the photo and chemically cross-linkable cohesin caused no change in DNA mobility (Figure 3-18, panel 2D). In order to test whether cohesin`s covalent circularisation was achieved in dimeric fractions that were used, the treated samples were divided into two: one part was loaded on 3-8% Tris-Acetate gels and probed by Western blot for epitope-tagged cohesin subunits (Figure 3-19, panel 2); the other part was separated on an agarose gel, and the minichromosomal DNA was detected by Southern blotting (Figure 3-19, panel 1). While the chemical cross-linker treatment of the samples extracted from the cross-linkable cohesin complex resulted in the detection of an up-shift in the molecular weight of the cohesin subunits probed for in the Western blot, no SDS-resistant dimers were observed in the Southern blot (Figure 3-19, panel 1D), indicating that the newly created photo and chemically cross-linkable cohesin molecule is not capable of creating SDS-resistant dimers.

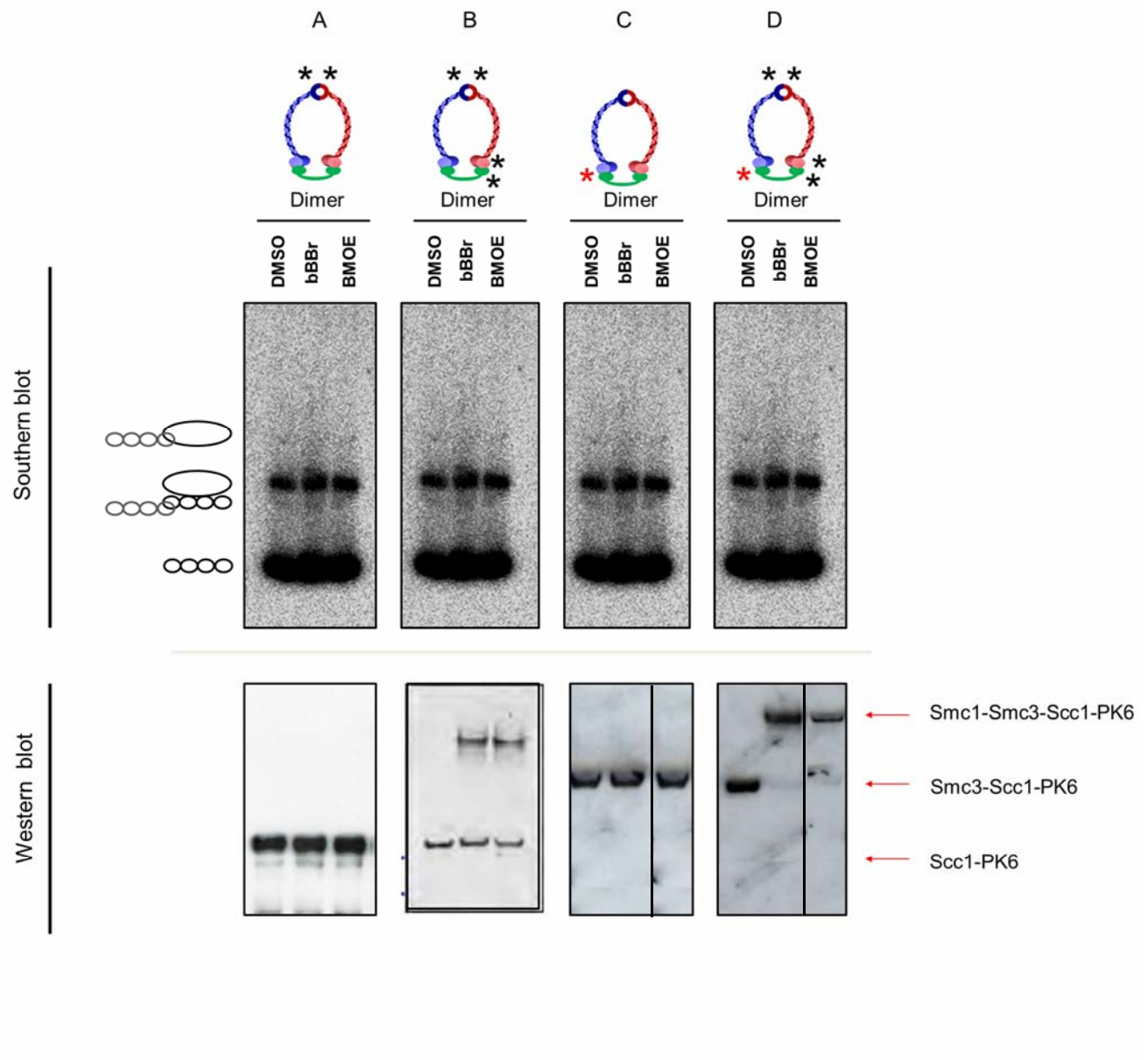

Figure 3-19: Inducing cohesin`s covalent circularisation

Fractions from dimeric populations of the 3kbp plasmid purified from the strains (A) K19413, (B) K19414, (C) K19415, (D) K14416 were dialysed against the reaction buffer for 1hr at 4°C and then treated with DMSO or with 5mM bBBr or 25 mM BMOE for 10 min at 4°C. Crosslinking reactions were then stopped by the addition of DTT and samples were denatured with 1% SDS at 65°C. Treated samples were split in two: one part was resolved on 0.8% agarose gel, transferred to a NY plus membrane, and the minichromosomal DNA was detected by Southern blotting (panel #1); the other part was run on a 3-8% Tris-Acetate Gel and proteins were detected by Western blot using antibodies against epitope tagged cohesin subunits (Scc1-PK6) (panel #2).

3.3. Discussion

In order to characterise the nature of "non-cohesive" cohesin`s interaction with DNA, I needed a new system that permitted covalent circularisation of cohesin complexes. The previously created cross-linkable cohesin molecule (Haering *et al*., 2008) abolished the experimental set up to test how "non-cohesive" cohesin interacts with chromatin, due to the presence of Smc3-Scc1 fusion protein which enabled cells to grow in the absence of Eco1. In order to overcome these problems, I tried two different methods in order to connect Smc3-Scc1 interface in a protein-denaturant resistant manner. In my first attempt, the C-terminus of Smc3 and the N-terminus of Scc1 were fused to FRB and FKBP12 respectively, proteins that can form a complex upon addition of the drug rapamycin (Belshaw *et al*., 1996; Chen *et al*., 1995). Crystal structure of the ternary complex of FKP12/rapamycin/FRB helped me to design cysteine pairs for the crosslinking FRB and FKBP12 only in the presence of rapamycin. Although I was able to obtain covalently linked products *in vitro* with purified FRB and FKBP12 proteins with a good cross-linking efficiency, I could not achieve the same efficiency in experiments where FRB and FKBP12 are fused to Smc3 and Scc1, respectively. Despite having long flexible linkers, being attached to Smc3 and Scc1, FKBP12 and FRB might lose their flexibility, and their orientation in the ternary complex might be altered even in the presence of rapamycin and therefore not behave the same way as they did under *in vitro* conditions. Alternatively, they might still bind each other but in a slightly different configuration. Even one degree rotation either in FRB or FKBP12 repositions the interaction surface between FRB and FKBP12 in the ternary complex and this could be enough to abolish the pairing of cysteine residues, which in turn would result a decrease in the cross-linking efficiency.

A different and more efficient method of crosslinking the Smc3-Scc1 interface was achieved in the second attempt. Amino acids within the coiled coil region of Smc3 were replaced by the non-natural amino acid ρ-benzoyl-phenylalanine (*ρ*BPA) (T. Gligoris, unpublished data), and an efficient crosslinking was obtained between the N-terminal domain of Scc1 and Smc3 *in vivo*. Photo and chemically cross-linkable interfaces of cohesin were then integrated with each other to generate a new version of the cohesin molecule. However, circularisation of the photo and chemically cross-linkable cohesin ring failed to create SDS-resistant dimers as *ρ*BPA substitution at position A181 or position K185 in Smc3 causes a significant reduction in the acetylation levels of cohesin (T.Gligoris, unpublished data). Although the cells bearing the photo and chemically cross-linkable cohesin molecule is alive, this version of cohesin molecule is deficient in holding sister chromatids together topologically. Acetylation of a pair of lysine residues (K112 and K113) on the surface of Smc3`s NBD by Eco1 acetyltransferase is a crucial event in establishing cohesion (Ben-Shahar *et al*., 2008; Unal *et al*., 2008; Zhang *et al*., 2008; Rowland *et al*., 2009), which occurs during S-phase and is maintained until anaphase when it is removed by Hos1 deacetylase (Beckouet *et al*., 2010; Borges *et al*., 2010). Preliminary experiments performed by T. Gligoris in our lab indicates that Smc3 K113 acetylation of *ρ*BPA substituted Smc3 at position A181 or position K185 is on average three- to four-fold less than the wild type (T.Gligoris, unpublished data). Given that Smc3 acetylation has been thought to convert non-cohesive cohesin to cohesive cohesin (Beckouet *et al*., 2010), the reduced acetylation levels of *ρ*BPA substituted Smc3 could also be the cause of the decrease in the amount of dimeric minichromosomes in strains containing the photo and chemically cross-linkable version of cohesin. Importantly, in addition to the decreased levels of acetylation, it has also been reported that only 30% of the acetylated Smc3 photo-cross-links to Scc1 (T. Gligoris, unpublished data). Why not all but only 30% of the acetylated Smc3 photo-cross-links to Scc1? The conformation between Smc3 and Scc1 which

allows 90% cross-linking might belong to the configuration of "non-cohesive" cohesin. Acetylation of Smc3 could therefore alter this configuration and cause a reduction in the cross-linking efficiency. Although a small amount of acetylated Smc3 has been shown to photo-cross-link to Scc1(T. Gligoris, unpublished data), this low efficiency cross-linking may not be enough to obtain SDS-resistant dimers.

Moreover, poor incorporation of *ρ*BPA in response to the amber codon in Smc3 has also been observed, as cells were still able to grow in the absence of *ρ*BPA (data not shown). Although the expression levels of *ρ*BPA substituted Smc3 was slightly increased in the presence of *ρ*BPA, *ρ*BPA substituted Smc3 can still be expressed in the absence of *ρ*BPA, indicating that the expression of *ρ*BPA substituted Smc3 at position A181 or position K185 is not fully dependent on the presence of *ρ*BPA in the growth medium (data not shown). This could happen if the orthogonal aminoacyl tRNA synthetase-tRNA pair is not working very efficiently in terms of incorporating *ρ*BPA into Smc3 in response to the amber codon. Poor incorporation of *ρ*BPA therefore could lead to the formation heterogeneous cohesin populations inside the cell. Those cohesin molecules, whose Smc3 subunit has not incorporated *ρ*BPA in response to amber codon, could also cause toxicity affecting the cell growth.

The fact that Eco1 mediates cohesion establishment by acetylating the lysine residues in the Smc3`s NBD (Ben-Shahar *et al*., 2008; Unal *et al*., 2008; Zhang *et al*., 2008; Rowland *et al*., 2009) also highlights the importance of understanding how Scc1 binds to Smc3 NBDs. The interaction between Scc1`s N terminal region and NBD domain of Smc3 was first identified by the finding that the N-terminal half of Scc1 copurifies with monomeric Smc3 protein when expressed in insect cells (Haering *et al*., 2002; Gruber *et al*., 2003). Subsequent experiments performed in yeast confirmed that this interaction also occurs *in vivo*. Insertion of TEV protease cleavage sites both into Scc1 and the coiled-coil region of Smc3 releases

Scc1`s N terminal cleavage fragment associated with Smc3`s NBD upon activation of TEV protease (Gruber *et al*., 2003). Consistent with the previous findings, a greater fluorescence resonance energy transfer (FRET) has been reported *in vivo* between the N-terminus of Scc1 fused to cyan fluorescent protein (CFP) and the C-terminus of Smc3 fused to yellow fluorescent protein (YFP) than to the YFP fused to the C-terminus of Smc1 (McIntyre *et al*.,2007).

While interaction between Smc1`s NBD and the C-terminal domain of α-kleisin take place independently, interaction between Smc3`s NBD and the N-terminal domain of α-kleisin depends on the binding of Smc1`s NBD to α-kleisin (Arumugam et al., 2003; Haering et al., 2002). Up to date, due to the absence of a crystal structure, it has been assumed that the interaction between the N-terminus of Scc1 and Smc3`s NBD is similar to that of between the C-terminus of Scc1 and Smc1`s NBD. The finding that the N-terminal domain of Scc1 cross-links to the coiled-coil region of Smc3 (T. Gligoris, unpublished data) challenge also the assumption that Smc3-Scc1 interaction behaves in a similar manner to the Smc1-Scc1 interaction. The photo-cross-linking between Smc3 and Scc1 might be an accurate representation of the location of the interaction *in vivo*. If the N-terminal domain of Scc1 binds to the conserved coiled-coil region of Smc3 instead of its NBD, then this could also be an explanation of the lower efficiency obtained in the *in vivo* cross-linking between cysteine containing Smc3-FRB and FKBP12-Scc1 in the presence of rapamycin. However, in order to confirm that the N-terminal of Scc1 is indeed interacting with the coiled-coiled regions of Smc3, more experiments need to be performed. Further efforts are also being made to find out where exactly on Scc1 Smc3 is cross-linking to.

A major limitation of the *ρ*BPA dependent photo-cross-linking technique is the inability to identify the residue in the protein which *ρ*BPA crosslinks. Moreover, due to the fact that many of the mutants were either dead or too sick to use for cross-linking attempts, a large

number of mutants need to be analysed in order to find cross-linking sites. Although *ρ*BPA cross-linking can confirm protein-protein interactions, where *ρ*BPA is forming covalent bonds in the other protein cannot be known. Despite these limitations, the *ρ*BPA dependent photo-cross-linking technique provides an alternative way of mapping protein-protein interaction sites *in vivo* in situations where a crystal structure is not available.

Chapter 4 - General Discussion

Cohesin is a key constituent of both interphase and mitotic chromosomes. It not only mediates sister chromatid cohesion necessary for chromosome segregation and DNA repair, but also, at least in animal cells, regulates gene expression during embryonic development. Understanding how cohesin interacts with DNA is essential in order to find out how it mediates such diverse functions.

The association between DNA and cohesin involves a topological mechanism, which has been demonstrated by the finding that purified sister minichromosomes are still held together by a modified cohesin complex that can be covalently circularized prior to protein denaturation (Haering *et al*., 2008). These cross-linking experiments led to the postulation that cohesin may also function as a "concatenase" which also captures individual chromatin fibres. It is still unknown whether cohesin complexes that associate with chromatin but are not involved in the establishment of sister chromatid cohesion entrap DNA topologically. In other words, how "non-cohesive" cohesin complexes interact with DNA is currently not known. The lack of stably bound cohesin during G1-phase suggests that cohesin dynamically exchanges on and off the chromatin. Whether this is the case for budding yeast is unclear. Cohesin complexes mediating its non-canonical functions like gene regulation are less stably bound to chromatin than cohesive cohesin. However, different dynamics does not mean that the physical nature of interaction between cohesin and DNA differs.

The conclusion, namely that cohesin entraps sister DNAs inside its tripartite ring structure, deriving from the experiments, that have used differential sedimentation velocity and gel electrophoresis to measure the physical properties of cohesin-mediated linkages between 2.3 kb circular sister minichromosomes, have been questioned mostly on the grounds that such small minichromosomes are dominated by their centromeres and may have unique properties

due to their circularity (Heidinger-Pauli *et al*., 2010; Skibbens, 2010; Yanagida, 2009). However, it has been shown that the same techniques can be applied to a larger and more natural minichromosome (a 26 kb circular minichromosome), which contains extensive arm sequences for about half of the sister chromatid cohesion (Farcas *et al.*, 2011). Using the original version of the cross-linkable cohesin, it has also been demonstrated that chemical cross-linking of cohesin entraps sister DNAs of a larger and circular but not linear minichromosomes, indicating that cohesin functions using a topological principle (Farcas *et al*., 2011).

Nevertheless, experiments performed with the original version of the cross-linkable cohesin ring still suffer from the limitation that they use a potentially artefactual cross-link for the Smc3-Scc1 interface, namely fusion of Smc3`s C-terminus to Scc1`s N-terminus (Haering *et al*., 2008). This is due to the absence of a crystal structure for the Smc3-Scc1 interface, which remains a key challenge for the cohesin field. In addition to that, for reasons that are not understood, the Smc3-Scc1 fusion is partially dysfunctional (Gruber *et al*., 2006). Moreover, the presence of fusion bypassed the requirement for Eco1, and therefore prevented me testing how "non-cohesive" cohesin interacts with chromatin, using the original version of cross-linkable cohesin complex.

The finding that the presence of Smc3-Scc1 fusion protein rescues the lethality caused by the absence of Eco1 implies that Smc3 acetylation can be mimicked by fusion of Smc3's nucleotide binding domain to α-kleisin (Chan *et al*., 2012). Based on these findings, it has also been suggested that releasin complex, which is a feature of cohesin complexes that enables them to disengage from chromatin in the absence of α-kleisin cleavage (Nasmyth, 2011), catalyzes cohesin's dissociation from chromatin by opening the ring's Smc3/α-kleisin

interface and that an essential function of acetylation is to block this process (Chan *et al*., 2012).

The presence of a mechanism responsible for opening of the Smc3/Scc1 interface points out the possibility that cohesin ring might have separate DNA entry and exit gates. Entrance of DNA into the cohesin ring has been proposed to involve a transient dissociation of the Smc1/Smc3 hinge interface (Gruber *et al*., 2006) and that dissociation could occur by reversing of this process (Nishiyama *et al*., 2010). However, it is not yet clear whether Smc hinges really are entry and exit gates for DNA. Genetic experiments in yeast have suggested that the SMC hinge domain and the Smc3/Scc1 interface serve as entry and exit gates for DNA, respectively (Gruber *et al*., 2006; reviewed in Nasmyth *et al*., 2011; Chan *et al*., 2012). The finding that fusion of Smc3`s NBD to α-kleisin but not that of Smc1 enabled cells to proliferate without Eco1 has led to the postulation that cohesin`s exit gate might be located at Smc3/Scc1 interface (Chan *et al*., 2012). Given that dissociation of cohesin from chromosomes takes place via two pathways, one in which the cohesin associated with mitotic chromosomes is removed after cleavage of its α-kleisin subunit by separase (Uhlmann *et al*., 1999; Uhlmann *et al*., 2000), and the other where prophase pathway causes dissociation of most cohesin associated with chromosome arms via a separase independent mechanism (Losada *et al*., 1998; Waizenegger *et al*., 2000), the mechanism responsible for opening of the Smc3/Scc1 interface might be also responsible for the prophase pathway.

Cohesin associates with replicated as well as unreplicated chromatin fibres. Results from FRAP studies in mammalian cells have identified two distinct dynamic behaviours of cohesin bound to DNA (Gerlich *et al*., 2006). About one third of cohesin was found to be stably associated with the chromosomes from S phase until the onset of anaphase. Due to the fact that the mean residence time for this pool of DNA-associated cohesin complexes is about six hours, this stable fraction has been presumed to involve in holding sister DNAs together.

Another third of the total amount of cohesin during G2 as well as all cohesin during the G1-phase was found to associate dynamically to chromatin, with a mean residence time of 25 minutes. This dynamic association of cohesin with chromosomes may be important for distribution of cohesin molecules along the genome, for remodelling intra-chromatid loops, and for removing topological barriers during transcription, repair or replication. Therefore, presence of an exit gate may be important to protect a large fraction of cohesin pool from separase, in order for cohesin to mediate its 'non-cohesive' functions, as a consequence of its prior dissociation during prophase.

Cohesin DNA-embracing cohesin complexes are thought to be distinguished from dynamic ones by Eco1 acetylation of Smc3 NBDs (Chan *et al*., 2012). Stably bound cohesin molecules are considered to resist cohesin-release pathways by acetylation of their Smc3 subunit. Dynamically bound cohesin complexes lack the acetylation mark and are thus unable to resist releasin activity. Acetylation can therefore be viewed as a key that locks cohesin rings shut once sister DNAs have been trapped inside.

Understanding how these dynamic and 'non-cohesive' cohesin molecules are associated with DNA fibres is essential if we are to grasp how cohesin regulates gene expression during embryonic development in animal cells and how sister chromatid cohesion is established during DNA replication in budding yeast. In order to investigate whether "non-cohesive" cohesin interacts with the DNA topologically in budding yeast, it was absolutely crucial to develop a new system where cohesin interfaces can be covalently cross-linked and introduced modifications do not cause major cohesion defects. Due to the reasons explained above and in Chapter 2, the original version of cross-linkable cohesin molecule is not suitable for this purpose. Therefore, I created two new versions of cross-linkable cohesin molecule either utilizing FRB-FKBP12 system or photo-cross-linking. Unfortunately however, as explained in detail in Chapter 3, these newly created cross-linkable cohesin molecules either gave poor

cross-linking efficiencies or had major cohesion defects due to the modifications making them cross-linkable. Thus, newly created cross-linkable cohesin molecules were also not suitable to address the question I would like to answer.

Despite being unsuccessful in generating a new and Eco1 dependent version of cross-linkable cohesin molecule, it is still feasible to investigate the nature of "non-cohesive" cohesin`s association with DNA. By the time I was writing my dissertation, we have started a collaboration with Stephan Gruber and his colleagues, who have examined the molecular architecture of condensin in *B. subtilis* (*Bacillus subtilis*) by biochemically and structurally *in vitro* and by site-specific cysteine cross-linking and genetic *in vivo* (Bürmann *et al.*, submitted). It has been demonstrated that bacterial SMC proteins harbour two essential interfaces for binding kleisin ScpA. As structural basis for one of the interfaces, their crystallographic analysis has revealed an extended three-stranded coiled coil formed between an N-terminal helix in ScpA and parts of the Smc coiled coil located next to the ATPase domain (Bürmann et al., submitted). It has been found out that only one kleisin subunit is bound to SMC dimers *in vivo*, indicating the asymmetric nature of bacterial condensin despite the symmetry of its Smc core. This asymmetric nature of bacterial condensin has been shown to be essential in *B. subtilis* by artificial conversion of asymmetric SMC/kleisin complexes into symmetric complexes (Bürmann et al., submitted).

Is the asymmetric nature of bacterial condensin present in eukaryotic SMC/kleisin complexes? The finding that residues (A181 and K185) in a conserved coiled coil region of Smc3 located next to its ATPase domain photo-cross-link to the N-terminus of Scc1 *in vivo* (T.Gligoris, unpublished data) is an indication that the asymmetry observed in bacterial condensin is likely to be conserved in eukaryotic SMC/kleisin complexes. Based on *B.subtilis* condensin crystal structure and the photo-cross-linking experiments performed in yeast by T. Gligoris, Gruber and his co-workers have modelled how cohesin`s Smc3 might bound to the

N-terminus of Scc1 *in silico*. Smc3 (S1043C) has been found to cross-link to a natural cysteine (C56) in the N-terminus of Scc1 (F.Bürmann, unpublished data). Their model has also been confirmed by additional cysteine specific cross-linkings of Scc1 and Smc3 proteins in *S.cerevisiae* cells (N.Petela, unpublished data). This strongly suggests that the N-terminus of Scc1 interacts with the Smc3`s conserved coiled coil region, indicating that the cohesin complex in yeast is likely to have a similar asymmetric configuration observed in *B.subtilis* condensin complex.

The finding that Smc3 (S1043C) has been identified to cross-link to a natural cysteine in Scc1 makes it possible to create a new version of cross-linkable cohesin molecule where all three cohesin interfaces, Smc3/Scc1 hinge, Smc1/C-terminus of Scc1 and Smc3/N-terminus of Scc1, can be covalently closed via cysteine specific cross-linkings. The cohesin complex with the above modifications was found out to be functional (P.Uluocak, unpublished data). Cysteine-based covalent closure of the three interfaces of cohesin`s Smc1-Smc3-Scc1 tripartite ring has been shown to entrap 28% of the sister DNAs of 2.3 kb minichromosomes inside circularised cohesin rings (P.Uluocak, unpublished data). The reason not all DNA are entrapped is because circularization efficiency is less than 50% (P.Uluocak, unpublished data). These cross-linking results thus exclude one more time that the connection between sister DNAs is mediated by non-topological interactions between cohesin complexes associated with each sister (Milutinovich and Koshland, 2003). Given that we now have a functional tool which allows us to cross-link cohesin complex in Eco1 dependent mannet, the focus of our future research consists of proving or disproving whether cohesin uses the same topological principle to trap individual chromatin fibres.

Chapter 5 – Materials and methods

5.1. Strains and plasmids generation

5.1.1. Strain Construction

The Frb domain was fused to the C-terminus of the endogenous *Smc3* gene by the one-step PCR-mediated technique (Longtine *et al*., 1998) using the cassette pSMC3-FRB-HisMx. All constructs were confirmed by PCR amplification and sequencing. The YIplac211 plasmids carrying the wild type and mutant *FKBP12-Scc1-PK6-avitag* genes were linearised with *EcoRV* enzyme for direct integration at the *ura3* locus and introduced into a diploid strain heterozygous for *scc1* deletion. After dissecting the tetrads and checking the viability of spores, all the *FKBP12-Scc1* mutants were found to be functional. The strain containing *Smc3-FRB::HISMX* was combined with the spore carrying YIplac211_ *FKBP12-Scc1-PK6-avitag* construct inserted at *Ura3* locus over deletion of *scc1*. For the minichromosome assay, a 2.3kb *TRP1ARS1 CEN4* minichromosome was transformed to the resulting strain.

The *Smc3-FRB* and *FKBP12-Scc1* cysteine mutants were created by site-directed mutagenesis using Phusion Polymerase. The constructs obtained and confirmed by sequencing were: *Smc3-FRB(V2094C), Smc3-FRB(R2042C), Smc3-FRB(K2095C)* in puc19, and *FKBP12(G89C)-Scc1-pk6-avitag, FKBP12(T85C)-Scc1pk6-avitag, FKBP12(D37C)-Scc1 pk6-avitag* in YIplac211.

The pRS305H plasmids carrying the wild type or mutant *Smc1-myc9* genes were digested with *KpnI* enzyme for integration at the *leu2* locus and introduced into a diploid strain heterozygous for *smc1* deletion. The spore containing *Smc1(G22C, K639C)-myc9* over deletion of *smc1* was combined with the strain containing *Scc1(A547C)-PK6-*

avitag::KanMX4 and wild type *Smc3* on a centromeric plasmid YCplac33 over *smc3* deletion in order to make a shuffle strain. The amber-substituted Smc3 plasmids and pLH157 were co-transformed into this shuffle strain. In order to identify functional Smc3 proteins containing residues that are substituted by BPA, a plasmid assay was performed on media containing BPA and the 5-FOA to select against the wild-type *URA3* plasmid-borne copy of *smc3*. The transformants were then streaked onto –Trp-Leu plates containing 1 mM BPA. For the minichromosome assay, a 3kb *URA3ARS1CEN6* minichromosome was transformed.

The yeast strains used in the experiments are listed in Appendix 1.

5.1.2 Plasmid Construction

2.3 kb minichromosome containing *TRP1ARS1,* and *CEN4* sequences was obtained by digesting a 4.4kb pUC19 plasmid containing *TRP1*, *ARS1* and 850 bp long *CEN4* with *SalI* and *BglI* overnight to remove the pUC19 sequences of the construct. Yeast sequences containing *TRP1ARS1* and *CEN4* were gel purified as 2.3kb fragment, circularized by ligation and used for yeast transformation.

3kb minichromosome: The fragment containing *URA3, ARS1* and *CEN6* sequences were amplified from the vector YIplac211 using appropriate primers and digested with NotI and BamHI. The digested fragment was then circularized by ligation and used for yeast transformation.

pGST-FKBP12 was a gift from Jerry Crabtree`s laboratory. Mutations in FKBP12 were introduced by site-directed mutagenesis and confirmed by sequencing.

pMAL-c2X-FRB: cDNAs encoding aa 2015-2114 of the human FKBP12-rapamycin-binding domain (FRB domain) in FRAP were cloned into pMAL-c2X (New England Biolabs) expression vector as a *EcoRI* and *BamHI* fragment and a stop codon was placed

after Q2114. Mutations were introduced by site-directed mutagenesis and confirmed by sequencing

SMC3-FRB-HisMx in pUC19: The insert fragment was amplified from strain K13637 using appropriate primers. pUC19 vector was digested with EcoRI, and the fragment containing the *Smc3-FRB::HisMx* together with the 300bp of Smc3`s 3`UTR was inserted (Clontech In-Fusion cloning system). Mutations were introduced by site-directed mutagenesis and confirmed by sequencing. The linker sequence used to fuse FRB to C-terminal of Smc3:

ARGSGSGGSS-(I2021-mTOR (human)-K2113)-SSGSGSGSAS

FKBP12-Scc1-PK6-Avitag in YIplac211: The fragment encoding the fusion *FKBP12-GClinker-Scc1* under the Scc1 promoter was amplified from strain K13637 using appropriate primers and cloned as EcoRI fragment into YIplac211. The resulting plasmid was digested with ClaI and BamHI in order to insert the fragment containing PK6-Avitag. Mutations were introduced by site-directed mutagenesis and confirmed by sequencing. The linker sequence used to fuse FKBP12 to the N-terminal of Scc1:

ARGSGSGGSS-(G2-FKBP12 (human)-E108)-SSGSGSGSAS

Smc3-HA3 in YEpLac181: Amber codon TAG was substituted with 2 different codons in the Smc3 ORF (K185 and A181) by site directed mutagenesis. Mutations were confirmed by sequencing.

pLH157 (TRP1) containing the *E.coli* nonsense suppressor tRNA/tRNA synthetase system was a gift from Steven Hahn (Mohibullah and Hahn, 2008).

Smc1-myc9 in pRS305H: Full-length Smc1 containing 9 Myc epitope tags was amplified and cloned as a HindIII and BamHI fragment into pRS305H. Cysteine mutations were inserted by site-directed mutagenesis and confirmed by sequencing.

5.2. Growth Conditions

Cells were grown in YEP media supplemented with either 2% glucose (YEPD) or 2% Raffinose (YEPRaff). For the preparation of 2.3kb *TRP1* minichromosomes, cells were grown in synthetic medium without tryptophan containing 0.5% leucine and 2% raffinose as the carbon source. For the preparation of 3kb *URA3* minichromosomes, cells were grown in synthetic medium without uracil supplemented with 0.5% leucine, 0.5% tryptophan and 2% glucose.

For Eco1 inactivation experiments, strains transformed with 2.3kb plasmids containing *TRP1 ARS CEN4* sequences were grown overnight at 23°C in synthetic medium without tryptophan containing raffinose as the carbon source. The cells were then diluted to a final OD_{600} of 0.2 and grown at 23°C until the OD_{600} reached 0.65. In order to achieve a proper G2-M arrest, cells were then diluted to a OD_{600} of 0.15, alpha factor was added to a final concentration of 2 μg/ml (from a 10mg/ml stock solution in ethanol and stored at -20°C), and cells were incubated shaking at 23°C for 1 hour. Alpha factor was added to a final concentration of 1.5 μg/ml. The cells were checked under the microscope every fifteen minutes until the G1 arrest was complete (less than or equal to 1% budded cells). To release cells from the arrest, the cells were spun down at room temperature at 5,000rpm for 2 min in a Beckman-Coulter Avanti A26-XP centrifuge and resuspended in four culture volumes of the same pre-warmed media they were grown in. The cells were spun again at 5,000rpm for 2 minutes in a Beckman-Coulter Avanti A26-XP centrifuge, resuspended in 10ml pre-warmed media and topped up to the desired culture volume (i.e. 690ml for a final volume of 700ml). To arrest the cells in a metaphase-like state, nocodazole (Sigma) was added at a final concentration of 10μg/ml to the culture and cells were incubated further for 1h50' at 25°C.

For *in vivo* photo-cross-linking experiments, cells were grown in minimal media supplemented with 2% glucose, 1%-Leu-Trp drop out and 2mM BPA dissolved in 1M NaOH, pH adjusted to 7 with 1M HCI to OD_{600}~1 overnight at 30°C. Next day, cells were diluted to a final OD_{600} of 0.2 and grown at 30°C until the OD_{600} reached 0.65 in YEPD+2mM BPA. Cells were then harvested and poured into 2-cm^2 Petri dish for UV cross-linking. To prepare solid media containing BPA, 0.135 gram of BPA dissolved in 5ml of 1M NaOH was added to 1L of media along with 5mL of 1M HCI to a final BPA concentration of 1mM.

5.3. Yeast Transformation

An overnight culture was grown at 23-30^{0}C and 50 ml rich media were inoculated from an overnight culture to OD_{600}=0.2 and grown at 23-30^{0}C to OD_{600}=0.6. 10 mg/ml salmon sperm DNA was boiled for 5 minutes at 95^{0}C and was kept on ice while harvesting cells. Cells were centrifuged in a 50ml falcon tube at 3,500rpm at 4^{0}C for 5 minutes. The pellet was resuspended in 1ml LiAc and centrifuged at 3,500rpm at 4^{0}C for 5 minutes. The cells were resuspended in 350µl of 1M LiAc, 10µl of boiled salmon sperm DNA, 5µl of plasmid DNA, 30µl of resuspended cells, and 112.5µl 50% PEG 3350 were mixed and incubated at room temperature without shaking for 30 minutes. Then 15µl 60% glycerol were added and the cells were incubated at room temperature without shaking for another 30 minutes. The cells were incubated at 42^{0}C for 10 minutes. 300µl sterile dH_2O were added and 1x150µl and 1x200µl were plated on selective plates.

5.4. Chromatin Immunoprecipitation (ChIP) Protocol for *Saccharomyces Cerevisiae*

A 50 ml culture in rich media was inoculated from an overnight culture and grown to have cells in exponential phase at OD_{600}=0.6-0.9. The cells were then diluted in rich media to a final OD_{600} of 0.2 and grown until they reached an OD_{600} of 0.4. Once they reached the required $OD_{600,}$ 4.2 ml (3% final) fresh fixative (50mM Tris-HCl pH 8.0, 11mM NaCI, 0.5mM EGTA, 1mM EDTA, 30% (v/v) formaldehyde) was added to 42 ml of the culture, and cells were rocked at 16°C for 30 minutes. Fixation was stopped by adding 2.0 ml 2.5M Glycine, inverting the tube and rocking for 5 minutes at 16°C. Cells were spun for 2 minutes at 3300rpm at 4°C in a Heraeus Multifuge 3 S-R cooling centrifuge, washed in 20ml ice-cold PBS and spun again at 3300 rpm for 2 minutes in a Heraeus Multifuge 3 S-R cooling centrifuge. Cells were incubated in 1ml 100mM Pipes-KOH pH9.3, 10mM DTT for 20min. on ice in a 1.5mL Eppendorf tube. Cells were spun for 2 min at 5000rpm at 4°C in a Heraeus Biofuge fresco cooling centrifuge and resuspended in 1 ml HEMS (100mM Hepes-KOH pH7.5, 1mM EGTA, 1mM $MgSO_4$,1.2M Sorbitol, 1mM PMSF, Complete Protease inhibitor EDTA free (Roche)). Cells were spun for 2 min at 5000rpm at 4°C in a Heraeus Biofuge fresco cooling centrifuge. Cells were spheroplasted in 1mL 0.5mg/mL zymolyase T100 in HEMS for 20 min at 37°C. Cells were spun for 2 minutes at 7000rpm. Cells were washed once with ice-cold HEMS and spun for 2 minutes at 8700rpm. Cells were resuspended in 1ml HEMS and spun at 13.2 rpm at 4°C in a Heraeus Biofuge fresco cooling centrifuge for 2 min. The supernatant was removed and the pellet frozen in liquid nitrogen. The pellet was resuspended in 2ml ice-cold lysis buffer (50mM Hepes-KOH pH 7.5, 140mM NaCI, 1mM EDTA, 1% (v/v) Triton X-100, 0.1% (w/v) Sodium deoxycholate, 1mM PMSF, Complete Protease inhibitor EDTA free) and transferred to a 15ml Falcon tube. The cells were sonicated at 4°C in a Bioruptor cold sonicator for 9 minutes at high level with a rotating cycle

of 30 seconds on/1 minute off. The lysate was transferred into a 2ml tube and spun for 5 minutes at 13,200 rpm at 4°C in a Heraeus Biofuge fresco cooling centrifuge. The supernatant was transferred to a new 2 ml tube and spun for 15 minutes at 13,200 rpm at 4°C in a Heraeus Biofuge fresco cooling centrifuge. The supernatant was transferred to a new tube and pre-cleared with 50ul of protein G Dynabeads (Invitrogen) on a rotating plate at 4°C for 1 hour. The beads were then pelleted with a Dynabead magnet and 200 ul of supernatant were frozen at -20°C for whole cell extract (WCE) standards while 1600 ul were transferred to a new 2ml tube and mixed with 3ul anti-PK antibody (Serotec, MCA 1360). The supernatant was kept on the rotating plate for 2 hours at 4°C. After two hours 100 ul of protein G Dynabeads were added and the samples were incubated rotating at 4°C overnight (12 hours or more). The beads were pelleted and washed once for 5 min. shaking at 800rpm at 16°C with 1ml of each of the following buffers: Lysis Buffer, lysis buffer plus 500mM NaCI, wash buffer (10mM Tris-HCl pH 8.0, 0.25M LiCl, 0.5% NP-40, 0.5% (w/v) sodium deoxycholate, 1mM EDTA, 1mM PMSF, Complete protease inhibitor EDTA Free), and TE buffer (10mM Tris-HCl pH 8.0, 1mM EDTA). The beads were then resuspended in 520 ul TES buffer (50mM Tris-HCl pH 8.0, 10mM EDTA, 1% SDS (w/v), complete protease inhibitor EDTA Free). The WCE samples were thawed and combined with 300 ul TES buffer and 20 ul 10% SDS. All samples were shaken at 800rpm at 65°C for 6hrs to overnight. This reverses the crosslinks and elutes the DNA from the beads. The beads were pelleted and 300 ul of the supernatants were transferred to a fresh 2 ml tube. 1uL of RNAse was added to all samples and the tubes were shaken at 900rpm for 1hr. at 37°C. Afterwards, 10ul of Proteinase K (Roche 20mg/mL in TE) were added to all samples and the tubes were shaken at 900rpm for 2hrs. at 37°C. Then, 1.2ml PB Buffer were added and the samples were mixed gently. The DNA was then purified using QIAquick Gel Extraction Kit. However, before eluting the DNA, columns were first dried at 65°C for 2min and then the DNA was

eluted with 50 ul prewarmed (65°C) 20mM Tris pH 8.0 or EB buffer. While IP samples were diluted 1:2 in buffer EB or 20mM Tris pH 8.0, WCE samples were diluted 1:5 in EB or 20mM Tris pH8.0. In the QPCR, while 1:2 and 1:10 dilutions were used for the IP samples, 1:5, 1:50, 1:500, and 1:5000 dilutions were used for the WCE samples. The qPCR reaction tubes contained the following:

2X Abgene SYBR Mix 10uL
Primer 1 (1:100 dilution) 1.4uL
Primer 2 (1:100 dilution) 1.4uL
dH2O 2.2uL
Sample 5uL

Reactions were set up using a CAS1200 automatic liquid handling system (Corbett Research). The qPCR was performed in a Corbett Rotorgene cycler with cycles as follows:

Hold 95°C-15min
Cycle 65X: 10sec-95°C
20 sec-52°C
20 sec-72°C (Acquiring on SYBR Channel)
Melt Curve-60-95°C

Site	5'-3' primer
345.1 (Low Cohesin)	CCAGATGGCTCACAT
346.3 (Low Cohesin)	GCTCAGAATTGGGTTTGTC
357.3 (Outer Pericentromere)	CCAGGATAGCCACTGCTTCT

358.3 (Outer Pericentromere)	CGATGACGTCGCTACACTT
363 (Inner Pericentromere)	GACGAAAGAACGGAAACTCG
364.2 (Inner Pericentromere)	CCTTGGATAGCTTTGCTGGA
366.1 (Centromere)	GCGGCCTTAAGTTCGTAGTG
367.2 (Centromere)	AAGTGCCGGAAATTGTCTTG
371 (Inner Arm)	ACGGTTCAGTTCCTCCATTG

5.5. Yeast protein extraction using trichloroacetic acid (TCA method)

Exponentially growing cells (2-3x10^8, about 3-4 units of OD_{600}) were collected by centrifugation at 2,000 rpm for 5min in Heraeus multifuge. Harvested cells were resuspended with 1ml ice-cold 10% TCA, transferred to a 2ml tube. Cells were spun down at 13,000 rpm for 10 sec and the supernatant was discarded. The pellet was frozen in liquid nitrogen. Fixed cells were resuspended in 200ul 10% TCA, 200ul glass beads were added and the cells were broken by beat-beater for 5 min in the cold room. The extracts were transferred in a fresh 1.5ml tube, the remaining beads were washed with 1ml 10% TCA, and then added to the tube containing the extracts. The resulting extract was spun at 13,000 rpm for 10 min and the supernatant was discarded. The pellet was resuspended in 100ul 2x SDS gel-loading buffer (4% SDS, 20% glycerol, 0.1% bromphenol blue, 125mM TrisHCI pH 6.8) (the solution color should become yellow due to the low pH), DTT was added to 10mM final concentration and the pH was adjusted by adding 50ul 1M Tris-base (pH 8.8) (the solution color should now turn back to blue). The samples were then sonicated at 20% output level (Branson Sonifier 250) for 5 sec. Samples were boiled for 5 min at 95 ^oC, centrifuged for 5 min at 13,000 rpm,

and separated on SDS/PAGE (sodium dodecyl sulphate polyacrylamide gel electrophoresis) or Tris-Acetate gels.

5.6. Western blot analysis

SDS/PAGE or Tris-Acetate gel electrophoresis and immunoblot analysis were performed according to standard protocols (Sambrook and Russell, 2001). Denatured samples were separated by SDS-PAGE or Tris-Acetate gel electrophoresis, and transferred to a PVDF (polyvinylidene fluoride) membrane. The membrane was then blocked for 1 hr in 4% milk prepared in PBST, and probed with antibodies diluted in blocking solution. The detection of the proteins in Western blot was carried out according to standard protocols, by using antibodies against the HA (3F10, 12CA5), against the myc (Gramsch, 9E11, Santa Cruz) and against PK (Serotec, MCA 1360) epitopes.

5.7. FACS analysis

1 ml of culture was centrifuged for 1 min at 13,000rpm. The supernatant was removed and the pellet was resuspended into 70% ethanol and stored at -20^{o}C. The fixed cells were spun down again for 1 min at 13,000rpm, and the pellet was dissolved in 1 ml 50mM Tris-HCI pH 7.5 and 20 ul of 10mg/ml RNaseA, and incubated over night at 37 ^{o}C with shaking. Next day, cells were pelleted by 1 min centrifugation at 13,000rpm. The pellet was resuspended in 400ul FACS buffer (200mM Tris-HCI pH7.5, 211mM NaCI, 78mM $MgCI_2$ and 50ug/ml propidium iodide). The cells were sonicated for 5sec at 40% power, 50-100ul were taken into FACS tubes containing 1 ml 50mM Tris-HCI pH 7.5, and the samples were read using a Becton Dickinson FACSCalibur machine, by ensuring 10,000 events per sample.

5.8. Minichromosome preparation

Cells were grown as described in the previous section. Cells were harvested by centrifugation at 3500rpm and 4°C for 3min in a Heraeus multifuge 3S-R. The pellet was washed twice with cold milliQ H_2O, resuspended in 100mM Tris HCl pH 9.4, 10mM DTT, and 10µg/ml nocodazole, and incubated for 15min at room temperature. After washing the cells once with milliQ H_2O, the pellet was resuspended in spheroplasting buffer (1M sorbitol, 50mM Tris HCl pH7.5, 1mM CaCl2, 1mM MgCl2, 1.1mg lyticase (L-2524, Sigma), and 10µg/ml nocodazole) and incubated for 30min on a shaking platform at 25°C and 65rpm. The spheroplasts were centrifuged in a Beckman Coulter using a JA 25.50 rotor at 6000rpm for 6 minutes, washed with 1M sorbitol, recentrifuged for 6 minutes and resuspended in 150µl cold 0.4M sorbitol and lysed on ice for 30 min by the addition of 600µl lysis buffer (25mM Hepes/KOH pH 8, 50mM KCl, 10mM MgSO4, 0.25% Triton X-100, 1mM PMSF, 3mM DTT, 1×complete EDTA-free protease inhibitors [Roche]), supplemented with 100µg/ml RNaseA and 300mM NaCI. The lysate was cleared by centrifugation at 4°C, and 1000rpm for 5min.

The cleared lysates were loaded on a 10-30% sucrose gradient prepared using a Biocomp gradient station, and separated in a SW41 rotor (Beckman Optima^{TM} L-100 XP Preparative Ultracentrifuge) for 15h at 18000 rpm. The sucrose gradients were fractionated using a Gilson FC203B fractionator, collecting 15drops per fraction.

5.9. Southern blot analysis

Gradient fractions were separated on 1 % agarose gels in the presence of 5ug/ml ethidium bromide at 1.4V/cm and transferred to Immobilon-NY+ membrane (Millipore).

Southern blot detection was achieved by hybridising with a ^{32}P-radioactively labelled probe, probing with the CEN4 sequence of the 3kbp minichromosome (for the detection of 3kbp minichromosome) or the whole sequence of 2.3kbp minichromosome (for the detection of 2.3kbp minichromosome). Hybridised blots were exposed to imaging plates and the radioactive signal was detected with the FLA-7000IR bio-image analyser (Fuji Film). Collected data were analysed using Aide Image Analyzer v4.22.

5.10. Genomic DNA preparation

Cells cultures (7.5-10 ODs of cells) were spun down at 3500 rpm in a Heraeus centrifuge for 2 min, and resuspended with ice-cold 50% Ethanol. EDTA was added to 10mM final concentration, and samples were stored at -20^{o}C (for at least 30min). Cells were pelleted at 2000 rpm for 5min at 4 ^{o}C, resuspended with 1ml ice-cold milliQ H_2O and transferred into 1.5ml Eppendorf tubes. Cells were washed with 1 ml ice-cold milliQ H_2O three times and then shortly spun at 10,000 rpm to remove the supernatant. Pelleted cells were dissolved in 250ul spheroplasting buffer (1.2M sorbitol, 0.1 M sodium citrate pH7.0, 0.1 M EDTA, 1% β-mercaptoethanol, 0.1 %, Zymolyase T-100) and incubated at 37 ^{o}C for 1h with occasional shaking. Cells were spun down at 8000 rpm for 1min, and the supernatant was carefully discarded. Cells were then gently resuspended in 500ul proteinase K buffer (10mM Tris pH 8.0, 50mM EDTA, 0.5 % SDS, and 0.01 % proteinase K), and incubated for 30min at 65 ^{o}C. 100ul 5M KAc was added and samples were mixed thoroughly and incubated on ice for 40min. Subsequent to 15min centrifugation at 13,000 rpm at 4 ^{o}C, 500ul supernatant was taken in a 1.5ml Eppendorf tube. 500ul ice-cold 100% ethanol was then added to precipitate the DNA at room temperature. The precipitated DNA pellet was centrifuged for 10min at 13,000 rpm at 4 ^{o}C, and the supernatant was removed. The DNA pellet was suspended in 500ul 50% Ethanol and incubated at room temperature for 10 min on a rotator. Following the

centrifugation for 10min at 13,000 rpm at 4 ^{o}C, the pellet was dried at 65 ^{o}C in order to remove ethanol completely. Later on, DNA was resuspended in 250ul TE and 1.25ul 10mg/ml RNase A was added and incubated for 30min at 37 ^{o}C. Concentrations of the genomic DNA were measured using Nanodrop and equal amounts were used for agarose electrophoresis.

5.11. Expression and purification of FRB and FKBP12 proteins

pGST-FKBP12 was a gift from Jerry Crabtree`s laboratory. To express FRB as a MBP fusion protein, cDNAs encoding aa 2015-2114 of the human FKBP12-rapamycin-binding domain (FRB domain) in FRAP were cloned into pMAL-c2X (New England Biolabs) expression vector, according to manufacturer's instructions (Clontech In-Fusion cloning system). Cysteine mutations were introduced by two-step PCR mutagenesis using Phusion polymerase (NEB). Human FRB and FKBP12 proteins were expressed separately in 12 L cultures of *E.coli* strain BL21 (DE3)-RIPL (Stratagene) at 20 ^{o}C for 12 hours after induction with 400uM IPTG. Cells were lysed in 150mM Tris pH7.5, 300mM NaCI, 1mM EDTA, and 1mM DTT containing Complete EDTA free protease inhibitor mix (Roche) using French Press and spun at 20000 rpm for 40 minutes at 4°C in a Beckman centrifuge. The supernatant of GST-tagged FKBP12 fusion protein was incubated with glutathione beads (Glutathione Sepharose 4B, Pharmacia) for 30 minutes on a rotator in the cold room and eluted in 150mM Tris pH7.5, 300mM NaCI, 1mM EDTA, 1mM DTT and 10mM glutathione. Eluted proteins were further purified using a Superdex 200pg 26/60 column (GE Healthcare) in 100mM Tris pH7.5, 1mM EDTA, 100mM NaCI and 1mM DTT. MBP tagged FRB fusion protein were purified via amylose affinity chromatography followed by gel filtration on a Superdex 200pg 26/60 column (GE Healthcare) in 100mM Tris pH7.5, 1mM EDTA, 100mM NaCI and 1mM DTT.

After gel filtration, FKBP12-GST was concentrated to 6 mg/ml and FRB-MBP was concentrated to 2 mg/ml. Protein concentrations were measured by UV absorption.

5.12. Cross-linking conditions

5.12.1 Chemical cross-linking reaction

Purified proteins were re-buffered into reaction buffer (25mM NaPi pH7.4, 50mM NaCI, 10mM $MgCl_2$, 0/25% Triton X-100, 100uM Rapamycin) via a Superdex G-25 column, adjusted to 0.5mg/ml and mixed quickly into 1/25 volume of DMSO, bBBr (Sigma), or BMOE (Pierce). Both cross-linkers were dissolved into DMSO just before use. After 10 minutes incubation at 4 ^{o}C, sample loading buffer containing β-mercaptoethanol was added, the samples were denatured for 5 min at 90 ^{o}C and run on SDS-PAGE followed by Coomassie blue staining. Optimal cross-linking occurred at final concentrations of 200uM bBBr or 1mM BMOE and reached a maximum after a few minutes at 4 ^{o}C.

5.12.2 Photo-cross-linking reaction

Cells were grown as described in section 5.2. Cells were poured into 2-cm^2 Petri dish. Samples were placed in a Spectrolinker XL1500 UV cross-linker (Spectronics Corp.) and irradiated three times for 400seconds with a power of 15,000mJcm^{-2}. After irradiation, cells were collected and whole cell extracts were prepared by TCA method as described in section 5.5. For immunoprecipitation experiments, extracts were prepared as described in section 5.14.

5.13. FKBP12-Rapamycin-FRB binding assay

Wild type and mutant FKBP12-GST proteins were first pre-mixed with rapamycin in 1 ml of binding buffer (100mM NaCI, 50mM Tris pH 7.5 with 1mM DTT) at 1uM each, followed by addition of 1uM wild type or mutant FRB-MBP proteins and brief incubation on ice. Amylose resin or glutathione sepharose (20 ul) was then added to the mixture and rocked at 4 ^{o}C for 1 hr. The matrix was subsequently washed three times in 1 ml of binding buffer and boiled in SDS sample buffer and loaded on a 12% SDS gel.

5.14. Immunoprecipitation experiments

Cells were grown as described in the previous section. Cells were harvested by centrifugation at 3500rpm and 4°C for 3min in a Heraeus multifuge 3S-R. The pellet was washed twice with cold milliQ H_2O, resuspended in 100mM Tris HCl pH 9.4, 10mM DTT, and 10µg/ml nocodazole, and incubated for 15min at room temperature. After washing the cells once with milliQ H_2O, the pellet was resuspended in spheroplasting buffer (1M sorbitol, 50mM Tris HCl pH7.5, 1mM CaCl2, 1mM MgCl2, 1.1mg lyticase (L-2524, Sigma), and 10µg/ml nocodazole) and incubated for 30min on a shaking platform at 25°C and 65rpm. The spheroplasts were centrifuged in a Beckman Coulter using a JA 25.50 rotor at 6000rpm for 6 minutes, washed with 1M sorbitol, recentrifuged for 6 minutes and resuspended in 150µl cold 0.4M sorbitol and then resuspended in 150 µl 0.4M sorbitol and lysed on ice for 30 min by the addition of 600µl lysis buffer (25mM Hepes/KOH pH 8, 50mM KCl, 10mM MgSO4, 0.25% Triton X-100, 1mM PMSF, 3mM DTT, 1×complete EDTA-free protease inhibitors [Roche]), supplemented with 100µg/ml RNaseA and 300mM NaCI. The lysate was cleared by centrifugation at 4°C, 1000rpm for 5min.

In the case of Scc1-PK or FKBP12-Scc1-PK immunoprecipitation, extractions were clarified by centrifugation, and further cleared by incubation with immunoglobulin G sepharose beads (GE Healthcare) on a rotating wheel for 1 hr. A total of 3 mg antibody against the Scc1-Pk6 epitope was added for 1hr (clone SV5-Pk1, Serotec), and immunocomplexes were isolated by adsorption to protein A sepharose beads (GE Healthcare) for 2 hr. Beads were washed extensively in extraction buffer, and immunocomplexes were recovered by incubation with elution buffer (50 mM Tris/HCl [pH 8.0], 10mMEDTA, 1% SDS) for 15 min at 65 ^{o}C. Eluates were run on a 3-8% Tris-Acetate gels followed by western blotting with a-2 Pk and a-acetyl lysine antibodies (ST1027, Calbiochem) or with a mouse monoclonal a-Smc3 acetylated antibody.

References

Anderson, D.-E., Losada, A., Erickson, H.-P., and Hirano, T. (2002). Condensin and cohesin display different arm conformations with characteristic hinge angles. J Cell Biol *156*, 419-424.

Arumugam, P., Gruber, S., Tanaka, K., Haering, C.-H, Mechtler, K., Nasmyth, K. (2003). ATP Hydrolysis Is Required for Cohesin's Association with Chromosomes. Current Biology *13*, 1941-1953.

Arumugam, P., Nishino, T., Haering, C.-H., Gruber, S., and Nasmyth, K. (2006). Cohesin's ATPase activity is stimulated by the C-terminal Winged-Helix domain of its kleisin subunit. Curr Biol *16*, 1998-2008.

Bakkenist, C.J., and Kastan, M.B. (2004). Initiating cellular stress responses. Cell *118*, 9-17.

Banaszynski, L.-A., Liu, C.-W., Wandless. T.-J. (2005). Characterization of the FKBP-rapamycin-FRB ternary complex. J Am Chem Soc. *127*, 4715-4721.

Bartolomei. M.-S., Zemel, S., Tilghman, S.-M. (1991). Parental imprinting of the mouse H19 gene. Nature *351*, 153–155.

Bausch, C., Noone, S., Henry, J.-M., Gaudenz, K., Sanderson, B., Seidel, C., and Gerton, J.-L. (2007). Transcription alters chromosomal locations of cohesin in S. cerevisiae. Mol Cell Biol *27*, 8522-8532.

Beckouët, F., Hu, B., Roig, M.-B., Sutani, T., Komata, M., Uluocak, P., Katis, V.-L., Shirahige, K., Nasmyth, K. (2010). An Smc3 acetylation cycle is essential for establishment of sister chromatid cohesion. Mol Cell *39*, 689-99.

Bell, A.C., and Felsenfeld, G. (2000). Methylation of a CTCF-dependent boundary controls imprinted expression of the Igf2 gene. Nature *405*, 482-485.

Bell, S.P., and Dutta, A. (2002). DNA replication in eukaryotic cells. Annu. Rev. Biochem. *71*, 333-374.

Belshaw, P.J., Ho, S.N., Crabtree, G.R., and Schreiber, S.L. (1996). Controlling protein association and subcellular localization with a synthetic ligand that induces heterodimerization of proteins. Proc. Natl. Acad. Sci. USA *93*, 4604–4607.

Ben-Shahar, T.-R., Heeger, S., Lehane, C., East, P., Flynn, H., Skehel, M., and Uhlmann, F. (2008). Eco1-dependent cohesin acetylation during establishment of sister chromatid cohesion. Science *321*, 563-566.

Ben-Shahar, T., Borges, V., Lehane, C., Lopez-Serra, L., Flynn, H., Skehel, M., and Uhlmann, F.(2010) Hos1 deacetylates Smc3 to close the cohesin acetylation cycle. Mol Cell. *39*, 677-688.

Bernard, J., Horowitz, R.A., Grigoryev, S.A., Carruthers, L.M., Hansen, J.C., Koster, A.J., Woodcock, C.L. (1998). Nucleosomes, linker DNA, and linker histone form a unique structural motif that directs the higher-order folding and compaction of chromatin. Proc. Natl Acad. Sci. USA *95*, 14173-14178.

Bernard, P., Maure, J.-F., Partridge, J.-F., Genier, S., Javerzat, J.-P., and Allshire, R.-C. (2001). Requirement of heterochromatin for cohesion at centromeres. Science *294*, 2539-2542.

Bernard, P., Schmidt, C.K., Vaur, S., Dheur, S., Drogat, J., Genier, S., Ekwall, K., Uhlmann, F., and Javerzat, J.P. (2008). Cell-cycle regulation of cohesin stability along fission yeast chromosomes. Embo J *27*, 111-121.

Birkenbihl, R.-P., and Subramani, S. (1992). Cloning and characterization of rad21 an essential gene of Schizosaccharomyces pombe involved in double strand break repair. Nuc Acid Res *20*, 6605-6611.

Blat, Y., and Kleckner, N. (1999). Cohesins bind to preferential sites along yeast chromosome III, with differential regulation along arms versus the centric region. Cell *98*, 249-259.

Blow, J.J., and Tanaka, T.U. (2005). The chromosome cycle: coordinating replication and segregation. Second in the cycles review series. EMBO Rep *6*, 1028-1034.

Brown, E.J., Albers, M.W., Shin, T.B., Ichikawa, K., Keith, C.T., Lane, W.S., and Schreiber, S.-L.(1994). A mammalian protein targeted by G1-arresting rapamycin-receptor complex. Nature *369*, 756-758.

Bürmann, F., Basquin, J., Gimenez-Oya, V., Conti, E., and Gruber, S. (2011). Bacterial origin of asymmetric SMC2/kleisin rings. Submitted to Cell.

Campbell, J.-L., and Cohen-Fix, O. (2002). Chromosome cohesion: ring around the sisters? Trends in Biochemical Sciences *27*, 492.

Cardozo, T., and Pagano, M. (2004). The SCF ubiquitin ligase: insights into a molecular machine. Nat Rev Mol Cell Biol *5*, 739-751.

Chan, K.-L., Roig, M.B., Hu, B., Beckouët, F., Metson, J., and Nasmyth, K. (2011). Evidence that acetylation of cohesin`s Smc3 subunit blocks dissociation from chromatin by preventing ring opening. Accepted to Cell.

Chang, C.-R., Wu, C.-S., Hom, Y., and Gartenberg, M.-R. (2005). Targeting of cohesin by transcriptionally silent chromatin. Genes Dev *19*, 3031-3042.

Chen, J., Zheng, X.- F., Brown, E. -J. and Schreiber, S.- L. (1995). Identification of an 11-kDa FKBP12-rapamycin-binding domain within the 289-kDa FKBP12-rapamycin-associated protein and characterization of a critical serine residue. Proc.Natl Acad. Sci. USA *92*, 4947-4951.

Chen, H.T., Warfield, L., and Hahn, S. (2007). The positions of TFIIF and TFIIE in the RNA polymerase II transcription preinitiation complex. Nat. Struct. Mol. Biol.*14*, 696–703.

Chin JW, Martin AB, King DS, Wang L, and Schultz PG. (2002). Addition of a photo-cross-linking amino acid to the genetic code of *Escherichia coli*. Proc.Natl Acad. Sci. USA *99*, 11020-11024.

Chin, J.-W., Cropp, T.-A., Anderson, J.-C., Mukherji, M., Zhang, Z., and Schultz, P.G. (2003). An expanded eukaryotic genetic code. Science *301*, 964–967.

Choi, J., Chen, J., Schreiber, S.-L., and Clardy, J. (1996). Structure of the FKBP12-rapamycin complex interacting with the binding domain of human FRAP. Science *273*, 239-242.

Ciosk, R., Shirayama, M., Shevchenko, A., Tanaka, T., Toth, A., Shevchenko, A., and Nasmyth, K. (2000). Cohesin's binding to chromosomes depends on a separate complex consisting of Scc2 and Scc4 proteins. Mol Cell *5*, 243-254.

Cohen-Fix, O., Peters, J.-M., Kirschner, M.-W., and Koshland, D. (1996). Anaphase initiation in Saccharomyces cerevisiae is controlled by the APC-dependent degradation of the anaphase inhibitor Pds1p. Genes & Dev *10*, 3081-3093.

Cuylen, S., Haering, CH. (2010). A new cohesive team to mediate DNA looping. Cell Stem Cell *7*, 424-426.

De Antoni, A., Pearson, C.G., Cimini, D., Canman, J.C., Sala, V., Nezi, L., Mapelli, M., Sironi, L., Faretta, M., Salmon, E.D*., et al.* (2005). The Mad1/Mad2 complex as a template for Mad2 activation in the spindle assembly checkpoint. Curr Biol *15*, 214-225.

DeChiara, T.-M., Robertson, E.-J., and Efstratiadis, A. (1991). Parental imprinting of the mouse insulin-like growth factor II gene. Cell *64*, 849–859.

Deardorff, M.A., Kaur, M., Yaeger, D., Rampuria, A., Korolev, S., Pie, J., Gil-Rodriguez, C., Arnedo, M., Loeys, B., Kline, A.D*., et al.* (2007). Mutations in cohesin complex members SMC3 and SMC1A cause a mild variant of cornelia de Lange syndrome with predominant mental retardation. Am J Hum Genet *80*, 485-494.

Diffley, J.F. (1995). The initiation of DNA replication in the budding yeast cell division cycle. Yeast *11*, 1651-1670.

Donze, D., Adams, C.R., Rine, J., and Kamakaka, R.T. (1999). The boundaries of the silenced HMR domain in Saccharomyces cerevisiae. Genes Dev *13*, 698-708.

Dormán, G., and Prestwich, G.D. (1994). Benzophenone photophores in biochemistry. Biochemistry *33*, 5661-5673.

Dorsett, D. (2007). Roles of the sister chromatid cohesion apparatus in gene expression, development, and human syndromes. Chromosoma *116*, 1-13.

Dubey, R.N., and Gartenberg, M.R. (2007). A tRNA establishes cohesion of a neighbouring silent chromatin domain. Genes Dev *21*, 2150-2160.

Ebmeier, C.C., and Taatjes, D.J. (2010). Activator-Mediator binding regulates Mediator-cofactor interactions. Proc.Natl Acad. Sci. USA *107*, 11283-11291.

Farcas, A.M., Uluocak, P., Helmhart, W., and Nasmyth, K. (2011). Cohesin`s concatenation of sister DNAs maintains their intertwining. Mol Cell *44*, 97-107.

Felsenfeld, G., and Groudine, M. (2003). Controlling the double helix. Nature *421*, 448–453.

Funabiki, H., Yamano, H., Kumada, K., Nagao, K., Hunt, T., and Yanagida, M. (1996). Cut2 proteolysis required for sister-chromatid separation in fission yeast. Nature *381*,438-441.

Gandhi, R., Gillespie, P.J., and Hirano, T. (2006). Human Wapl is a cohesin-binding protein that promotes sister-chromatid resolution in mitotic prophase. Curr Biol *16*, 2406-2417.

Gerlich, D., Koch, B., Dupeux, F., Peters, J.M., and Ellenberg, J. (2006). Live-cell imaging reveals a stable cohesin-chromatin interaction after but not before DNA replication. Curr Biol *16*, 1571-1578.

Gillespie, P.J., and Hirano, T. (2004). Scc2 couples replication licensing to sister chromatid cohesion in Xenopus egg extracts. Curr Biol *14*, 1598-1603.

Glynn, E.F., Megee, P.C., Yu, H.G., Mistrot, C., Unal, E., Koshland, D.E., DeRisi, J.L., and Gerton, J.L. (2004). Genome-Wide Mapping of the Cohesin Complex in the Yeast Saccharomyces cerevisiae. PLoS Biol *2*, E259.

Gorr I. H., Boss, D., and Stemmann, O. (2005). Mutual inhibition of separase and Cdk1 by two-step complex formation. Mol Cell *19*, 135-141.

Grewal, S.I., and Moazed, D. (2003). Heterochromatin and epigenetic control of gene expression. Science *301*, 798-802.

Gruber, S., Haering, C.H., and Nasmyth, K. (2003). Chromosomal cohesin forms a ring. Cell *112*, 765-777.

Gruber, S., Arumugam, P., Katou, Y., Kuglitsch, D., Helmhart, W., Shirahige, K., and Nasmyth, K. (2006). Evidence that loading of cohesin onto chromosomes involves opening of its SMC hinge. Cell *127*, 523-537.

Guacci, V., Koshland, D., and Strunnikov, A. (1997). A direct link between sister chromatid cohesion and chromosome condensation revealed through analysis of MCD1 in S. cerevisiae. Cell *91*, 47-57.

Gullerova, M., and Proudfoot, N.J. (2008). Cohesin complex promotes transcriptional termination between convergent genes in S. pombe. Cell *132*, 983-995.

Haering, C.H., Lowe, J., Hochwagen, A., and Nasmyth, K. (2002). Molecular Architecture of SMC Proteins and the Yeast Cohesin Complex. Mol Cell *9*, 773-788.

Haering, C.H., Schoffnegger, D., Nishino, T., Helmhart, W., Nasmyth, K., and Lowe, J. (2004). Structure and stability of cohesin's Smc1-kleisin interaction. Mol Cell *15*, 951-964.

Hanna, J.S., Kroll, E.S., Lundblad, V., and Spencer, F.A. (2001). *Sacharomyces cerevisiae* CTF18 and CTF14 are required for sister chromatid cohesion. Mol cell Biol *21*, 3144-3158.

Hark, A.T., Schoenherr, C.J., Katz, D.J., Ingram, R.S., Levorse, J.M., and Tilghman, S.M. (2000). CTCF mediates methylation-sensitive enhancer-blocking activity at the H19/Igf2 locus. Nature *405*, 486-489.

Hauf, S., Waizenegger, I.C., and Peters, J.M. (2001). Cohesin cleavage by separase required for anaphase and cytokinesis in human cells. Science *293*, 1320-1323.

Hauf, S., Roitinger, E., Koch, B., Dittrich, C.M., Mechtler, K., and Peters, J.M. (2005). Dissociation of cohesin from chromosome arms and loss of arm cohesion during early mitosis depends on phosphorylation of SA2. PLoS Biol *3*, e69.

Heitz, E. (1928). Das Heterochromatin der Moose. Jahrb Wiss Botanik *69*, 762–818.

Hirano, T. (2006). At the heart of the chromosome: SMC proteins in action. Nat Rev Mol Cell Biol *7*, 311-316.

Haering, C.H., Farcas, A., Arumugam, P., Metson, J., and Nasmyth, K. (2008). The cohesin ring concatenates sister DNAs. Nature *454* 297-301.

Harding, M.W., Galat, A., Uehling, D.E., and Schreiber, S.L. (1989). A receptor for the immunosuppressant FK506 is a cis-trans peptidyl-prolyl isomerase. Nature *341*, 758-760.

Hartman, T., Stead, K., Koshland, D., and Guacci, V. (2000). Pds5p Is an Essential Chromosomal Protein Required for both Sister Chromatid Cohesion and Condensation in Saccharomyces cerevisiae. J Cell Biol *151*, 613-626.

Hartwell, L.H. and Weinert, T.A. (1989). Checkpoints: controls that ensure the order of cell cycle events. Science *246*, 629-634.

Heidinger-Pauli, J.M., Unal, E., Guacci, V., and Koshland, D. (2008). The kleisin subunit of cohesin dictates damage-induced cohesion. Mol Cell *31*, 47-56.

Heidinger-Pauli, J.M., Unal, E., and Koshland, D. (2009). Distinct targets of the Eco1 acetyltransferase moculate cohesion in S phase and in response to DNA damage. Mol Cell *34*, 311-321.

Heidinger-Pauli, J.M., Onn, I., and Koshland, D. (2010). Genetic evidence that the acetylation of the Smc3p subunit of cohesin modulates its ATP-bound state to promote cohesion establishment in *Saccharomyces cerevisiae*. Genetics *185*, 1249-1256.

Hopfner, K.P., Karcher, A., Shin, D.S., Craig, L., Arthur, L.M., Carney, J.P., and Tainer, J.A. (2000). Structural biology of Rad50 ATPase: ATP-driven conformational control in DNA double-strand break repair and the ABC-ATPase superfamily. Cell *101*, 789-800.

Hopfner, K.P., and Tainer, J.A. (2003). Rad50/SMC proteins and ABC transporters: unifying concepts from high-resolution structures. Curr Opin Struct Biol *13*, 249-255.

Hu, B., Itoh, T., Mishra, A., Katoh, Y., Chan, K., Upcher, W., Godlee, C., Roig, M.B., Shirahige, K., and Nasmyth, K. (2010). Identification of an intermediate in the cohesin loading reaction reveals chromatin fibre translocation. Curr Biol *21*, 12-24.

Irniger, S., Piatti, S., Michaelis, C., and Nasmyth, K. (1995). Genes involved in sister chromatid separation are needed for B-type cyclin proteolysis in budding yeast. Cell *81*, 269-278.

Ivanov, D., Schleiffer, A., Eisenhaber, F., Mechtler, K., Haering, C.H., and Nasmyth, K. (2002). Eco1 is a novel acetyltransferase that can acetylate proteins involved in cohesion. Curr Biol *12*, 1-20.

Ivanov, D. and K, Nasmyth. (2005). A Topological Interaction between Cohesin Rings and a Circular Minichromosome. Cell *122*, 849-855.

Ivanov D. and K, Nasmyth. (2007). *A physical assay for sister chromatid cohesion in vitro* . Mol Cell *27,* 300-310.

Jenuwein, T. and Allis, C.D. (2001). Translating the histone code. Science *293*, 1074-1080.

Kagey, M.H., Newman, J.J., Bilodeau, S., Zhan, Y., Orlando, D.A., van Berkum, N.L., Ebmeier, C.C., Goossens, J., Rahl, P.B., Levine, S.S., Taatjes, D.J., Dekker, and J., Young, R.A. (2010). Mediator and cohesin connect gene expression and chromatin architecture. Nature *467*, 430-435.

Kanduri, C., Pant, V., Loukinov, D. *et al.* (2000). Functional association of CTCF with the insulator upstream of the H19 gene is parent of origin-specific and methylation sensitive. Curr Biol *10*, 853–856.

Kauer, J.C., Erickson-Viitanen, S., and DeGrado, W.F. (1986). p-Benzoyl-L-phenylalanine, a new photoreactive amino acid. Photolabeling of calmodulin with a synthetic calmodulin-binding peptide. J Biol Chem. *261*, 10695-700.

Kitajima, T.S., Hauf, S., Ohsugi, M., Yamamoto, T., and Watanabe, Y. (2005). Human Bub1 defines the persistent cohesion site along the mitotic chromosome by affecting Shugoshin localization. Curr Biol *15*, 353-359.

Kitajima, T.S., Sakuno, T., Ishiguro, K., Iemura, S., Natsume, T., Kawashima, S.A., and Watanabe, Y. (2006). Shugoshin collaborates with protein phosphatase 2A to protect cohesin. Nature *441*, 46-52.

King, R.W., Peters, J., Tugendreich, S., Rolfe, M., Hieter, P., and Kirschner, M.W. (1995). A 20S complex containing CDC27 and CDC16 catalyzes the mitosis-specific conjugation of ubiquitin to cyclin B. Cell *81*, 279-288.

Klein, F., Mahr, P., Galova, M., Buonomo, S.B.C., Michaelis, C., Nairz, K., and Nasmyth, K. (1999). A central role for cohesins in sister chromatid cohesion, formation of axial elements, and recombination during yeast meiosis. Cell *98*, 91-103.

Kornberg, R.D. (2005). Mediator and the mechanism of transcriptional activation. Trends in Biochemical Sciences *30*, 235-239.

Koshland, D., and Hartwell, L.H. (1987). The structure of sister minichromosome DNA before anaphase in Saccharomyces cerevisiae. Science *238*, 1713-1716.

Krantz, I.D., McCallum, J., DeScipio, C., Kaur, M., Gillis, L.A., Yaeger, D., Jukofsky, L., Wasserman, N., Bottani, A., Morris, C.A*., et al.* (2004). Cornelia de Lange syndrome is caused by mutations in NIPBL, the human homolog of Drosophila melanogaster Nipped-B. Nat Genet *36,* 631-635.

Kueng, S., Hegemann, B., Peters, B.H., Lipp, J.J., Schleiffer, A., Mechtler, K., and Peters, J.M. (2006). Wapl controls the dynamic association of cohesin with chromatin. Cell *127*, 955-967.

Kurdistani, S.K., and Grunstein, M. (2003). Histone acetylation and deacetylation in yeast. Nat Rev Mol Cell Biol *4*, 276-284.

Kurze, A., Michie, K.A., Dixon, S.E., Mishra, A., Itoh, T., Khalid, S., Strmecki, L., Shirahige, K., Haering, C.H., Löwe, J., and Nasmyth, K. (2011). A positively charged channel within the Smc1/Smc3 hinge required for sister chromatid cohesion. Embo *30*, 364-378.

Laloraya, S., Guacci, V., and Koshland, D. (2000). Chromosomal addresses of the cohesin-component, Mcd1p. J Cell Biol *151*, 1047-1056.

Lafont, A.L., Song, J., and Rankin, S. (2010). Sororin cooperates with the acetyltransferase Eco2 to ensure DNA replication-dependent sister chromatid cohesion. Proc Natl Acad Sci U S A. *107*, 20364-20369.

Lammens, K., Bemeleit, D.J., Mockel, C., Clausing, E., Schele, A., Hartung, S., Schiller, C.B., Lucas, M., Angermuller, C., Soding, J., *et al*. (2011). The Mre11:Rad50 structure shows an ATP-dependent molecular clamp in DNA double-strand break repair. Cell *145*, 54-66.

Lau, A., Blitzblau, H., and Bell, S.P. (2002). Cell-cycle control of the establishment of mating-type silencing in S. cerevisiae. Genes Dev *16*, 2935-2945.

Lengronne, A., Katou, Y., Mori, S., Yokobayashi, S., Kelly, G.P., Itoh, T., Watanabe, Y., Shirahige, K., and Uhlmann, F. (2004). Cohesin relocation from sites of chromosomal loading to places of convergent transcription. Nature *430*, 573-578.

Lengronne, A., McIntyre, J., Katou, Y., Kanoh, Y., Hopfner, K.P., Shirahige, K., and Uhlmann, F. (2006). Establishment of sister chromatid cohesion at the S.cerevisiae replication fork. Mol Cell *23*, 787-799.

Lengronne, A., and Schwob, E. (2002). The yeast CDK inhibitor Sic1 prevents genomic instability by promoting origin licensing in late G1. Mol Cell *5*, 1067-1078.

Liang, J., Choi, J., and Clardy, J. (1999). Refined structure of the FKBP12-rapamycin-FRB ternary complex at 2.2 A resolution. Acta Crystallogr D Biol Crystallogr *55*, 736-744.

Lin, M.Z., and Wang, L. (2008). Selective labelling of proteins with chemical probes in living cells. Physiology *23*, 131-141.

Lim, H.S., Kim, J.S., Park, Y.B., Gwon, G.H., and Cho, Y. (2011). Crystal structure of the Mre11-Rad50-ATPgammaS complex: understanding the interplay between Mre11 and Rad50. Genes & Development *25*, 1091-1104.

Lodish, H., Berk, A., Matsudaira, P., Kaiser, A.C., Krieger, M., Scott, M.P., Zipursky, S.L., and Darnell, J. (2003). Molecular Cell Biology.

Longtine, M. S., McKenzie, A., Demarini, D. J., Shah, N. G., Wach, A., Brachat, A., Philippsen, P., and Pringle, J. R. (1998). Additional modules for versatile and economical PCRbasedgene deletion and modification in *Saccharomyces cerevisiae*. Yeast *14*, 953-961.

Losada, A., Hirano, M., and Hirano, T. (1998). Identification of Xenopus SMC protein complexes required for sister chromatid cohesion. Genes Dev *12*, 1986-1997.

Losada, A., Yokochi, T., Kobayashi, R., and Hirano, T. (2000). Identification and Characterization of SA/Scc3p Subunits in the Xenopus and Human Cohesin Complexes. J Cell Biol *150*, 405-416.

Losada, A., Hirano, M., and Hirano, T. (2002). Cohesin release is required for sister chromatid resolution, but not for condensin-mediated compaction, at the onset of mitosis. Genes Dev *16*, 3004-3016.

Lowe, J., Cordell, S.C., and van den Ent, F. (2001). Crystal structure of the SMC head domain: an ABC ATPase with 900 residues antiparallel coiled-coil inserted. J Mol Biol *306*, 25-35.

Luger, K., Mader, A.W., Richmond, R.K., Sargent, D.F., and Richmond, T.J. (1997). Crystal structure of the nucleosome core particle at 2.8 A resolution. Nature *389*, 251-260.

Marsden, M.P., and Laemmli, U.K. (1979). Metaphase chromosome structure: evidence for a radial loop model. Cell *17*, 849-858.

Mapelli, M., Filipp, F.V., Rancati, G., Massimiliano, L., Nezi, L., Stier, G., Hagan, R.S., Confalonieri, S., Piatti, S., Sattler, M.*, et al.* (2006). Determinants of conformational dimerization of Mad2 and its inhibition by p31comet. EMBO J *25*, 1273-1284.

Mayer, M.L., Gygi, S.P., Aebersold, R., and Hieter, P. (2001). Identification of RFC (Ctf18p, Ctf8p, and Dcc1p): an alternative RFC complex required for sister chromatid cohesion in S. cerevisiae. Mol Cell *7*, 959-970.

McGuinness, B.E., Hirota, T., Kudo, N.R., Peters, J.M., and Nasmyth, K. (2005). Shugoshin Prevents Dissociation of Cohesin from Centromeres during Mitosis in Vertebrate Cells. PLoS Biol *3*, 433-449.

Mc Intyre, J., Muller, E.G., Weitzer, S., Snydsman, B.E., Davis, T.N., and Uhlmann, F. (2007). In vivo analysis of cohesin architecture using FRET in the budding yeast Saccharomyces cerevisiae. Embo J *26*, 3783-3793.

Megee, P.C., Mistrot, C., Guacci, V., and Koshland, D. (1999). The centromeric sister chromatid cohesion site directs Mcd1p binding to adjacent sequences. Mol Cell *4*, 445-450.

Melby, T.E., Ciampaglio, C.N., Briscoe, G., and Erickson, H.P. (1998). The symmetrical structure of structural maintenance of chromosomes (SMC) and MukB proteins: Long, antiparallel coiled coils, folded at a flexible hinge. J Cell Biol *142*, 1595-1604.

Michaelis, C., Ciosk, R., and Nasmyth, K. (1997). Cohesins: Chromosomal proteins that prevent premature separation of sister chromatids. Cell *91*, 35-45.

Milutinovich, M. and Koshland, D.E. (2003). Molecular biology. SMC complexes--wrapped up in controversy. Science *300*, 1101-1102.

Mishra, A., Hu, B., Kurze, A., Beckouët, F., Farcas, A.M,, Dixon, S.E., Katou, Y., Khalid, S., Shirahige, K., and Nasmyth, K. (2010). Both interaction surfaces within cohesin's hinge domain are essential for its stable chromosomal association. Curr Biol *20*, 279-289.

Misulovin, Z., Schwart, Y.B., Li, X.Y., Kahn, T.G., Gause, M., MacArthur, S., Fay, J.C., Eisen, M.B., Pirrotta, V., Biggin, M.D., et al. (2008). Association of cohesin and Nipped-B with transcriptionally active regions of the Drosophila melanogaster genome. Chromosoma *117*, 89-102.

Miyazaki, W.Y., and Orr-Weaver, T.L. (1994). Sister-chromatid cohesion in mitosis and meiosis. Annu Rev Genet *28*, 167-187.

Mohibullah N., and Hahn S. (2008). Site-specific cross-linking of TBP in vivo and in vitro reveals a direct functional interaction with the SAGA subunit Spt3. Genes Dev *22*, 2994-3006.

Moldovan, G.L., Pfander, B., and Jentsch, S. (2006). PCNA controls establishment of sister chromatid cohesion during S phase. Mol. Cell *23*, 723-732.

Morgan, D.O. (1997). Cyclin-dependent kinases: engines, clocks, and microprocessors. Annu. Rev. Cell. Dev. Biol. *13*, 261-291.

Murray, A.W., and Szostak, J.W. (1985). Chromosome segregation in mitosis and meiosis, Annu Rev Cell Biol *1*, 289-315.

Musacchio, A., and Salmon, E.D. (2007). The spindle-assembly checkpoint in space and time. Nat Rev Mol Cell Biol *8*, 379-393.

Nasmyth, K. (2001). Disseminating the genome: joining, resolving, and separating sister chromatids during mitosis and meiosis. Annu Rev Genet *35*, 673-745.

Nasmyth, K. (2005). How might cohesin hold sister chromatids together? Philosophical Transactions of the Royal Society B: Biological Sciences *360*, 483.

Nasmyth, K. (2011). Cohesin: a catenase with separate entry and exit gates? Nat Cell Biol. 2011 13, 1170-1177.

Nasmyth, K., and Haering, C.H. (2005). The structure and function of SMC and kleisin complexes. Annu Rev Biochem *74*, 595-648.

Nasmyth, K., and Haering, C.H. (2009).Cohesin: Its roles and mechanisms. Annu Rev Genet. *43*, 525-558.

Neuwald, A.F. and Hirano, T. (2000). HEAT repeats associated with condensins, cohesins and other complexes involved in chromosome-related functions. Genome Res *10*, 1445-1452.

Nicklas, R.B. (1988). The forces that move chromosomes in mitosis. Annual review of biophysics and biophysical chemistry *17*, 431-449.

Nishiyama T, Ladurner R, Schmitz J, Kreidl E, Schleiffer A, Bhaskara V, Bando M, Shirahige K, Hyman AA, Mechtler K, and Peters JM. (2010). Sororin mediates sister chromatid cohesion by antagonizing Wapl. Cell *143*, 737-749.

Nagao, K., Adachi, Y., and Yanagida, M. (2004). Separase-mediated cleavage of cohesin at interphase is required for DNA repair. Nature *430*, 1044-1048.

Nonaka, N., Kitajima, T., Yokobayashi, S., Xiao, G., Yamamoto, M., Grewal, S.I., and Watanabe, Y. (2002). Recruitment of cohesin to heterochromatic regions by Swi6/HP1 in fission yeast. Nat Cell Biol *4*, 89-93.

Ocampo-Hafalla MT, Katou Y, Shirahige K, and Uhlmann F. (2007). Displacement and re-accumulation of centromeric cohesin during transient pre-anaphase centromere splitting. Chromosoma *116*, 531-544.

Oliveira, R.A., Hamilton, R.S., Pauli, A., Davis, I., and Nasmyth, K. (2010). Cohesin cleavage and Cdk inhibition trigger formation of daughter nuclei. Nat Cell Biol *12*, 185-192.

Oudet, P., Gross-Bellard, M., and Chambon, P. (1975). Electron microscopic and biochemical evidence that chromatin structure is a repeating unit. Cell *4*, 281–300.

Panizza, S., Tanaka, T., Hohchwagen, A., Eisenhaber, F., and Nasmyth, K. (2000). Pds5 cooperates with cohesin in maintaining sister chromatid cohesion. Curr Biol *10*, 1557-1564.

Parelho, V., Hadjur, S., Spivakov, M., Leleu, M., Sauer, S., Gregson, H.C., Jarmuz, A., Canzonetta, C., Webster, Z., Nesterova, T.*, et al.* (2008). Cohesins functionally associate with CTCF on mammalian chromosome arms. Cell *132*, 422-433.

Pauli, A., Althoff, F., Oliveira, R.A., Heidmann, S., Schuldiner, O., Lehner, C.F., Dickson, B.J., and Nasmyth, K. (2008). Cell-type-specific TEV protease cleavage reveals cohesin functions in Drosophila neurons. Dev Cell *14*, 239-251.

Pauli, A., van Bemmel, J.G., Oliveira, R.A., Itoh, T., Shirahige, K., van Steensel, B., and Nasmyth K. (2010). A direct role for cohesin in gene regulation and ecdysome response in Drosophila salivary glands. Curr Biol *20*, 1787-1798.

Paweletz, N. (2001). Walther Flemming: pioneer of mitosis research. Nat Rev Mol Cell Biol *2*, 72-75.

Peters, J.M., Tedeschi, A., and Schmitz, J. (2008). The cohesin complex and its roles in chromosome biology. Genes Dev *22*, 3089-30114.

Phair, R.D., Scaffidi, P., Elbi, C., Vecerova, J., Dey, A., Ozato, K., Brown, D.T., Hager, G., Bustin, M., and Misteli, T. (2004). Global nature of dynamic protein-chromatin interactions *in vivo*: three-dimensional genome scanning and dynamic interaction networks of chromatin proteins. Mol Cell Biol *24*, 6393-6402.

Potts, P. R., Porteus, M.H., and Yu, H. (2006). Human SMC5/6 complex promotes sister chromatid homologous recombination by recruiting the SMC1/3 cohesin complex to double-strand breaks. Embo J *25*, 3377-3388.

Rankin, S., Ayad, N.G., and Kirschner, M.W. (2005). Sororin, a substrate of the anaphase-promoting complex, is required for sister chromatid cohesion in vertebrates. Mol Cell *18*, 283-288.

Rao, P.N., and Johnson, R.T. (1970). Mammalian cell fusion: studies on the regulation of DNA synthesis and mitosis. Nature *225*, 159-164.

Riedel, C.G., Katis, V.L., Katou, Y., Mori, S., Itoh, T., Helmhart, W., Galova, M., Petronczki, M., Gregan, J., Cetin, B.*, et al.* (2006). Protein phosphatase 2A protects centromeric sister chromatid cohesion during meiosis I. Nature *441*, 53-61.

Rollins, R.A., Korom, M., Aulner, N., Martens, A., and Dorsett, D. (2004). Drosophila Nipped-B protein supports sister chromatid cohesion and opposes the stromalin/Scc3 cohesion factor to facilitate long-range activation of the cut gene.Mol Cell Biol *24*, 3100-3111.

Rollins, R.A., Morcillo, P., and Dorsett, D. (1999). Nipped-B, a Drosophila homologue of chromosomal adherins, participates in activation by remote enhancers in the cut and Ultrabithorax genes. Genetics *152*, 577-593.

Rowland, B.D., Roig, M.B., Nishino, T., Kurze, A., Uluocak, P., Mishra, A., Beckouët, F., Underwood, P., Metson, J., Imre, R.*, et al.* (2009). Building sister chromatid cohesion: Smc3 acetylation counteracts an anti-establishment activity. Mol Cell *33*, 763-774.

Rubio, E.D., Reiss, D.J., Welcsh, P.L., Disteche, C.M., Filippova, G.N., Baliga, N.S., Aebersold, R., Ranish, J.A., and Krumm, A. (2008). CTCF physically links cohesin to chromatin. Proc Natl Acad Sci U S A *105*, 8309-8314.

Sabatini, D.M., Erdjument-Bromage, H., Lui, M., Tempst, P., and Snyder, S.H. (1994). RAFT1: a mammalian protein that binds to FKBP12 in a rapamycin-dependent fashion and is homologous to yeast TORs. Cell *78*, 35-43.

Salic, A., Waters, J.C., and Mitchison, T.J. (2004). Vertebrate shugoshin links sister centromere cohesion and kinetochore microtubule stability in mitosis. Cell *118*, 567-578.

Sambrook, J., and Russell, D.W. (2001). Molecular Clonning: A Laboratory Manual, 3rd edition. (Cold Spring Harbor Laboratory Press) .

Schleiffer, A., Kaitna, S., Maurer-Stroh, S., Glotzer, M., Nasmyth, K., and Eisenhaber, F. (2003). Kleisins: a superfamily of bacterial and eukaryotic SMC protein partners. Mol Cell *11*, 571–575.

Schule, B., Oviedo, A., Johnston, K., Pai, S., and Francke, U. (2005). Inactivating mutations in ESCO2 cause SC phocomelia and Roberts syndrome: no phenotype-genotype correlation. Am J Hum Genet *77*, 1117-1128.

Schmitz, J., Watrin, E., Lenart, P., Mechtler, K., and Peters, J.M. (2007). Sororin is required for stable binding of cohesin to chromatin and for sister chromatid cohesion in interphase. Curr Biol *17*, 630-636.

Schreiber, S.L. (1991). Chemistry and biology of the immunophilins and their immunosuppressive ligands. Science *251*, 283-287.

Schuldiner, O., Berdnik, D., Ma Levy, J., Wu, J.S.-Y., Luginbuhl, D., Gontag, A.C., and Luo, L. (2007). PiggyBac-based mosaic screen identifies a postmitotic function for cohesin in regulating developmental axon pruning. Dev Cell *14*, 227-238.

Schwob, E., Bohm, T., Mendenhall, M.D., and Nasmyth K. (1994). The B-type cyclin kinase inhibitor p40SIC1 controls the G1 to S transition in S. cerevisiae. Cell *2*, 233-244,

Sehgal, S.N., Baker, H., and Vézina, C. (1975). Rapamycin (AY-22,989), a new antifungal antibiotic. II. Fermentation, isolation and characterization. J Antibiot (Tokyo) *28*, 727-732.

Sheaff, R.J., and Roberts, J.M. (1996). End of the line: proteolytic degradation of cyclin-dependent kinase inhibitors. Chem Biol *11*, 869-873.

Siekierka, J. J., Hung, S. H. Y., Poe, M., Lin, C. S., and Sigal, N. H. (1989). A cytosolic binding protein for the immunosuppressant FK506 has peptidyl-prolyl isomerase activity but is distinct from cyclophilin. Nature *341*, 755-757.

Sjoegren, C., and Nasmyth, K. (2001). Sister chromatid cohesion is required for post-replicative double strand break repair in Saccharomyces cerevisiae. Curr Biol *11*, 991-995.

Skibbens, R.V., Corson, L.B., Koshland, D., and Hieter, P. (1999). Ctf7p is essential for sister chromatid cohesion and links mitotic chromosome structure to the DNA replication machinery. Genes and Dev *13*, 307-319.

Skibbens, R.V. (2010). Buck the establishment: reinventing sister chromatid cohesion. Trends Cell Biol *20*, 507-513.

Sullivan, M., Higuchi, T., Katis, V.L., and Uhlmann, F. (2004). Cdc14 phosphatase induces rDNA condensation and resolves cohesin-independent cohesion during budding yeast anaphase. Cell *117*, 471-482.

Sumara, I., Vorlaufer, E., Gieffers, C., Peters, B.H., and Peters, J.-M. (2000). Characterization of vertebrate cohesin complexes and their regulation in prophase. J Cell Biol *151*, 749-762.

Sumara, I., Vorlaufer, E., Stukenberg, P.T., Kelm, O., Redemann, N., Nigg, E.A., and Peters, J.M. (2002). The dissociation of cohesin from chromosomes in prophase is regulated by Polo-like kinase. Mol Cell *9*, 515-525.

Sutani, T., Kawaguchi, T., Kanno, R., Itoh, T., and Shirahige, K. (2009). Budding yeast Wpl1(Rad61)-Pds5 complex counteracts sister chromatid cohesion-establishing reaction. Curr Biol *19*, 492-97.

Stedman, W., Kang, H., Lin, S., Kissil, J.L., Bartolomei, M.S., and Lieberman, P.M. (2008). Cohesins localize with CTCF at the KSHV latency control region and at cellular c-myc and H19/Igf2 insulators. EMBO J *27*, 654-666.

Stemmann, O., Zou, H., Gerber, S.A., Gygi, S.P., and Kirschner, M.W. (2001). Dual inhibition of sister chromatid separation at metaphase. Cell *107*, 715-726.

Stillman, B. (2005). Origin recognition and the chromosome cycle. FEBS Lett *579*, 877-884.

Strom, L., Lindroos, H.B., Shirahige, K., and Sjogren, C. (2004). Postreplicative recruitment of cohesin to double-strand breaks is required for DNA repair. Mol Cell *16*, 1003-1015.

Strom, L., Karlsson, C., Lindroos, H.B., Wedahl, S., Katou, Y., Shirahige, K., and Sjogren, C. (2007). Postreplicative formation of cohesion is required for repair and induced by a single DNA break. Science *317*, 242-245.

Struhl, K. (1999). Fundamentally different logic of gene regulation in eukaryotes and prokaryotes. Cell *98*, 1–4.

Tachibana-Konwalski, K., Godwin, J., van der Weyden, L., Champion, L., Kudo, N.R., Adams, D.J., Nasmyth, K. (2010). Genes Dev. *24*, 2505-2521.

Takahashi, T.S., Yiu, P., Chou, M.F., Gygi, S., and Walter, J.C. (2004). Recruitment of Xenopus Scc2 and cohesin to chromatin requires the pre-replication complex. Nat Cell Biol *6*, 991-996.

Takahashi, T.S., Basu, A., Bermudez, V., Hurwitz, J., and Walter, J.C. (2008). Cdc7- Drf1 kinase links chromosome cohesion to the initiation of DNA replication in Xenopus egg extracts. Genes Dev *22*, 1894-1905.

Tanaka, T., Cosma, M.P., Wirth, K., and Nasmyth, K. (1999). Identification of cohesin association sites at centromeres and along chromosome arms. Cell *98*, 847-858.

Teif V.B. and Bohinc K. (2011). Condensed DNA: condensing the concepts. Progress in Biophysics and Molecular Biology *105*, 208–222.

Toth, A., Ciosk, R., Uhlmann, F., Galova, M., Schleifer, A., and Nasmyth, K. (1999). Yeast Cohesin complex requires a conserved protein, Eco1p (Ctf7), to establish cohesion between sister chromatids during DNA replication. Genes and Dev *13*, 320-333.

Uhlmann, F. and K. Nasmyth (1998). Cohesion between sister chromatids must be established during DNA replication. Curr Biol *8*, 1095-101.

Uhlmann, F., Lottspeich, F., and Nasmyth, K. (1999). Sister chromatid separation at anaphase onset is promoted by cleavage of the cohesin subunit Scc1p. Nature *400*, 37-42.

Uhlmann, F., Wernic, D., Poupart, M.A., Koonin, E., and Nasmyth, K. (2000). Cleavage of cohesin by the CD clan protease separin triggers anaphase in yeast. Cell *103*, 375-386.

Unal, E., Arbel-Eden, A., Sattler, U., Shroff, R., Lichten, M., Haber, J.E., and Koshland, D. (2004). DNA damage response pathway uses histone modification to assemble a double-strand break-specific cohesin domain. Mol Cell *16*, 991-1002.

Unal, E., Heidinger-Pauli, J.M., and Koshland, D. (2007). DNA double-strand breaks trigger genome-wide sister-chromatid cohesion through Eco1 (Ctf7). Science *317*, 245-248.

Unal, E., Heidinger-Pauli, J.M., Kim, W., Guacci, V., Onn, I., Gygi, S.P., and Koshland, D.E. (2008). A molecular determinant for the establishment of sister chromatid cohesion. Science *321*, 566-569.

Vega, H., Waisfisz, Q., Gordillo, M., Sakai, N., Yanagihara, I., Yamada, M., van Gosliga, D., Kayserili, H., Xu, C., Ozono, K.*, et al.* (2005). Roberts syndrome is caused by mutations in ESCO2, a human homolog of yeast ECO1 that is essential for the establishment of sister chromatid cohesion. Nat Genet *37*, 468-470.

Verdel, A., Jia, S., Gerber, S., Sugiyama, T., Gygi, S., Grewal, S.I., and Moazed, D. (2004). RNAi-mediated targeting of heterochromatin by the RITS complex. Science *303*, 672-676.

Verdel, A., and Moazed, D. (2004). RNAi-directed assembly of heterochromatin in fission yeast. FEBS Lett *579*, 5872-5878.

Visintin, R., Prinz, S., and Amon A. (1997). CDC20 and CDH1: A family of substrate-specific activators of APC-dependent proteolysis. Science *278*, 460-463.

Volpe, T.A., Kidner, C., Hall, I.M., Teng, G., Grewal, S.I., and Martienssen, R.A. (2002). Regulation of heterochromatic silencing and histone H3 lysine-9 methylation by RNAi. Science *297*, 1833-1837.

Waizenegger, I., Hauf, S., Meinke, A., and Peters, J.M. (2000). Two distinct pathways remove mammalian cohesin from chromosome arms in prophase and from centromeres in anaphase. Cell *103*, 399-410.

Waga, S., and Stillman, B. (1998). The DNA replication fork in eukaryotic cells. Annu. Rev. Biochem. *67*, 721-751.

Warren, W.D., Steffensen, S., Lin, E., Coelho, P., Loupart, M., Cobbe, N., Lee, J.Y., McKay, M.J., Orr-weaver, T., Heck, M.M., and Sunkel, C.E. (2000). The Drosophila RAD21 cohesin persists at the centromere region in mitosis. Curr Biol *10*, 1463-1466.

Wang, L., Brock, A., Herberich, B., and Schultz, P.G. (2001). Expanding the genetic code of *Escherichia coli*. Science *292*, 498-500.

Watrin, E., and Peters, J.M. (2006). Cohesin and DNA damage repair. Exp Cell Res *312*, 2687-2693.

Watrin, E., Schleiffer, A., Tanaka, K., Eisenhaber, F., Nasmyth ,K., and Peters, J.M. (2006). Human Scc4 is required for cohesin binding to chromatin, sister-chromatid cohesion, and mitotic progression. Curr Biol *16*, 863-874.

Weber, S.A., Gerton, J.L., Polancic, J.E., DeRisi, J.L., Koshland, D., and Megee, P.C. (2004). The kinetochore is an enhancer of pericentric cohesin binding. PLoS Biol *2*, E260.

Weitzer, S., Lehane, C., and Uhlmann, F. (2003). A model for ATP hydrolysis-dependent binding of cohesin to DNA. Curr Biol *13*, 1930-1940.

Wendt, K.S., Yoshida, K., Itoh, T., Bando, M., Koch, B., Schirghuber, E., Tsutsumi, S., Nagae, G., Ishihara, K., Mishiro, T.*, et al.* (2008). Cohesin mediates transcriptional insulation by CCCTC-binding factor. Nature *451*, 796-801.

Williams, G.J., Williams, R.S., Williams, J.S., Moncalian, G., Arvai, A.S., Limbo, O., Guenther, G., SilDas, S., Hammel, M., Russell, P., *et al.* (2011). ABC ATPase signature helices in Rad50 link nucleotide state to Mre11 interface for DNA repair. Nature structural & molecular biology *18*, 423-431.

Woo, J.S., Lim, J.H., Shin, H.C., Suh, M.K., Ku, B., Lee, K.H., Joo, K., Robinson, H., Lee, J., Park, S.Y., Ha, N.C., and Oh, B.H. (2009). Structural studies of a bacterial condensin complex reveal ATP-dependent disruption of intersubunit interactions. Cell *136*, 85-96.

Xiong, B., Lu, S., and Gerton, J.L. (2010). Hos1 is a lysine deacetylase for the Smc3 subunit of cohesin. Curr Biol *20*, 1660-1665.

Yanagida, M. (2009). Clearing the way for mitosis: is cohesin a target? Nat Rev Mol Cell Biol *10*, 489-496.

Zhang, B., Jain, S., Song, H., Fu, M., Heuckeroth, R.O., Erlich, J.M., Jay, P.Y., and Milbrandt, J. (2007). Mice lacking sister chromatid cohesion protein PDS5B exhibit developmental abnormalities reminiscent of Cornelia de Lange syndrome. Development *134*, 3191-3201.

Zhang, J., Shi, X., Li, Y., Kim, B.J., Jia, J., Huang, Z., Yang, T., Fu, X., Jung, S.Y., Wang, Y.*, et al.* (2008). Acetylation of Smc3 by Eco1 is required for S phase sister chromatid cohesion in both human and yeast. Mol Cell *31*, 143-151.

Appendix 1: yeast strains

Strain number	Genotype
K699	Mat a, ade2-1, trp1-1, can1-100, leu2-3,112, his3-11,15, ura3, GAL, psi+
K700	Mat alpha, ade2-1, trp1-1, can1-100, leu2-3,112, his3-11,15, ura3, GAL, psi+
K13637	Mat alpha,fpr1::NatMX Smc3-GL-mFRB::HIS3,scc1::HIS3 trp1::FKBP12-GL-Scc1::TRP1
K14727	Mat a, ade2-1, trp1-1, can1-100, leu2-3,112, his3-11,15, ura3, GAL, psi+ eco1(G211H)
K14601	Mat a, ade2-1, trp1-1, can1-100, leu2-3,112, his3-11,15, ura3, GAL, psi+, SCC1-PK9::kanMX
K15103	Mat a, ade2-1, can1-100, leu2-3,112, his3-11,15, ura3, GAL, psi+, 2.3kb TRP1-Cen4- ARS1 minichromosome
K16107	Mat a, ade2-1, can1-100, leu2-3,112, his3-11,15, ura3, GAL, psi+, eco1-1 (G211D), 2.3kb TRP1-CEN4-ARS1 plasmid
K16292	Mat a, smc3::HIS3, scc1::KanMx, ura3::Scc1P-Smc3-TEV3-Scc1::URA3
K16431	Mat a, eco1::NatMx4, rad61::HphMx
K16456	Mat alpha, smc3::HIS3, scc1::KanMx, ura3::Scc1P-Smc3-TEV3-Scc1::URA3, eco1-1 (G211D).
K16459	Mat alpha, smc3::HIS3, scc1::KanMx, ura3::Scc1P-Smc3-TEV3-Scc1::URA3
K16460	Mat a, smc3::HIS3, scc1::KanMx, ura3::Scc1P-Smc3-TEV3-Scc1::URA3, eco1::NatMx4
K16558	Mat a, smc3::HIS3, scc1::KanMx, ura3::Scc1P-Smc3-TEV3-Scc1::URA3, eco1::NatMx4, YEplac112-pGAL1-NLS-myc9-TEV protease-NLS-NLS
K16560	Mat a, smc3::HIS3, scc1::KanMx, ura3::Scc1P-Smc3-TEV3-Scc1::URA3, eco1::NatMx4, YEplac112
K16562	Mat a, smc3::HIS3, scc1::KanMx, ura3::Scc1P-Smc3-TEV3-Scc1::URA3, YEplac112
K16564	Mat a, smc3::HIS3, scc1::KanMx, ura3::Scc1P-Smc3-TEV3-Scc1::URA3, YEplac112-pGAL1-NLS-myc9-TEV protease-NLS-NLS
K18654	Mat a, smc3::HIS3, smc1::NatMx, YEplac181-Smc3(E570C)-HA3, pLH157(TRP+), Scc1(A547C)-PK6-Avitag::KanMx,leu2: Smc1(G22C, K639C)-myc9::hphNT1::leu2
K18655	Mat a, smc3::HIS3, smc1::NatMx, YEplac181-Smc3(E570C, K185→Amber codon)-HA3, pLH157(TRP+), Scc1(A547C)-PK6-Avitag::KanMx,leu2: Smc1(G22C, K639C)-myc9::hphNT1::leu2
K18656	Mat a, smc3::HIS3, smc1::NatMx, YEplac181-Smc3(E570C, A181→Amber codon)-HA3, pLH157(TRP+), Scc1(A547C)-PK6-Avitag::KanMx,leu2: Smc1(G22C, K639C)-myc9::hphNT1::leu2
K18664	Mat alpha, smc3::HIS3, smc1::NatMx, YEplac181-Smc3(E570C, A181→Amber codon)-HA3, pLH157(TRP+),Scc1(A547C)-PK6-Avitag::KanMx, leu2: Smc1(G22C, K639C)-myc9::hphNT1::leu2
K18665	Mat alpha, smc3::HIS3, smc1::NatMx, YEplac181-Smc3(E570C, K185→Amber codon)-HA3, pLH157(TRP+),Scc1(A547C)-PK6-Avitag::KanMx, leu2: Smc1(G22C, K639C)-myc9::hphNT1::leu2
K19139	Mat a, ura3::Scc1P-Smc3-TEV3-Scc1-HA6::URA3, smc3::HIS3, scc1::KanMx, 2.3kb TRP1-Cen4- ARS1 minichromosome
K19140	Mat alpha, ura3::Scc1P-Smc3-TEV3-Scc1-HA6::URA3, smc3::HIS3, scc1::KanMx, 2.3kb TRP1-Cen4- ARS1 minichromosome
K19141	Mat a, ade2-1, trp1-1, can1-100, leu2-3,112, his3-11,15, GAL, psi+, 3kb URA3-Cen6- ARS1 minichromosome
K19142	Mat alpha, ade2-1, trp1-1, can1-100, leu2-3,112, his3-11,15, GAL, psi+, 3kb URA3-

	Cen6- ARS1 minichromosome
K19143	Mat a, Smc3-GL-mFRB::HIS3,scc1::NatMx, ura3::FKBP12-GL-Scc1-PK6-Avitag::URA3
K19144	Mat alpha, Smc3-GL-mFRB::HIS3,scc1::NatMx, ura3::FKBP12-GL-Scc1-PK6-Avitag::URA3
K19145	Mat a, Smc3-GL-mFRB::HIS3,scc1::NatMx, ura3::FKBP12-GL-Scc1-PK6-Avitag::URA3, 2.3kb TRP1-Cen4- ARS1 minichromosome
K19146	Mat alpha, Smc3-GL-mFRB::HIS3,scc1::NatMx, ura3::FKBP12-GL-Scc1-PK6-Avitag::URA3, 2.3kb TRP1-Cen4- ARS1 minichromosome
K19147	Mat a, ura3::FKBP12-GL-Scc1-PK6-Avitag::URA3, Smc3(E570C)-GL-mFRB::HIS3, scc1::NatMx, leu2:Smc1(K639C)-myc9::LEU2, smc1::KanMx
K19148	Mat alpha, ura3::FKBP12-GL-Scc1-PK6-Avitag::URA3, Smc3(E570C)-GL-mFRB::HIS3, scc1::NatMx, leu2:Smc1(K639C)-myc9::LEU2, smc1::KanMx
K19149	Mat a, ura3::FKBP12-GL-Scc1-PK6-Avitag::URA3, Smc3-GL-mFRB::HIS3, scc1::NatMx, leu2:Smc1-myc9::LEU2, smc1::KanMx
K19150	Mat alpha, ura3::FKBP12-GL-Scc1-PK6-Avitag::URA3, Smc3-GL-mFRB::HIS3, scc1::NatMx, leu2:Smc1-myc9::LEU2, smc1::KanMx
K19151	Mat a, Smc3-GL-mFRB(R2042C)::HIS3,scc1::NatMx, ura3::FKBP12(T85C)-GL-Scc1-PK6-Avitag::URA3
K19152	Mat alpha, Smc3-GL-mFRB(R2042C)::HIS3,scc1::NatMx, ura3::FKBP12(T85C)-GL-Scc1-PK6-Avitag::URA3
K19153	Mat a, smc3::HIS3, smc1::NatMx, YEplac181-Smc3-HA3, pLH157(TRP+), Scc1-PK6-Avitag::KanMx, leu2: Smc1-myc9::hphNT1::leu2
K19154	Mat alpha, smc3::HIS3, smc1::NatMx, YEplac181-Smc3-HA3, pLH157(TRP+), Scc1-PK6-Avitag::KanMx, leu2: Smc1-myc9::hphNT1::leu2
K19155	Mat a, smc3::HIS3, smc1::NatMx, YEplac181-Smc3(A181→Amber codon)-HA3, pLH157(TRP+), Scc1-PK6-Avitag::KanMx, leu2: Smc1-myc9::hphNT1::leu2
K19156	Mat alpha, smc3::HIS3, smc1::NatMx, YEplac181-Smc3(A181→Amber codon)-HA3, pLH157(TRP+), Scc1-PK6-Avitag::KanMx, leu2: Smc1-myc9::hphNT1::leu2
K19157	Mat a, smc3::HIS3, smc1::NatMx, YEplac181-Smc3(K185→Amber codon)-HA3, pLH157(TRP+), Scc1-PK6-Avitag::KanMx, leu2: Smc1-myc9::hphNT1::leu2
K19158	Mat alpha, smc3::HIS3, smc1::NatMx, YEplac181-Smc3(K185→Amber codon)-HA3, pLH157(TRP+), Scc1-PK6-Avitag::KanMx, leu2: Smc1-myc9::hphNT1::leu2
K19159	Mat a, smc3::HIS3, smc1::NatMx, YEplac181-Smc3(A181→Amber codon)-HA3, pLH157(TRP+), Scc1(A547C)-PK6-Avitag::KanMx,leu2: Smc1(G22C)-myc9::hphNT1::leu2
K19160	Mat alpha, smc3::HIS3, smc1::NatMx, YEplac181-Smc3(A181→Amber codon)-HA3, pLH157(TRP+),Scc1(A547C)-PK6-Avitag::KanMx, leu2: Smc1(G22C)-myc9::hphNT1::leu2
K19161	Mat a, smc3::HIS3, smc1::NatMx, YEplac181-Smc3(K185→Amber codon)-HA3, pLH157(TRP+), Scc1(A547C)-PK6-Avitag::KanMx, leu2:Smc1(G22C)-myc9::hphNT1::leu2
K19162	Mat alpha, smc3::HIS3, smc1::NatMx, YEplac181-Smc3(K185→Amber codon)-HA3, pLH157(TRP+), Scc1(A547C)-PK6-Avitag::KanMx, leu2:Smc1(G22C)-myc9::hphNT1::leu2
K19163	Mat a, smc3::HIS3, smc1::NatMx, YEplac181-Smc3-HA3, pLH157(TRP+), Scc1(A547C)-PK6-Avitag::KanMx,leu2: Smc1(G22C)-myc9::hphNT1::leu2
K19164	Mat alpha, smc3::HIS3, smc1::NatMx, YEplac181-Smc3-HA3, pLH157(TRP+), Scc1(A547C)-PK6-Avitag::KanMx, leu2: Smc1(G22C)-myc9::hphNT1::leu2
K19165	Mat a, smc3::HIS3, YEplac181-Smc3-HA3, pLH157(TRP+), Scc1-PK6::KanMx, 3kb URA3-Cen6-ARS1 minichromosome
K19166	Mat alpha, smc3::HIS3, YEplac181-Smc3-HA3, pLH157(TRP+), Scc1-PK6::KanMx, 3kb URA3-Cen6-ARS1 minichromosome
K19167	Mat a, smc3::HIS3, YEplac181-Smc3(K185→Amber codon)-HA3, pLH157(TRP+),

	Scc1-PK6::KanMx, 3kb URA3-Cen6-ARS1 minichromosome
K19168	Mat alpha, smc3::HIS3, YEplac181-Smc3(K185→Amber codon)-HA3, pLH157(TRP+), Scc1-PK6::KanMx, 3kb URA3-Cen6-ARS1 minichromosome
K19169	Mat a, smc3::HIS3, YEplac181-Smc3(A181→Amber codon)-HA3, pLH157(TRP+), Scc1-PK6::KanMx, 3kb URA3-Cen6-ARS1 minichromosome
K19170	Mat alpha, smc3::HIS3, YEplac181-Smc3(A181→Amber codon)-HA3, pLH157(TRP+), Scc1-PK6::KanMx, 3kb URA3-Cen6-ARS1 minichromosome
K19171	Mat a, ade2-1, can1-100, leu2-3,112, his3-11,15, ura3, GAL, psi+, eco1-1 (G211D), 2.3kb TRP1-CEN4-ARS1 plasmid
K19172	Mat a, Smc3-GL-mFRB(V2094C)::HIS3,scc1::NatMx, ura3::FKBP12(G89C)-GL-Scc1-PK6-Avitag::URA3
K19173	Mat alpha, Smc3-GL-mFRB(V2094C)::HIS3,scc1::NatMx, ura3::FKBP12(G89C)-GL-Scc1-PK6-Avitag::URA3
K19174	Mat a, Smc3-GL-mFRB(K2095C)::HIS3,scc1::NatMx, ura3::FKBP12(D37C)-GL-Scc1-PK6-Avitag::URA3
K19175	Mat alpha, Smc3-GL-mFRB(K2095C)::HIS3,scc1::NatMx, ura3::FKBP12(D37C)-GL-Scc1-PK6-Avitag::URA3
K19413	Mat a, smc3::HIS3, smc1::NatMx, YEplac181-Smc3-HA3, pLH157(TRP+), Scc1(A547C)-PK6-Avitag::KanMx,leu2: Smc1(G22C)-myc9::hphNT1::leu2, 3kb URA3-Cen6-ARS1 minichromosome
K19414	Mat a, smc3::HIS3, smc1::NatMx, YEplac181-Smc3(E570C)-HA3, pLH157(TRP+), Scc1(A547C)-PK6-Avitag::KanMx,leu2: Smc1(G22C, K639C)-myc9::hphNT1::leu2, 3kb URA3-Cen6-ARS1 minichromosome
K19415	Mat a, smc3::HIS3, smc1::NatMx, YEplac181-Smc3(A181→Amber codon)-HA3, pLH157(TRP+), Scc1(A547C)-PK6-Avitag::KanMx,leu2: Smc1(G22C)-myc9::hphNT1::leu2, 3kb URA3-Cen6-ARS1 minichromosome
K19416	Mat a, smc3::HIS3, smc1::NatMx, YEplac181-Smc3(E570C, A181→Amber codon)-HA3, pLH157(TRP+), Scc1(A547C)-PK6-Avitag::KanMx,leu2: Smc1(G22C, K639C)-myc9::hphNT1::leu2, 3kb URA3-Cen6-ARS1 minichromosome
K19417	Mat a, smc3::HIS3, smc1::NatMx, Scc1P-Smc3-TEV3-Scc1::KanMx, leu2: Smc1-myc9::hphNT1::leu2, 3kb URA3-Cen6-ARS1 minichromosome
K19418	Mat a, smc3::HIS3, smc1::NatMx, Scc1P-Smc3(E570C)-TEV3-Scc1(A547C)::KanMx, leu2: Smc1(G22C, K639C)-myc9::hphNT1::leu2, 3kb URA3-Cen6-ARS1 minichromosome
TG1	Mat a, smc3::HIS3, YEplac181-Smc3-HA3, pLH157(TRP+), Scc1-PK6::KanMx
TG2	Mat alpha, smc3::HIS3, YEplac181-Smc3-HA3, pLH157(TRP+), Scc1-PK6::KanMx
TG3	Mat a, smc3::HIS3, YEplac181-Smc3(K185→Amber codon)-HA3, pLH157(TRP+), Scc1-PK6::KanMx
TG4	Mat alpha, smc3::HIS3, YEplac181-Smc3(K185→Amber codon)-HA3, pLH157(TRP+), Scc1-PK6::KanMx
TG5	Mat a, smc3::HIS3, YEplac181-Smc3(A181→Amber codon)-HA3, pLH157(TRP+), Scc1-PK6::KanMx
TG6	Mat alpha, smc3::HIS3, YEplac181-Smc3(A181→Amber codon)-HA3, pLH157(TRP+), Scc1-PK6::KanMx

Appendix 2: Abbreviations

ABC-like	ATP binding cassette
APC/C	anaphase promoting complex/cyclosome
ARS	autonomous replication sequences
ATP	adenosine triphosphate
B.subtilis	*Bacillus subtilis*
bBBr	bibromobimane
BMOE	bis-maleimidoethane
bp	base pairs
*ρ*BPA	*ρ*-benzoyl-phenylalanine
BSA	bovine serum albumin
C-terminal	carboxy-terminal
Cap-H	chromosome associated protein
CARs	cohesin-associated regions
Cdc6, Cdc7, Cdc14, Cdc20	cell division cycle
Cdh1	Cdc20 homolog 1
CDK	cyclin dependent kinase
CdLS	Cornelia de Lange Syndrome
cDNA	complementary DNA
CEN	centromere
CFP	cyan fluorescent protein
ChIP	chromatin immunoprecipitation
ChIP-CHIP	chromatin IP followed by hybridization to DNA microarrays
Ch	chromosome
CKI	cyclin dependent kinase inhibitors
CTCF	CCCTC binding factor
Cut 1	cell ultimately torn protein 1
Dbf4	dumbell former 4
DNA	deoxyribonucleic acid

DMSO	dimethyl sulfoxide
DTT	dithiothreitol
DSBs	double strand breaks
dsRNA	double stranded RNA
E.coli	*Escherichia coli*
Eco1	establishment of cohesion 1
EcR	Ecdysone Receptor
EDTA	ethylenediamine tetraacetic acid
EGTA	ethylene glycol tetraacetic acid
Esp1	extra spindle poles of protein 1
EtOH	ethanol
FRAP	fluorescent recovery after photobleaching
FRAP	FKBP-rapamycin-associated protein
FRET	fluorescence resonance energy transfer
G1/G2-phase	gap1/gap2-phase
g, mg, µg	gram, milligram, microgram
GFP	green fluorescent protein
H1, H2A, H2B, H3, H4	histone proteins
HMR	Hidden MAT Right
HP1	heterochromatin protein 1
ICR	interlocus control region
IgG	immunoglobulin G
IP	immunoprecipitate or immunoprecipitation
kbp	kilobasepairs
KCI	potassium chloride
kDa	kilodalton
km, m, cm, µm, nm	kilometre, metre, centimetre. Micrometre, nanometre
l, ml, µl	litre, millilitre, microlitre
M (or M-phase)	mitotic phase
M, mM, uM, nM	molar, millimolar, micromolar, nanomolar
Mad2	mitotic arrest deficient protein 2

Mcd1	mitotic chromosome determinant 1
MCS	multiple cloning site
N-terminal	amino-terminal
NaPi	sodium phosphate buffer
NBD	nucleotide binding protein
o.n	overnight
ORF	open reading frame
pBS	cloning vector pBlueScribe
PBS	phosphate-buffered saline
PBST	phosphate-buffered saline/Tween 20
PCNA	proliferating cell nuclear antigen
PCR	polymerase chain reaction
Pds1	premature dissociation of sisters
pH	power of hydrogen
Plk1	polo-like kinase 1
PMSF	phenylmethylsulphonyl fluoride
PP2A	protein phosphatase 2A
preRC	pre-replicative complex
PVDF	polyvinylidene fluoride
qRT-PCR	quantitative Real-Time PCR
Rad21	radiation sensitive mutant 21
Rad50	radiation sensitive mutant 50
RBS/SC	Roberts/SCphocomelia
rDNA	ribosomal DNA
RNAi	RNA interference
rpm	revolutions per minute
RT	room temperature
S (or S-phase)	synthesis phase
S.cerevisiae	*Saccharomyces cerevisiae*
S.D.	Standard deviation
S.pombe	*Schizosaccharomyces pombe*

SA1, SA2	stromal antigen
SAC	spindle assembly checkpoint
Scc1-4	sister chromatid cohesion protein
SCF	Skp1-cull-Fbox protein
SDS	sodium dodecyl sulphate
SDS-PAGE	sodium dodecyl sulphate polyacrylamide gel electrophoresis
Sgo	shugoshin
Smc1-6	structural maintenance of chromosome proteins
t	time
TE	Tris/EDTA
ts	temperature-sensitive
TEV	tobacco etch virus
TPR	tetratricopeptide
Tris	2-amino-2-(hydroxymethyl) propane-1,3-diol
UTR	untranslated region
Wapl	wing apart like
X.laevis	*Xenopus laevis*
YEPD	yeast extract peptone dextrose
YEPRaff	yeast extract peptone raffinose
YFP	yellow fluorescent protein
γ-neurons	gamma neurons
5-FOA	5-fluoroorotic acid

Appendix 3: Acknowledgements

A PhD has been the most difficult thing I have done so far in my life, and it would not have been possible without the support and understanding of my DPhil supervisor, Kim Nasmyth. Thank you Kim for giving me the opportunity to work in your lab!

I also have been very lucky to work with my colleagues in the laboratory, especially Ana-Maria Farcas, who have helped me a lot to develop as a scientist. Ana, you were always available and willing to help throughout my studies. Thank you very much for patiently answering my questions about gradients, going through almost every blot that I made and never leaving me alone in the cold room when our "lovely" fractionator was broken down! Working with you was always fun and I missed your company a lot in the lab when you are gone to Zurich.

Thank very much Maria Demidova and Sarah Dixon for being good friends throughout my PhD. Maria, thanks very much for keeping me company when we had to go home in the middle of the night after a very long day in the lab. Though it was short, our Arabic class adventure was lots of fun! Sarah, I will always keep our emergency "glass-room" conversations in good memory! ☺

Maurici Brunet was a great source of help on the issues related to protein biochemistry. Maurici, I will never forget our fight about cooling down the French Press! Despite everything, I still think that I was right☺

Thank you very much Frederique Becquet for the brain-storming sessions you have carried out with me. Thank you for being such a nice and fun mate to work with☺

Thank you Ahmed Rattani for the lengthy conversations that you carried out with me about music, world politics and how to make a career outside of science☺

Thank you Raquel Oliveira, Frederique Becquet, and Maurici Brunet for critically reading parts of my thesis and for providing valuable comments.

This work is also dedicated to my very supportive Turkish friends in UK; Gamze Camdere, Eda Suer, Cihangir Yandim and Asli Ermis, who helped me through this period and made my life in Oxford memorable. Arkadaslar iyi ki varsiniz! Hersey icin cok tesekkurler!

Thank you to all my colleagues, past and present, for discussions and for creating such a wonderful working atmosphere: Ajay Mishra, Alexander Kurze, Anca Farcas, Andrea Pauli, Bin Hu, Bulent Cetin, Chris Chan, Jean Metson, Johanna Scheinost, Martin Houlard, Mayte Siswick, Tatsuya Hirano, Vitorio Katis, William Upcher, Wolfgang Helmhart, Lana Strmecki, Magda Wolna, Ryo Kawamura, Kikue Tachibana, Naomi Petela, Sarah Dixon, Christian Eichinger, Mickael Ploquin, Elwy Okaz, Nik Watson, Madhu Srinivasan, Benjamin Rowland, and Barry McGuinness.